A

RESONANCE RAMAN STUDIES OF BOVINE AND OCTOPUS VISUAL PIGMENTS

By

Liewen Huang

A dissertation submitted to the Graduate Faculty in Physics in partial fulfillment of the requirements for the degree of Doctor of Philosophy, The City University of New York

1995

This manuscript has been read and accepted for the Graduate Faculty in Physics in the satisfaction of the dissertation requirement for the degree of Doctor of Philosophy

2/7/95
Date

Chair of Examining Committee

2/10/95
Date

Executive Officer

Supervisory Committee

The City University of New York

ABSTRACT

RESONANCE RAMAN STUDIES OF BOVINE AND OCTOPUS VISUAL PIGMENT

BY

Liewen Huang

Advisor: Professor Robert H. Callender

We have regenerated bovine and octopus visual pigments with retinals containing isotopic labels at three positions, i.e., 8-^{13}C-11,12-D_2, 10-^{13}C-11,12-D_2, 11-^{13}C-11,12-D_2, 14-^{13}C-11,12-D_2, for the studies of bound chromophore ethylenic and Schiff base vibrational modes by resonance Raman spectroscopy. Also regenerated were octopus visual pigments with singly or doubly ^{13}C labeled retinals, i.e., 9-^{13}C, 10,11-$^{13}C_2$, 12,13-$^{13}C_2$, 13-^{13}C, 14,15-$^{13}C_2$, 14,15-$^{13}C_2$-ND, for the studies of vibrational modes in the fingerprint region. We have analyzed the resonance Raman spectra based upon the observation of the response of individual bands in the spectrum of rhodopsin, isorhodopsin, or bathorhodopsin to a particular label. The observed peaks in the fingerprint and ethylenic regions have been tentatively assigned to specific C-C and C=C stretches.

We have also studied a model retinal protonated Schiff base analog and its isotopically labeled derivatives as well as calculations using *ab initio* methods. Based on the vibrational analysis, new criteria to determine the

Schiff base C=N configuration from Raman spectroscopy have been developed, and the C=N configuration in octopus rhodopsin, isorhodopsin and bathorhodopsin has been determined.

We have continued the resonance Raman study of the Schiff base hydrogen/deuterium exchange for rhodopsin and bacteriorhodopsin by employing the continuous-flow experiment. The exchange of a deuteron on the Schiff base with a proton is very fast, with half-times of 6.9 ± 0.9 and 1.3 ± 0.3 ms for rhodopsin and bacteriorhodopsin, respectively, faster than the proton-deuteron exchange rate of a protonated Schiff base in aqueous solution (16 ± 2 ms). This anomalous result can be understand if a structural water molecule (or molecules) is present next to the protonated Schiff base in the two pigments.

To My Family

ACKNOWLEDGMENT

I thank my thesis advisor Professor Robert Callender for patiently guiding me through this work. His strict scientific attitude, creative imagination and astute advice have made my graduate career a very rewarding one, both in professional and personal growth.

My special gratitude goes to Dr. Hua Deng for his considerable valuable advise and assistance.

I thank Dr. Yiannis Koutalos greatly for helping me in preparation of octopus samples. I thank Prof. Thomas Ebrey, Dr. Jie Liang, for the great help in my thesis research and in my staying in UIUC. I thank Drs. R. Gebhard, M. Groesbeek and Prof. J. Lugtenburg for the gift of isotopic derivatives, Prof. M. Tsuda for octopus eyeballs. All of these were key elements of my thesis research.

I am grateful to Prof. Myriam Sarachik for lending me the dye laser which are used in the pump-probe experiments for octopus pigments. I thank Prof. Marilyn Gunner for her worthy suggestion in my research and generous assistance in using the computers. I thank Ms. Sheila Ehlinger in Biology Department for kindly letting me use the dark room and the high-speed centrifuges. I would like to thank Mr. Joseph Altmann and his colleagues in the machine shop for their help in configuring optical system and for providing liquid nitrogen for low temperature experiments.

I would like to thank the members of my thesis committee for their time and guidance.

I thank past and present members of our lab and the department, Dr. Jim Ball, Dr. Danny Manor, Dr. Zheng Jie, Dr. Xiaoke Chen, Dr. Gezhi Weng, Dr. Yongqing Chen, Dr. Jeroen van Beek, Dr. Rudolf Gilmanshin, Dr. Larry Senak, Dr. Ming Yan, Mr. Dongguang Xiao, Mr. Guang Bai, Mr. Zhongmo Ju, Mr. Zunhai Dong, Mr. Hui Zhong, Mr. Jianghua Wang, Mrs. Naomi Hellman for their plentiful help during the course of this study. Specifically, I thank Dr. Senak for his proof reading my thesis and thoughtful suggestions.

I thank all my teachers, especially Prof. Steve Orenstein. I thank all people who ever helped me to pursue this degree in any ways.

Finally, I extremely thank my parents, my wife, my brother and sister, and my grand parents, for their encouragement, supporting and love. I would also like to thank my best friend, Dr. Yuping Cai, for his momentous help in my scientific career.

TABLE OF CONTENTS

LIST OF TABLES

LIST OF CHARTS

LIST OF FIGURES

Chapter 1

INTRODUCTION

I. GENERAL INTRODUCTION

Rhodopsin, the protein responsible for converting light into an optic nerve impulse, and bacteriorhodopsin, the light transducing protein of the purple membrane of Halobacterium halobium (Birge, 1990) have been intensively studied by resonance Raman spectroscopy for more than two decades (Rimai *et al.*, 1970; Oseroff and Callender, 1974) (for reviews, see Callender and Honig, 1977; Warshel, 1977; Ottolenghi, 1980; Callender, 1982a; Smith *et al.*, 1985a; Applebury and Hargrave, 1986; Doukas *et al.*, 1986; Mathies *et al.*, 1987; Birge, 1990; Birge, 1990; Mathies *et al.*, 1991). During this time, experiment techniques, that have been developed for studying the photolabile samples, include: pump-probe (Oseroff and Callender, 1974), flow through and rotating cell (Callender *et al.*, 1976; Mathies *et al.*, 1976; Stockburger *et al.*, 1979; Terner *et al.*, 1979; Braiman and Mathies, 1982a; Braiman and Mathies, 1982b), and continuous flow mixing (Ehrenberg *et al.*, 1980; Doukas *et al.*, 1981; Deng *et al.*, 1994a). Studies of the isotopically substituted artificial chromophores combined with data from IR and time-revolved (El-Sayed, 1982), has provided a great deal of information concerning chromophore conformation and its interactions with the apoprotein (Curry *et al.*, 1985; Smith *et al.*, 1985a; Mathies *et al.*, 1987; Palings

et al., 1987; Palings *et al.*, 1989; Deng *et al.*, 1991a; Deng *et al.*, 1991b; Lin *et al.*, 1992; Lin *et al.*, 1994).

We will extend the resonance Raman spectroscopy to the study of visual pigment bacteriorhodopsin, bovine and octopus rhodopsins, and model compounds in some more detail.

II. THEORETICAL BACKGROUND

Raman and Resonance Raman

The physical origin of Raman scattering lies in inelastic collisions between molecules and photons. In inelastic collision the photon exchanges energy with the molecule, resulting in the change of the wavelength of the scattered light. The shift in frequency of the incident light, hence the change in energy, is equal to the energy difference between the vibrational states of the molecular. The Raman effect in which the incident light wavelength is close to absorption band of the chromophore, is known as resonance Raman (see Figure 1.1). The Raman cross-sections of the vibrational modes, in which the predominantly moving atoms are also involved in the equilibrium displacement of molecule upon aborption of a photon, may be greatly enhanced in resonance Raman (see the detailed discussion in the Raman Intensity Section). Thus, the resonance Raman spectroscopy provides a way to measure a small part constituent with a special absorption center in a very complicated biological system.

The Raman effect has been well studied (Raman and Krishnan, 1928; Van Vleck, 1929; Placzek, 1934; Roothaan, 1951; Albrecht, 1961; Tang and Albrecht, 1970; Albrecht and Hutley, 1971; Friedman and Hochstrasser, 1974; Inagaki *et al.*, 1974; Warshel and Karplus, 1974; Johnson and Peticolas, 1976; Warshel, 1977). In this section we discuss the factors that determine Raman

intensities of normal modes, as well as internal coordinate, mixing, and coupling (Curry *et al.*, 1985; Tavan *et al.*, 1985; Garriga et al., 1986; Kakitani *et al.*, 1983).

Normal Mode and Normal Coordinate

Any complicated motion of atoms vibrating within a molecule can be broken down into simple components known as normal modes of vibration . Normal coordinate is defined as that a normal mode is described by a single (normal) coordinate which varies with time. Each normal coordinate independently contributes to the kinetic and potential energy of the system. The internal coordinate in normal mode calculation is defined, as the geometrically localized basis set of coordinates as set out by Wilson *et al.* (1955), and is referred as C=C, C-C, C-H stretching, CCC, CCH bending, etc.

Raman Intensity

For randomly oriented molecules the total Raman intensity for the transition from an initial vibronic state m to a final vibronic state n is given by

$$I_{m,n} = \frac{8\pi}{9C^4} I_0 \omega^4 \sum_{\rho\sigma} |\alpha^{\rho\sigma}_{m,n}|^2$$

where $I_{m,n}$ and ω is the total intensity and frequency of the scattered light, respectively. I_0 is the intensity of the incident light. $\alpha^{\rho\sigma}_{m,n}$, the component of the polarizability tensor, is expressed by

$$\alpha^{\rho\sigma}_{m,n} = \frac{1}{h} \sum_{\nu} \frac{\langle gi|\mu^\sigma|ev\rangle\langle ev|\mu^\rho|gf\rangle}{\nu_{gi,ev} - \nu_0 + i\,\Gamma_{ev}} + \frac{\langle gi|\mu^\rho|ev\rangle\langle ev|\mu^\sigma|gf\rangle}{\nu_{gi,ev} + \nu_0 + i\,\Gamma_{ev}}$$

where Γ_{ev} the damping factor with the finite lifetime of each molecule state vibronic state $|ev\rangle$ denotes the νth vibrational level in the eth excited electronic state, $\nu_{gi,ev}$ is the frequency difference between the indicated

vibronic levels gi and ev, ν is the frequency of the incident light, and μ^{σ} the electronic dipole moment operator along direction σ. The sum over index ν runs all vibrational states on the eth electronic state.

The first term of the above expression, the Albrecht A-term, is the predominant term in the Raman tensor in the resonance case for the retinal chromophore (Warshel and Dauber, 1977; Doukas *et al.*, 1978a).

$$A^{\rho\sigma} = \frac{1}{h} \sum_{\nu} \frac{R_{\sigma}^{ge} R_{\rho}^{eg}}{\nu_{gi,ev} - \nu_0 + i\,\Gamma_{ev}} \langle i \mid \nu \rangle \langle \nu \mid f \rangle$$

where R is the electronic transition moment as a function of normal coordinate and <i | v> etc. are overlap integrals between vibrational wave functions of the ground and excited states, g and e.

Kakitani (1979) showed that in a near resonance case, if the damping factor G can be neglected, relative Raman intensity I of two modes s and t can be expressed as:

$$\frac{I_s}{I_t} \approx \left(\frac{\Delta_s \nu_s}{\Delta_t \nu_t}\right)^2$$

where Δ_i is proportional to the equilibrium geometry shift upon excitation of the normal mode i and n_i is its vibrational frequency.

Thus, the frequency of scattered photons in the Raman spectra, including that is the resonance Raman spectra, is the property of the ground state vibrational modes, while the intensity of scattering light in resonance Raman is related with the exited electronic state (Carey, 1982).

This relation is need to understand the Raman intensity consideration in our analysis of the resonance Raman spectra of retinal.

Mixing and Coupling

Two concepts, mixing and coupling, are used in analysis of the patterns of vibrational frequencies and intensities in retinal isomers and isotopic

derivatives (Curry *et al.*, 1985). Mixing of two local symmetry coordinates (LSC's) affects the observed Raman band *intensity*, since the intrinsic amplitudes of the LSC's will be in- or out-of-phase. The intensities reinforce in the in-phase, and partially cancel in the out-of-phase combination. Coupling happens when there are substantial kinetic or potential energy interactions between the intrinsic coordinates. The *frequencies* of the resulting normal modes appear shifted (usually "pushed" apart) from the "intrinsic" frequencies of the LSC's in which the interaction is absent (Curry *et al.*, 1985).

Isotopic Substitution

Isotopic substitution can be an invaluable aid in the analysis of normal modes in vibrational spectra. Usually, the force constants are unaltered by isotopic substitution, so the shift in observed frequency can be attributed principally to mass effects (Carey, 1982). The resulting frequency shifts of the normal modes provide a good measure of the degree to which the substituted local coordinates' contribute to each normal mode of the original molecule (Curry *et al.*, 1985).

In this work, ^{13}C- and Deuterium labeled retinal derivatives have been employed. The observed shift of particular band upon isotopic substitution is used to assign normal modes for model compounds, as well as bovine and octopus visual pigments.

III. VISUAL PIGMENTS

The retina of the most animal eye contains two types of receptor cells. They are known as rods and cones because of their shape. The rods are responsible for vision in dim light. They consist of an inner segment that

contains the nucleus and mitochondria and an outer segment (ROS) that is attached by a number of small fibrils. Cones are responsible for vision in bright light, as well as color vision (Solomons, 1988), Rhodopsin is found in the disk membrane of retinae (Daemen, 1973; Papermaster and Dryer, 1973). The rhodopsin molecules have considerable freedom of rotational (Brown *et al.*, 1972; Cone, 1972) and translational (Poo and Cone, 1974) movement which is temperature dependent (Blasie and Worthington, 1969). The amino acid sequence of a number of opsins (Ovchinnikov, 1982; Hargrave *et al.*, 1983; Applebury and Hargrave, 1986; Nathans *et al.*, 1986; Ovchinnikov *et al.*, 1988) have been determined. This makes it possible to identify protein perturbations that may be responsible for the opsin-shift (Kosower, 1988; Loppnow *et al.*, 1989; Sakmar *et al.*, 1989; Zhukovsky and Oprian, 1989; Lin *et al.*, 1992).

It is shown that the chromophore (light-absorbing group) of rhodopsin is the polyunsaturated aldehyde, 11-*cis*-retinal (Figure 1.2c). The 11-*cis* retinal is connected to a specific lysine residue in the protein known as opsin via a Schiff base linkage (Lews *et al.*, 1974; Oseroff and Callender, 1974). Bovine pigment has an absorption band centered at 498 nm. The principal result of absorption of a photon by rhodopsin is the isomerization of the chromophore from 11-*cis* to all-*trans* (Hubbard and Kropf, 1958; Wald, 1968). After absorption of a photon, rhodopsin goes through a series of intermediates (Callender and Honig, 1977; Bennett, 1978)(Figure 1.3), culminating in chromophore detachment from the opsin. This process is known as bleaching because pigments absorb in the visible while the final product, retinal and opsin, absorbs in the UV (Hubbard and Wald, 1952; Yoshizawa and Wald, 1963). An artificial pigment, called isorhodopsin (Collins and

Morton, 1950), which contains 9-*cis* retinal (Figure 1.2d) as a chromophore follows the same bleaching sequence of rhodopsin upon absorption of light.

The first intermediate of bovine rhodopsin, bathorhodopsin (also known as prelumirhodopsin; Yoshizawa and Wald, 1963), is formed photochemically in less than 6 psec. (Busch *et al.*, 1972; Monger *et al.*, 1979). Bovine bathorhodopsin (λ_{max} = 543 nm) has an absorption center that is red shifted from rhodopsin (λ_{max} = 497 nm). At temperature lower than 130 K, rhodopsin, isorhodopsin and bathorhodopsin can be photochemically interconverted without further decay (Yoshizawa and Wald, 1963). Some 60% of the incident photon energy (about 35 kcal/mole) is converted to chemical energy upon photon absorption (Cooper, 1979).

It is generally believed that the primary photochemical event in vision, the formation of bathorhodopsin, involves a *cis-trans* isomerization of the retinal chromophore (Rosenfeld *et al.*, 1977). This is based on liquid nitrogen temperature absorption studies (Yoshizawa and Wald, 1963; Hubbard and Kropf, 1965) and supported by resonance Raman and picosecond studies (Honig *et al.*, 1976; Callender and Honig, 1977; Aton *et al.*, 1978; Aton *et al.*, 1980; Eyring *et al.*, 1980a; Narva and Callender, 1980; Doukas *et al.*, 1985). Some proposed models (Fransen *et al.*, 1976; van der Meer *et al.*, 1976; Peters *et al.*, 1977), however, were not completely consistent with all the experimental data. The analysis of the Raman data with intense hydrogen out of plane modes suggest that the all-*trans* retinal (Figure 1.2a) chromophore in bathorhodopsin could be twisted (Eyring *et al.*, 1980b; Loppnow *et al.*, 1990; Deng *et al.*, 1991a).

Our understanding of visual photochemistry results mainly from studies on bacteriorhodopsin (Aton *et al.*, 1979; Eyring and Mathies, 1979; Narva *et al.*, 1981; Pande *et al.*, 1981; Crouch *et al.*, 1984; Lam *et al.*, 1984; Pande

et al., 1986; Rao *et al.*, 1986; Fodor *et al.*, 1988b; Pande *et al.*, 1989; Pande *et al.*, 1989; Fahmy *et al.*, 1991), retinal isomers (Doukas *et al.*, 1978a; Curry *et al.*, 1984; Curry *et al.*, 1985), and vertebrate pigments (mainly bovine rhodopsin [Callender, 1979; Eyring *et al.*, 1982; Lewis, 1982; Buchert *et al.*, 1983; Doukas *et al.*, 1984; Birge and Callender, 1987; Palings *et al.*, 1987; Callender, 1989; Pajares and Rando, 1989; Palings *et al.*, 1989; Morrison *et al.*, 1991; Pande *et al.*, 1991; Pugh and Lamb, 1993] and its meta product [Doukas *et al.*, 1978b; Tsuda, 1979b; Pande *et al.*, 1982; Yoshizawa and Shichida, 1982], as well as iodopsin, the chicken rhodopsin [Loppnow *et al.*, 1989; Lin *et al.*, 1994]). By comparison, we know relatively little about invertebrate pigments. Octopus perhaps is one of the most often studied invertebrate pigments.

There are some similarities and interesting differences in the photochemical behavior of vertebrate and invertebrate pigments (Suzuki and Callender, 1981; Ohtani *et al.*, 1988; Koutalos *et al.*, 1990). In general, both type rhodopsins contain 11-*cis* chromophores and meta products contain the *trans* chromophore (Pande *et al.*, 1987). The bathorhodopsins of both species absorb at the same frequencies (540 nm for octopus and 543 nm for bovine bathorhodopsin). Both pigment systems absorb the energy of a single photon at ca. 55 kcal/mol, and convert the same fraction of this light energy, some 60%, to form the high-energy batho products. On the other hand, there is a larger difference between the λ_{max}'s of octopus rhodopsin (λ_{max} = 472) and bathorhodopsin (λ_{max} = 540 nm) in comparison to their bovine counterparts (500 and 543 nm, respectively). Additionally, the opsin pocket differs in the pigments of the two species as do their photochemical cycles.

Previous work has shown that the resonance Raman spectra of the vertebrate and invertebrate rhodopsin are very different as are the spectra of their two batho products (Pande *et al.*, 1984; Pande *et al.*, 1987). In order to

understand how those differences in spectra relate to chromophore structure, a series of resonance Raman measurements of octopus bathorhodopsin were performed where the chromophores have been isotopically labeled by deuterium at virtually every chromophore hydrogen position individually. This has led to an understanding of bathorhodopsin's HOOP modes, indicating that the (presumably *trans*) chromophore is twisted differently in octopus bathorhodopsin than in bovine bathorhodopsin. This data suggests specific active site interactions between chromophore and protein are quite different for the two species (Deng *et al.*, 1991a; Deng *et al.*, 1991b).

In this work, we extend these studies. The spectra of octopus rhodopsin containing deuterated chromophores are measured as are those of ^{13}C labeled chromophores in both octopus rhodopsin and bathorhodopsin. Normal modes are assigned to peaks based on the isotopic shifts. Chromophore structure and the interaction between the chromophore and the protein are also discussed.

IV. EXPERIMENTAL TECHNIQUES

Photolability Problem and Special Methods

A major difficulty in the measurement of the resonance Raman effect in visual pigments or model compounds is that they readily isomerize upon absorption of a photon. The Raman effect, even for resonance enhanced cross-sections, is an extremely weak phenomenon. The chromophore absorption cross-section of visual pigments is about 10^{-16} cm^2/mol, about eight orders of magnitude larger than the resonance Raman cross-section of the most intense Raman active mode. It is clear that it is much more probable for a rhodopsin molecule to absorb light, and thus be effectively "destroyed" relative to the original sample, than for it to Raman scatter a

photon. Special techniques have been developed for obtaining Raman spectra of light sensitive samples (Callender, 1982b).

'Pump and Probe' Method

The central idea of this method is that thermal decay of bathorhodopsin is blocked at low temperatures, and three pigments (rhodopsin, bathorhodopsin and isorhodopsin) are rapidly interconverted under laser irradiation. Their relative concentrations are determined at equilibrium by the laser frequency (Hurley *et al.*, 1977). The quantum yield for one species to the other upon absorption of a photon has been studied (Strackee, 1972). Thus a weak "probe" laser beam is used to produce the Raman signal, and a relatively stronger "pump" laser beam simultaneously irradiating the sample controls sample composition (Oseroff and Callender, 1974). Practically, in these experiments, resonance Raman measurements were performed at 80 K in a home-made liquid nitrogen coldfinger, utilizing the dual-beam pump-probe technique. The regenerated membranes were centrifuged to a thick pellet that was applied to the sample tip of the coldfinger and then cooled down to 80 K. The photostationary mixtures of rhodopsin, isorhodopsin, and bathorhodopsin at 80 K are obtained and their Raman spectra taken with the "probe" beam (457.9 nm line from an Ar+ laser). The composition of this mixture can be changed by simultaneously irradiating the sample with a second high-intensity "pump" laser beam. The spectra of various sample compositions are then added and subtracted appropriately to yield the individual spectra of rhodopsin bathorhodopsin, and isorhodopsin. A major advantage of the "pump-probe" method is that the amount of pigment needed for the experiment is minimal. This is

especially crucial for pigments containing rare isotopically labeled chromophores.

Flowing Sample

This method measures flowing solution samples contained either in a jet stream (Mathies *et al.*, 1976) or a capillary tube (Callender *et al.*, 1976) passing through the laser beam with a velocity sufficient to insure that any given molecule has a low probability of absorbing a photon in the laser-sample interaction area.

Kinetics of Mixed Reactants

The time evolution of two reacting systems, for example, the exchange of a proton of the protonated Schiff base for a deuteron, can be monitored by Raman spectroscopy. Two reactants are mixed rapidly via two jets meeting in a mixing chamber. The mixed sample exits through a capillary tube, the exit flow speed and the position of the focused Raman exciting laser beam control the time at which the reaction is monitored after initialization (Deng, 1987).

Instruments

Raman spectra are obtained with an optical multichannel analyzer (OMA) system, consisting of a Spex triplemate spectrometer (Spex Industries, Metuchen, NJ) and a model DIDA-100 reticon detector connected to a ST-100 detector controller (Princeton Instruments, Trenton, NJ), which is interfaced to a Macintosh II microcomputer (Apple Computer, Cupertino, CA). The laser excitation beam is 457.9 nm, allowing a spectral window of about 1400 cm^{-1} with resolution of 8 cm^{-1} to be detected. The Raman band positions are

calibrated against the known Raman peaks of toluene and are accurate to ±1.5 cm^{-1}.

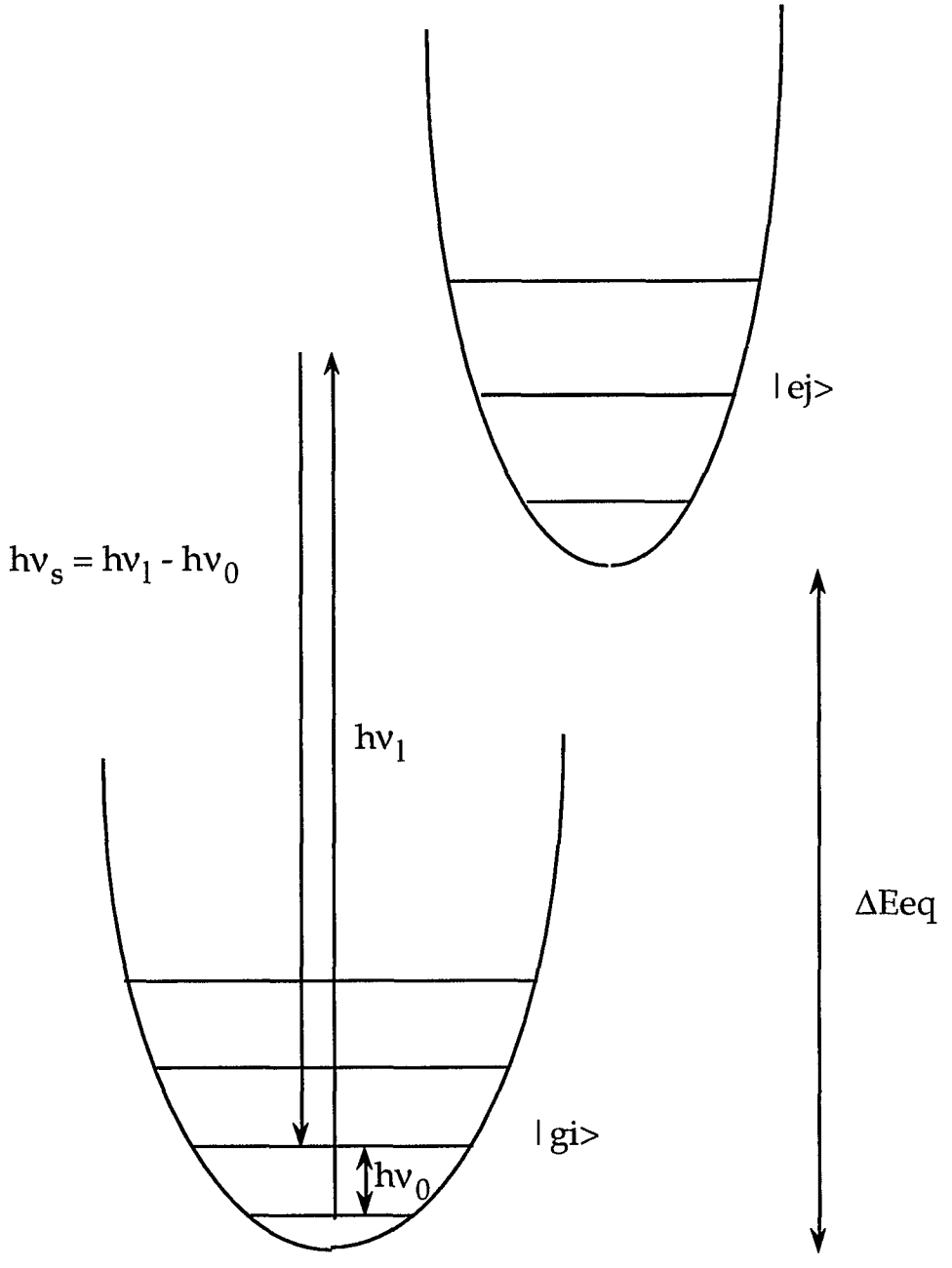

Figure 1.1: A schematic drawing of Raman scattering. A resonance enhancement happens when $h\nu_l \approx \Delta E_{eq}$. In a standard nonresonance Raman experiment $h\nu_l < \Delta E_{eq}$.

Figure 1.2: Conformations of various isomers of retinal (X = O), its Schiff base (X = N), and its protonated Schiff base (X = NH+). (a) all-*trans*; (b) 13-*cis*; (c) 11-*cis*; (d) 9-*cis*. Flexible bonds whose equilibrium configuration is not planar are indicated by arrows .

(a)

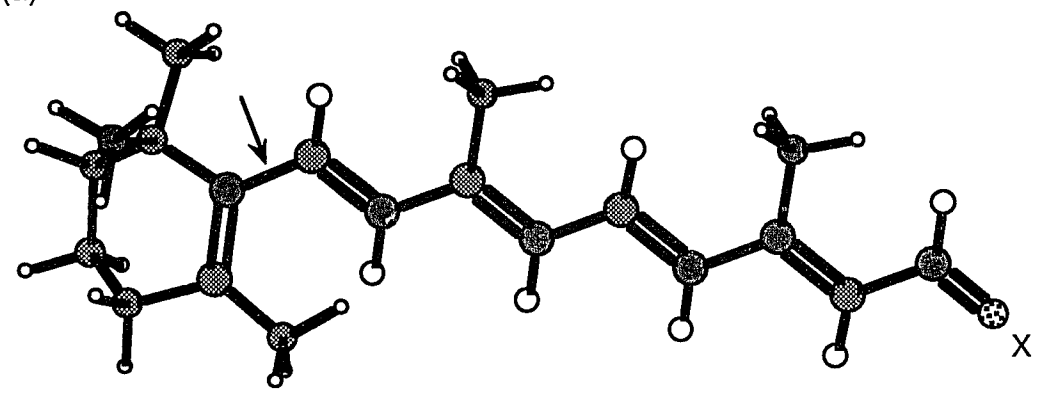

(b)

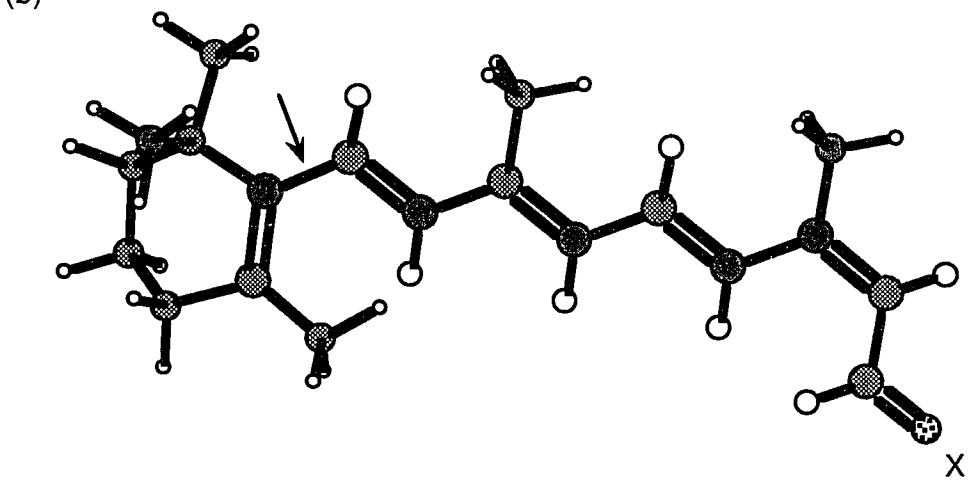

(c)

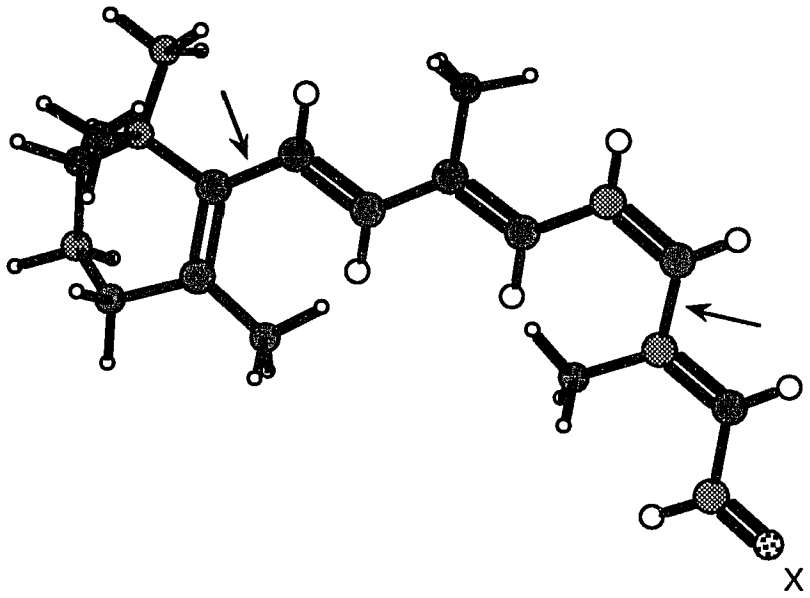

(d)

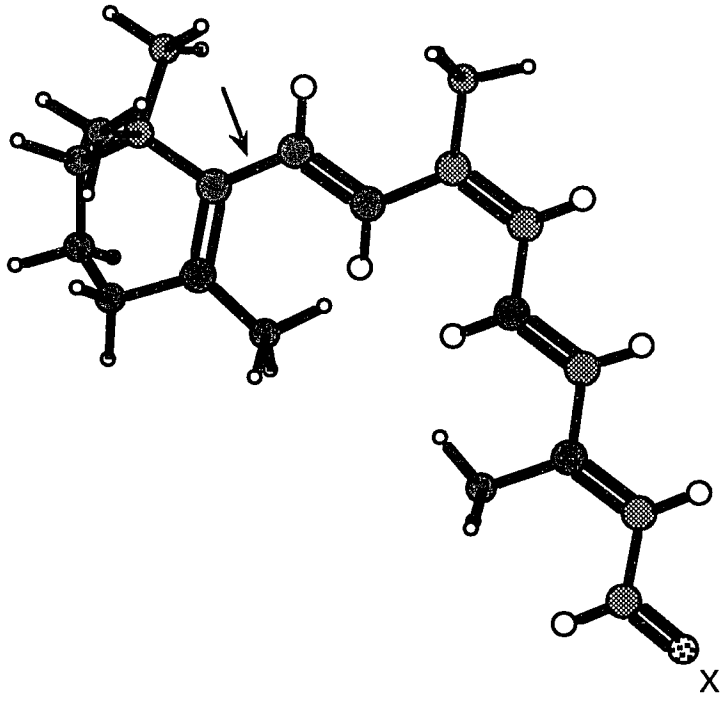

Figure 1.3: The bleaching sequence of rhodopsin. Rhodopsin and isorhodopsin are placed lowest in the figure to indicate they have lower free energy than their common photoproducts.

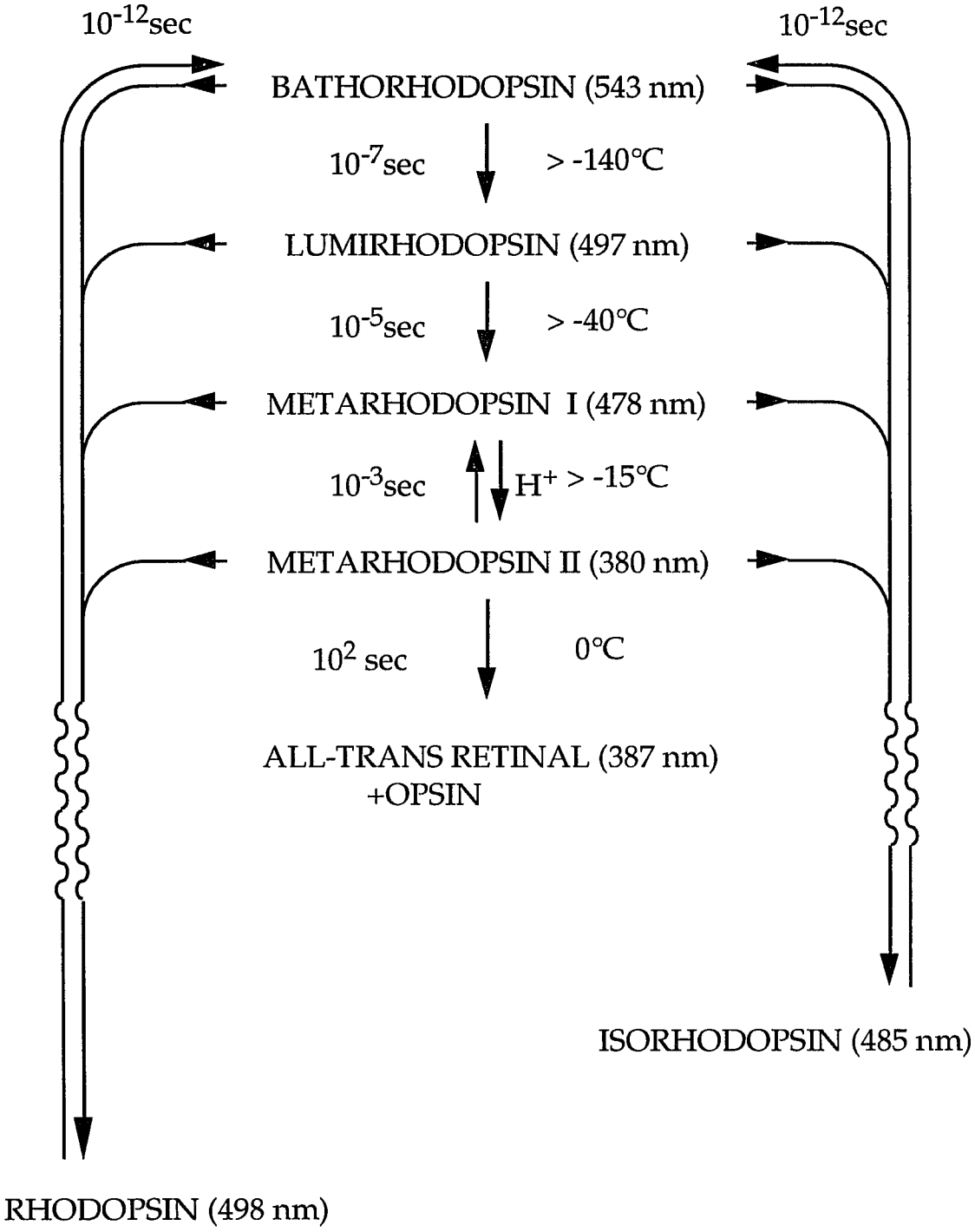
10^{-12}sec
10^{-12}sec
BATHORHODOPSIN (543 nm)
10^{-7}sec
> -140°C
LUMIRHODOPSIN (497 nm)
10^{-5}sec
> -40°C
METARHODOPSIN I (478 nm)
10^{-3}sec
H^+ > -15°C
METARHODOPSIN II (380 nm)
10^2 sec
0°C
ALL-TRANS RETINAL (387 nm)
+OPSIN
ISORHODOPSIN (485 nm)
RHODOPSIN (498 nm)

Chapter 2

EVIDENCE FOR A BOUND WATER MOLECULE NEXT TO THE RETINAL SCHIFF BASE IN BACTERIORHODOPSIN AND RHODOPSIN: A RESONANCE RAMAN STUDY OF THE SCHIFF BASE HYDROGEN/DEUTERON EXCHANGE *

I. ABSTRACT

The retinal chromophores of both rhodopsin and bacteriorhodopsin are bound to their apoproteins via a protonated Schiff base. We have employed continuous-flow resonance Raman experiments on both pigments to determine that the exchange of a deuteron on the Schiff base with a proton is very fast, with half times of 6.9±0.9 ms and 1.3±0.3 ms for rhodopsin and bacteriorhodopsin, respectively. When these results are analyzed using standard hydrogen-deuteron exchange mechanisms, that is acid, base or water catalyzed schemes, it is found that none of these can explain the experimental results. Since the exchange rates are found to be independent of pH, the deuterium-hydrogen exchange can not be hydroxyl (or acid) catalyzed. Moreover, the deuterium-hydrogen exchange of the retinal Schiff base can not be catalyzed by water acting as a base since in that case the estimated

---

* Content of this chapter has been published in the Biophysical Journal (Deng, H., L. Huang, R. Callender, and T. Ebrey. (1994). Evidence For a Bound Water Molecule Next to the Retinal Schiff Base in Bacteriorhodopsin and Rhodopsin: A Resonance Raman Study of the Schiff Base Hydrogen/Deuterium Exchange. *Biophys. J.* **66**: 1129-1136).

exchange rate is predicted to be orders of magnitude slower than that observed. The relatively slow calculated exchange rates are essentially due to the high pKa values of the Schiff base in both rhodopsin (pKa > 17) and bacteriorhodopsin (pKa ~ 13.5). We have also measured the deuterium-hydrogen exchange of a protonated Schiff base model compound in aqueous solution. Its exchange characteristics, in contrast to the Schiff bases of the pigments, is pH dependent and consistent with the standard base catalyzed schemes. Remarkably, the water catalyzed exchange, which has a half time of 16±2 ms and which dominates at pH 3.0 and below, is slower than the exchange rate of the Schiff base in rhodopsin and bacteriorhodopsin. Thus, there are two anomalous results, the inconsistency of the observed hydrogen exchange rates of retinal Schiff base in the two pigments with those predicted from the standard exchange schemes and the enhancement of the rate of hydrogen exchange in the two proteins over the model Schiff base in aqueous solution. We suggest that these results can be explained by the presence of a structural water molecule (or molecules) at the retinal binding sites of the two pigments, quite close, probably hydrogen bonded, to the Schiff base proton. In this case, the rate of exchange can be faster than that found for the model compound due to an 'effective water concentration' near the Schiff base that is increased from that found in aqueous solution.

II. INTRODUCTION

Rhodopsin, the protein responsible for sensing light in vision, consists of a chromophore, the 11-cis isomer of the aldehyde of vitamin A, retinal, and the colorless apoprotein, opsin. The chromophore is covalently attached by a protonated Schiff base, $-C=NH^+-$, linkage to an ε-amino group of a lysine in opsin. The absorption of light results in the very rapid photoisomerization

of the 11-*cis* chromophore to a *trans* form (Schoenlein *et al.*, 1991; Yan *et al.*, 1991). In this process, about half of the energy of the absorbed photon is converted to chemical energy by forming a high energy chemical species called bathorhodopsin (Honig *et al.*, 1979b). Bacteriorhodopsin (bR), a protein located in the cell membrane of the bacterium, *Halobacterium salinarium* (formerly *Halobacterium halobium*), has as its chromophore the *trans* isomer of retinal, which is also attached to its apoprotein by a protonated Schiff base. The photophysics of the bound chromophore is quite similar to rhodopsin, although there are differences in detail. For example, the photoconversion of bR to K, the primary photoproduct analogous to bathorhodopsin, is a *trans* to *cis* isomerization, takes somewhat longer, and converts less of the photon's energy to chemical energy. This photophysical behavior of rhodopsin and bacteriorhodopsin is very unusual. In contrast to the pigments, model compounds of protonated Schiff bases of retinal in solution, for example, differ in energy by less than a kcal/mol amongst their *cis* and *trans* forms compared to the about 35 kcal/mol difference in energy between rhodopsin and bathorhodopsin (cf., Birge, 1990; Mathies *et al.*, 1991).

For some time it has been supposed that the protein structure around the bound retinal, particularly near the protonated Schiff base linkage, is key to this remarkable photochemical behavior. Certainly, calculations show that the specific arrangement of the group or groups that 'solvate' the positively charged protonated Schiff base linkage have direct and strong effects on the ground and excited states of the chromophore, on the reaction coordinates, and on the dynamics of the excitation process (cf., Birge *et al.*, 1988; Birge, 1990; Mathies *et al.*, 1991). Also, it has been supposed that electrostatic considerations, the separation of the positively charged protonated Schiff base from its putative negative counter-ion or solvating groups, is a major factor

in the energy storage shown by these pigments (Honig *et al.*, 1979b; Deng and Callender, 1987; Birge *et al.*, 1988). High resolution structures for rhodopsin and bacteriorhodopsin would help immensely in understanding these questions but unfortunately none exist.

One method for studying the structure of a group with a labile proton, like that of the protonated Schiff base linkage of rhodopsin and bacteriorhodopsin, is hydrogen-deuterium exchange. Such studies have been used extensively to study various properties of proteins, especially protein folding (for recent reviews, see Kim, 1986; Englander and Mayne, 1992). The standard reaction mechanism for hydrogen-deuterium exchange in aqueous solution involves acid/base catalysis (cf. Eigen, 1964). For a protonated Schiff base, only the base (hydroxyl or water acting as base) catalyzed hydrogen exchange reaction is significant (see results, below). The hydroxyl catalyzed exchange reaction, for example, proceeds via two steps given by the following scheme:

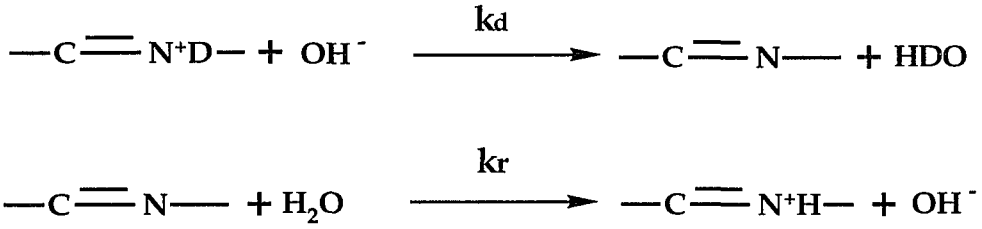

Scheme 2.1

In some cases the factors which influence the exchange rate have been well characterized. For example, in studies of amide hydrogen exchange in proteins, a decrease in exchange rate by 2 to 10 orders of magnitude compared to model compounds has been observed and attributed to stronger hydrogen

bonding of the amide hydrogen (e. g. in an α-helix structure) and/or the change in the accessibility of the amide to the solvent (Kim, 1986; Jeng and Englander, 1991; Englander and Mayne, 1992).

The stretching frequency of the protonated Schiff base, at 1657 cm^{-1} in rhodopsin and at 1640 cm^{-1} in bR, is easily observed in the resonance Raman spectroscopy of these pigments and undergoes a downward frequency shift of 32 and 16 cm^{-1}, respectively, upon deuteration. It is thus quite easy to determine the amount of either the protonated or deuterated form. The hydrogen-deuterium exchange rate of the retinal Schiff base in bR has been previously measured by continuous flow resonance Raman measurements (Ehrenberg *et al.*, 1980; Doukas *et al.*, 1981). A theoretical analysis of the results suggested that the experimentally determined exchange time, on the order of a few milliseconds or less and independent of pH, is three orders of magnitude faster than the hydroxyl catalyzed reaction and five orders of magnitude faster than the water catalyzed reaction (Doukas *et al.*, 1981). On the basis of this analysis, a new reaction mechanism was proposed for the hydrogen exchange reaction. This mechanism did not involve proton dissociation from the protonated Schiff base, but rather consisted of the direct exchange of a proton with a water molecule in a concerted reaction.

We have revisited this problem here. The time resolution of the exchange apparatus has been improved substantially so that we are now able to resolve the exchange time for bacteriorhodopsin. The exchange time of bovine rhodopsin as a function of pH has also been determined in order to explore its similarity or difference with bacteriorhodopsin. In addition, we have performed the hydrogen-deuterium exchange experiments on a Schiff base model compound which was sufficiently stable in aqueous solution so

that we could quantitatively compare its exchange reaction with that of the pigments.

III. MATERIALS AND METHODS

An aqueous suspension of bR was prepared as previously described (Becher and Cassim, 1975) and deuterated by centrifugation and resuspension in D_2O. The concentration of the sample was adjusted to about 4 OD at 570 nm. Before the exchange experiment, the bR sample was light-adapted with 568.2 nm laser light from a krypton ion laser for about half an hour. The initial pD of bR was about 6.5 (uncorrected pH meter reading); no buffer was used.

Bovine rhodopsin containing rod outer segment membranes were prepared (Papermaster and Dryer, 1973), and kept frozen at -60 °C. Just before the Raman experiments, the membranes were thawed and pelleted by centrifugation. The pellet was washed with D_2O once and then the rhodopsin solubilized with 10 mM of the detergent CHAPSO (Boerhinger Mannhaim Co., Indianapolis, IN) in D_2O. The concentration of the rhodopsin was about 4 OD at 500 nm. The pD of the rhodopsin sample was 6.5 (uncorrected pH meter reading) in the unbuffered solution.

The deuterated Schiff base model compound, 3-methyl-2-butene butylamine, ($CH_3C(CH_3)$=CH-CH=NH^+-$CH_2CH_2CH_2CH_3$), was prepared as follows. 2.5 ml 3-methyl-2-butenal (Sigma Chemical Co., St. Louis, MO) and 2.8 ml butylamine (Sigma) were mixed on ice. The reaction mixture, mostly unprotonated Schiff base, was then dissolved in 25 ml n-hexane, followed by centrifugation to remove the water formed in the reaction. After 2.5 ml of a 37% aqueous DCl solution was added to the unprotonated Schiff base in hexane on ice, the mixture was shaken vigorously for a few minutes. The

deuterated Schiff base, separated from hexane by centrifugation, was diluted by D_2O to a final volume of about 40 ml and its pD adjusted by NaOD to about 2.5 (uncorrected pH meter reading). The Schiff base hydrolyzed slowly to aldehyde at a rate of about 5-10% per hour under these conditions. The time required for the D-H exchange experiment was about 2-3 hours, so up to 25% of the Schiff base could have hydrolyzed by the end of the experiment.

A mixing chamber was constructed with two jets meeting at a small angle (about 15°), and the mixed sample exited through a 0.5 mm diameter glass capillary at a flow rate of 60 ml/min. The dead time of the flow apparatus, 0.9 ms ±0.3, was calculated from the measured flow rate and the volume of the flow cell. This dead time was verified by following the reaction of potassium ferricyanide with ascorbic acid at pH 8 ($t_{1/2}$ = 6.5 ms; Tonomura *et al.*, 1987), and by the reduction of 2,6-dichlorophenalindophenol with ascorbic acid at pH 3 ($t_{1/2}$ = 0.65 ms; Tonomura *et al.*, 1987). The error in the delay time was mainly from the fluctuation of the pump flow rate because the experiments allow only a short stabilization time after initiating the mixing, due to sample limitations. Therefore, estimated error at longer delay times was about 10%, rather than a fixed time.

Continuous flow experiments were carried out by mixing the deuterated pigments or model compound with 20 fold aqueous solution. For bR, the pD value was always kept at 6.5 (uncorrected pH meter reading), but the water pH was adjusted to 2.5, 6.5 or 10.5 in the three sets of D-H exchange experiments for bR. In the pH 6.5 experiment, distilled water was used. In the pH jump experiments from pD 6.5 to pH 2.5 and pH 10.5, 1M NaCl was added to the water to stabilize the pH after mixing. In the D-H exchange experiments with rhodopsin, the pD value of rhodopsin was kept at pD 6.5 (uncorrected pH meter reading), and a dilute phosphate buffer (1 mM) was

used to stabilize the pH at 3 or 7, in two separate exchange experiments. The following were used as the aqueous mixing solutions in the D-H exchange experiments of the Schiff base model compound: 1M HCl; 0.1M HCl; 10 mM NaCl at pH 2; 10 mM phosphate buffer at pH 2; 10 mM NaCl at pH 3; 10 mM phosphate buffer at pH 3; 10 mM formate at pH 4; 10 mM acetate at pH 5; 10 mM phosphate at pH 6 and pH 6.5.

The resonance Raman spectra of bacteriorhodopsin were measured with a 530.1 nm line from a krypton ion laser at a power level of 40 mW, and those of rhodopsin were measured with 488.0 nm line from an argon ion laser at the same power level. A cylindrical lens was used to focus the laser beam onto the sample so that more laser power could be used to enhance the Raman signal without introducing too much sample photolysis. Under these conditions, less than 15% of the bacteriorhodopsin or rhodopsin undergoes photolysis (Callender *et al.*, 1976). The Raman spectrum of the protonated Schiff base model compound was measured with 514.5 nm line from an argon laser at a power level of 200-300 mW. All experiments were conducted at room temperature.

The Raman spectra were taken with an optical multichannel analyzer (OMA) system consisting of a triplemate spectrometer (Spex Industries, Metuchen, NJ), a model DIDA-1000 reticon detector connected to a ST-100 detector controller (Princeton Instruments, Trenton, NJ), which was interfaced to a MAC II computer (Apple Computer, Cupertino, CA). With the above laser excitation wavelengths, a spectral window of about 1000 cm^{-1} with resolution of 8 cm^{-1} could be detected. The Raman band positions were calibrated against the known Raman peaks of toluene and are accurate to ±2 cm^{-1}.

IV. RESULTS

Bacteriorhodopsin. Resonance Raman spectra of deuterated bacteriorhodopsin (Figure 2.1) were obtained at various delay times after mixing with a 20-fold excess H_2O at pH 6.5. Also shown in Figure 2.1 are bacteriorhodopsin spectra in D_2O and H_2O, respectively. The intensity of the protonated Schiff base, $C{=}NH^+$, stretch mode at 1640 cm^{-1} increases with delay time while the deuterated, 1624 cm^{-1}, $C{=}ND^+$, stretch band decreases with delay time. Since there was a 20-fold excess of H_2O over D_2O after mixing, the D-H exchange reaction should depend little on the concentration of water. We assume below that the reactions approximately follow first order reaction kinetics. At a delay time, t, after mixing, the intensity, I(t), of the protonated Schiff base C=N stretch band at 1640 cm^{-1} and the deuterated Schiff base C=N stretch band at 1624 cm^{-1} can then be expressed by the following two equations:

$$I_{1640}(t) = I_{1640}(1 - e^{-kt}) \tag{1}$$

and

$$I_{1624}(t) = I_{1624} \bullet e^{-kt} \tag{2}$$

The maximum intensities, I_{1640} and I_{1624}, are obtained from the spectra of bacteriorhodopsin in H_2O and D_2O, respectively. Taking the ratio of $I_{1640}(t)$ and $I_{1624}(t)$, it can be shown that:

$$\ln[\frac{I_{1624} \bullet I_{1640}(t)}{I_{1640} \bullet I_{1624}(t)} + 1] = kt \tag{3}$$

Figure 2.2 shows a plot of the left hand side of eq. 3 versus t. The biggest problem with determining the accuracy of the peak intensities has to do with the determination of the background levels. All the spectra contain a sloping background. This has been removed by approximating the background as a straight line and assuming that the Raman intensity is zero at 1470 and 1720 cm^{-1}. The latter value is perfectly justified since it is known that no Raman intensity (apart from very small overtone bands) lies in this region (see e.g. Callender *et al.*, 1976; Aton *et al.*, 1977). There is no Raman structure at or near 1470 cm^{-1} as well so this value seems well justified as well. In addition, the accuracy of each data point has been improved by comparing each spectrum in Figure 2.1 with a series of resonance Raman spectra of bacteriorhodopsin in solution with different D_2O/H_2O ratios, which were measured in separate experiments. These controls employed the same samples so that their backgrounds are the same as those found in the kinetic measurements. Thus, only a matching of the relative peak heights of a particular kinetic experiment with the control series is needed, and this minimizes the problem of ambiguity of the position of the background. Using a non-linear least square fitting procedure, these data are adequately fit to a linear function, which has been plotted in Figure 2.2. However, the data points in Figure 2.2 appear to deviate from first order kinetics at the later time points. A fit to a second-order function also yielded satisfactory results, but the errors in the data points are such that it is not possible to determine whether the kinetics are first or second order (note estimated error bars in the Figure). The ambiguity in the value of the background is the essential determinant in the error in the data points along the y axis. The accuracy of the data points along the x-axis in the plot is limited by the fluctuations in pump velocity (see Methods) yielding a $\pm$ (0.3 + (t - 1)•10%) ms of the time

value. The rates quoted below arise from calculating the slope of the best straight line fitted to the data of Figure 2.2. Values of $t_{1/2}$ can be calculated from this rate. Also, $t_{1/2}$ is the time at which half exchange occurs and this can be also determined from a comparison of the series of kinetic runs (Figure 2.1) with the spectrum of bacteriorhodopsin in a 50-50 mixture of H_2O and D_2O in a steady state measurement. Since the baseline is the same for the kinetic runs and the steady state run, a comparison only of relative peak heights in the raw spectra is required. We estimate that the accuracy of the half-times obtained in this way is probably more accurate than that obtained from the calculated rate, and is limited by the uncertainty in the pump flow rate. In any case, the $t_{1/2}$ values obtained from either method agree within our estimated errors.

The first order exchange reaction rate thus obtained was k=530 s^{-1}, and a half time of $t_{1/2}$ = 1.3 (±0.3) ms. A similar analysis, performed on data obtained in D-H exchange experiments with a pH jump from either pD 6.5 to pH 2.5 or to pH 10.5, yielded exchange rate constants of 460 s^{-1} ($t_{1/2}$=1.5±0.4 ms) and 440 s^{-1} (1.6±0.4 ms), respectively. Therefore, there is no obvious pH dependence of D-H exchange rate of the retinal Schiff base hydrogen in bR.

The pH independent nature of the D-H exchange reaction in bR has been observed previously (Ehrenberg *et al.*, 1980; Doukas *et al.*, 1981). The reaction time constant obtained here is consistent with the latter (who reported kinetics had $t_{1/2}$ less than 3.0 ms, the instrument deadtime in that report) but is about 3 times faster than the former (who reported a $t_{1/2}$=4.7 ms exchange time). We found that under conditions favoring protein aggregation (very high salt concentration and/or repeated usage of the sample) the D-H exchange time was slowed by about 2 to 4 times (data not shown).

Rhodopsin. Figure 2.3 shows the resonance Raman spectra of rhodopsin in D_2O at various delay times after mixing with 1 mM phosphate buffer at pH 3. The band at 1657 cm^{-1} and at 1625 cm^{-1} have been assigned to the protonated and deuterated Schiff base C=N stretch mode, respectively. As in the D-H exchange experiments of bR, the intensity of the 1657 cm^{-1} band increases, and that of the 1625 cm^{-1} band decreases with the delay time. A similar analysis as that used for bacteriorhodopsin is shown in Figure 2.4 and yields a pseudo first order reaction rate of k= 120 s^{-1} ($t_{1/2}$ = 5.8±0.8 ms) at pH 3 and k=100 s^{-1} ($t_{1/2}$ = 6.9±0.9) ms at pH 6.5. Thus, the kinetics, like those of bacteriorhodopsin, show no pH dependence over this range.

Model Schiff Base. Retinal Schiff bases would be the ideal model; however, these are quite unstable in aqueous solution (hydrolyzing very fast to the aldehyde). Therefore, we have turned to measurement of 3-methyl-2-butene butylamine, which is just stable enough for measurement. The chemistry of this compound is very similar to that of a retinal Schiff base, being a polyene joined to an alkane group via the -C=NH^+- linkage. Most important, the pK_a of 3-methyl-2-butene butylamine and a retinal Schiff base are virtually the same (Favrot *et al.*, 1978; see below). In Figure 2.5, Raman spectra taken of 3-methyl-2-butene butylamine in D_2O are shown at various delay times after mixing with H_2O. In series A, the deuterated Schiff base in D_2O was mixed with a 20 fold excess of 10 mM phosphate buffer at pH 3. In series B, the same sample was mixed with 20 fold excess 10 mM NaCl at pH 3. Up to three bands are observed in these spectra. The spectrum in H_2O contains the protonated Schiff base band, C=NH^+ stretch, at 1672 cm^{-1} (top spectrum of panels A and B) and also contains a band at 1629 cm^{-1} which can be assigned to the butene C=C stretch. The spectrum in D_2O is dominated by the in-phase combination of the C=C and C=ND^+ stretches at 1647 cm^{-1}

(bottom spectrum of panels A and B). The delay time spectra, however, are also complicated by the presence of hydrolyzed aldehyde product, 3-methyl-2-butenal, whose spectrum contains strong bands at 1630 and 1650 cm^{-1} (data not shown). We have estimated that up to 25% of the model protonated Schiff base may form hydrolyzed product within the two to three hour time period required to obtain the delay time data (see Materials). Therefore, in the Raman spectra taken after mixing, the band intensity at 1647 cm^{-1} is significantly higher than the expected C=N stretch band intensity. After correction for this artifact, the data was analyzed as above, and the exchange time as a function of pH is plotted in Figure 2.6.

It is evident from the data in Figure 2.5, by comparing the data in series A (with buffer) with the no buffer conditions of series B, that the D-H exchange reaction of the Schiff base model compound was not affected significantly by the presence of buffer at pH 3.0. Similar results were found for measurements performed for pH values less than 3.5. However, the pH of the mixed sample could not be reproducibly measured when the buffer concentration was lower than 10 mM at pH higher than 3.5. We believe that the observed exchange rate for pH>3.5 likely contains a component of buffer catalysis (see below).

The three standard mechanisms for hydrogen exchange involve acid, base or water catalyzed reactions. Thus, the pH dependent total exchange reaction rate k, can be expressed by the following equation:

$$k=k_H[H^+] + k_{OH}[OH^-] + k_w [H_2O] \quad (4)$$

where k_H and k_{OH} are the second order acid and base catalyzed exchange rate constant, respectively. $k'_w = k_w [H_2O]$ is the water catalyzed exchange rate and is independent of pH. Buffer in general may also contribute to the exchange

reaction (cf. Eigen, 1964; Englander *et al.*, 1972). Fitting the data in Figure 2.6 to equation (4) yields: $k_{OH} = 1.1 \bullet 10^{12}$ $M^{-1}s^{-1}$ and $k'_w = 43$ s^{-1}; k_H is negligible in the pH range of our study. A general expression to estimate the second order rate constants, $k_{(H, OH, w)}$ on the right side of equation (4) is given by the following equation (Englander *et al.*, 1972):

$$k_{(H, OH, w)} = k_r [10^{\Delta pK_s}/(10^{\Delta pK_s} +1)] \quad (5)$$

where ΔpKs is equal to the pKa of proton acceptor (e.g. OH^-) minus that of proton donor (e.g. the Schiff base). The recombination rate constant, k_r (see Scheme 2.1), is limited to the maximum diffusion rate, which is of the order of 10^{10}-10^{11} $M^{-1}s^{-1}$ (Eigen, 1964). The pKa of our Schiff base model compound is about 7 (Favrot *et al.*, 1978), very close to that of retinal Schiff bases (Sheves *et al.*, 1986). Using this and $pK_a(H_2O) = -1.7$ and $pK_a(OH^-) = 15.7$ and the limiting value of $k_r < 10^{10}$-10^{11} $M^{-1}s^{-1}$, we find that k'_w and k_{OH} are constrained so $k'_w < 10^3$-10^4 s^{-1} and $k_{OH} < 10^{10}$-10^{11} $M^{-1}s^{-1}$. The observed k'_w of 43 s^{-1} is well below this upper limit and therefore consistent with the conventional reaction mechanism. However, the experimentally derived value of $k_{OH}=1.1 \bullet 10^{12}$, is one to two orders of magnitude higher than the estimated limit. For this reason, we believe that the observed exchange rate in Figure 2.6 above pH 3.5 may have a contribution from buffer catalysis and that this effect is masking the true value of k_{OH}.

V. DISCUSSION

The measured H-D exchange time constants for bacteriorhodopsin ($t_{1/2}$ = 1.3±0.3 ms) and for rhodopsin ($t_{1/2}$ = 6.9±0.9 ms) are very fast, and the rates are essentially independent of pH over the range of our measurements. As we have shown previously for bacteriorhodopsin (Doukas *et al.*, 1981), these

fast exchange times cannot be explained using standard base catalyzed mechanisms involving either OH^- or the general base H_2O (see Scheme 2.1). An upper bound on the OH^- catalyzed reaction rate is given by $k_{OH^-} = k_r[OH^-]$, where the recombination rate is limited by diffusional encounters with the protonated Schiff base, i.e. $k_r < 10^{10}$-10^{11} $M^{-1}s^{-1}$ (Eigen, 1964). At pH 3, the lowest pH studied for rhodopsin, and at pH 2.5, the lowest value for the bacteriorhodopsin experiments, the use of the diffusion controlled upper bound for k_r yields an exchange time no faster than 1-10 s, some three orders of magnitude slower than the observed rates in the two proteins. Moreover, a OH^- catalyzed reaction is pH dependent while that observed for the two pigments is not. Thus neither rhodopsin's nor bacteriorhodopsin's Schiff base exchange reaction is base (or acid) catalyzed.

Although the standard mechanism for a water catalyzed reaction is pH independent, it can also be excluded. In this case, Eq. 5 collapses to the familiar form of a pseudo first order deprotonation rate, $k'_w=k_w[H_2O]$, as given by $k'_w=k_r10^{-pKa}$. Again an upper limit of k'_w can be determined once the pKa of the Schiff base is known by taking a diffusion rate limiting value for k_r. The pKa of the Schiff base, as complexed in the retinal binding site of the two proteins, is 13.5 for bacteriorhodopsin (Druckmann *et al.*, 1982; Sheves *et al.*, 1986) and may be as high as 17 in rhodopsin (Steinberg *et al.*, 1993). Using a pKa value of 13.5 and $k_r < 10^{10}$-10^{11} $M^{-1}s^{-1}$, then $k'_w < 3x10^{-3}$ s^{-1} or $t_{1/2}$ >230 s. The observed exchange time is five orders of magnitude faster than this estimated upper limit. And the use of the pK_a appropriate for rhodopsin obviously yields an even slower upper limit of the exchange time, on the order of 10^{-5} or less, or $t_{1/2} > 7x10^4$ s. On the other hand, similar analysis of the model Schiff base yield an upper limit of the water catalyzed exchange rate of 10^3 s^{-1} , entirely consistent with the observed value, which is

43 s^{-1} . We therefore conclude that neither hydroxyl nor water based catalyzed reactions can explain the fast exchange times observed for the Schiff base proton in bacteriorhodopsin and rhodopsin.

We emphasize that at pH 2-3, the hydrogen exchange rate in rhodopsin (120 s^{-1}) and bR (460 s^{-1}) is higher than that of the model compound at the same pH (43 s^{-1}), where the water based catalysis dominates the exchange in solution. This observation is in clear contrast with all previous studies on the exchange of protein amide hydrogens. Compared to model amides, it was found that the amide hydrogen exchange rate in proteins can be delayed substantially by hydrogen bonding (Kim, 1986; Englander and Mayne, 1992,Jeng and Englander, 1991) or virtually eliminated by a hydrophobic pocket (Maeda *et al.*, 1992). The real enhancement of the Schiff base deuteron exchange with water in these two pigments must be enormous because it has not only overcome the delays caused by possible protein dependent mechanisms, but also the unfavorable pKa increase of the Schiff base.

A plausible explanation for the rate enhancement of the Schiff base H-D exchange in rhodopsin and bR is that there is a water molecule next to the Schiff base hydrogen which is well oriented and positioned for the reaction. The rate acceleration induced by the proper positioning of the reactants should be similar to that observed in a monomolecular enzymatic or intermolecular reaction compared to a bimolecular reaction. In bimolecular reactions, the transition state of the reaction is necessarily monomolecular, therefore three translational and up to three rotational degrees of freedom are lost, which corresponds to a large entropy loss and contributes to the transition barrier of the reaction in solution. However, when the reactants are bound together by an enzyme or joined by a chemical bond before the reaction occurs, the entropy loss will not contribute to the transition barrier of

the reaction (but to a barrier of a non rate limiting step, such as the diffusion of the water molecule to the Schiff base in rhodopsin or bR) and substantial rate enhancements can then be achieved (Page and Jencks, 1971). It has been shown that such entropic effects can contribute to a rate enhancement of up to $10^{6.5}$ (cf. Page and Jencks, 1971).

The proposed water molecule can be constrained to the proper position by hydrogen bonding to protein residues and/or to the retinal Schiff base. A number of studies point towards to the conclusion, with more or less certainty, that a water molecule or molecules are at the binding site of rhodopsin and bacteriorhodopsin, some suggesting that the putative water molecule is hydrogen bonded directly to the protonated Schiff base linkage. For example, rhodopsin (Rafferty and Schchi, 1981) and bacteriorhodopsin (Hildebrandt and Stockburger, 1984) have been shown to undergo substantial changes in their respective absorption maxima upon dehydration; for both pigments the changes in absorption maxima are fully reversible upon rehydration. Since the position of the absorption maxima of these proteins is quite sensitive to the binding arrangement at the protonated Schiff base linkage, varying strongly with the nature of the hydrogen bond of the apoprotein to the Schiff base proton and with nearby charges, such behavior has been taken to suggest that water forms part of the structure of the binding site. Birge and co-workers have performed extensive semi-empirical and quantum mechanical calculations modeling the results of two photon spectroscopy (Birge and Zhang, 1990) and kinetics of the primary photophysical event of these pigments (Birge *et al.*, 1988; Birge, 1990). In order to satisfactorily model these results and a number of the spectroscopic properties of the binding site, they have found it necessary to place a water molecule at the binding site, hydrogen bonded to the Schiff base proton.

Finally, the position of the protonated Schiff base, C=NH^+ stretch, frequency and its change upon deuteration of the pigment and the Schiff base suggest that a water molecule interacts strongly with the protonated Schiff base. In bacteriorhodopsin, the width of the observed C=NH^+ stretch is relatively broad for this band and narrows considerably upon deuteration of the protein (see e.g. Figure 2.1). This was interpreted by Hildebrandt and Stockburger (Hildebrandt and Stockburger, 1984) as arising from a vibrational energy exchange transfer between the C=NH^+ stretch, which lies at 1641 cm^{-1}, and the bending mode of H_2O, which lies at 1635 cm^{-1}. This coupling is largely abolished when H_2O is replaced by D_2O since the D_2O bend lies at 1205 cm^{-1}. This type of coupling is a short range effect so that this analysis places a water molecule very close to the protonated Schiff base. In rhodopsin, the shift in frequency between the protonated C=NH^+ stretch and the deuterated C=NH^+ stretch, some 32 cm^{-1}, is generally believed to imply a strong hydrogen bond to the imine proton of the protonated Schiff base (Bagley *et al.*, 1985; Deng and Callender, 1987; Palings *et al.*, 1987). What is unusual is that this large isotope shift decreases either very slightly or not at all upon the photochemical formation of the primary photoproduct, bathorhodopsin. This suggests that the strength of the hydrogen bond is largely unaffected despite the photo-isomerization of the bound retinal chromophore that takes place in the rhodopsin (an 11-*cis* chromophore) to bathorhodopsin (a trans chromophore) transformation. This despite the fact that the photoisomerization would cleave a putative salt bridge between the protonated Schiff base and a negative counter-ion and despite the rather large red shift in absorption maximum that distinguishes bathorhodopsin from rhodopsin. One way of explaining such results is that a water molecule is hydrogen bonded between the Schiff base and its counter-ion in rhodopsin and that this molecule and its hydrogen

bond follows the retinal chromophore during photoisomerization (Deng and Callender, 1987; Birge *et al.*, 1988).

Assuming that a water molecule is at the binding site of the two pigments and hydrogen bonded to the Schiff base imine proton, the rate of H-D exchange can be cast as the sum of two physically distinct steps. The first is the rate of diffusion of water to the Schiff base site and binding of this water molecule to the proper position. The second step is the rate at which hydrogens of the structural water molecule exchange with the Schiff base hydrogen. Our current results can not distinguish which of the two steps is rate limiting, although there is some hint that the diffusion of the water molecule to the Schiff base may be rate limiting due to the fact that the exchange time in bacteriorhodopsin slows down somewhat under experimental conditions where the protein aggregates. However, more experiments, such as kinetic isotope effect of the hydrogen exchange experiments, are needed for such a conclusion.

Finally, the exchange results of this work bear on recent titration studies of rhodopsin which suggest that the pK_a of the protonated Schiff base linkage in rhodopsin is greater than 17 (Steinberg *et al.*, 1993). Given that the pK_a of model retinal Schiff bases are around 7 in solution, an increase of 10 pH units is a remarkable if not a spectacular result. However, the analysis of the titration studies assumed explicitly that the binding site is accessible to water. Clearly, the results presented here show that the Schiff base binding site is quite accessible to aqueous solvent. In fact, if the molecular model presented here is correct, the diffusion of water to the Schiff base binding site in rhodopsin and bacteriorhodopsin occurs on the millisecond time scale (or faster).

This work is supported by grants from the National Institutes of Health (EYO3142 to RC and EYO1323 and to TE) and the Department of Energy (DE-FG02-88ER13948 to TE), and this support is gratefully acknowledged.

Figure 2.1: Resonance Raman spectra of bR at various delay times after mixing the bR sample in D_2O with 20 fold excess of H_2O at pH 6.5. The spectra of bR in H_2O and D_2O are also shown for comparison. The spectra were obtained with 530.1 nm laser line from a krypton laser at a power level of 40 mW; a cylindrical lens was used to reduce sample photolysis while maintaining efficient Raman scattering. The spectra had a resolution of 8 cm^{-1}.

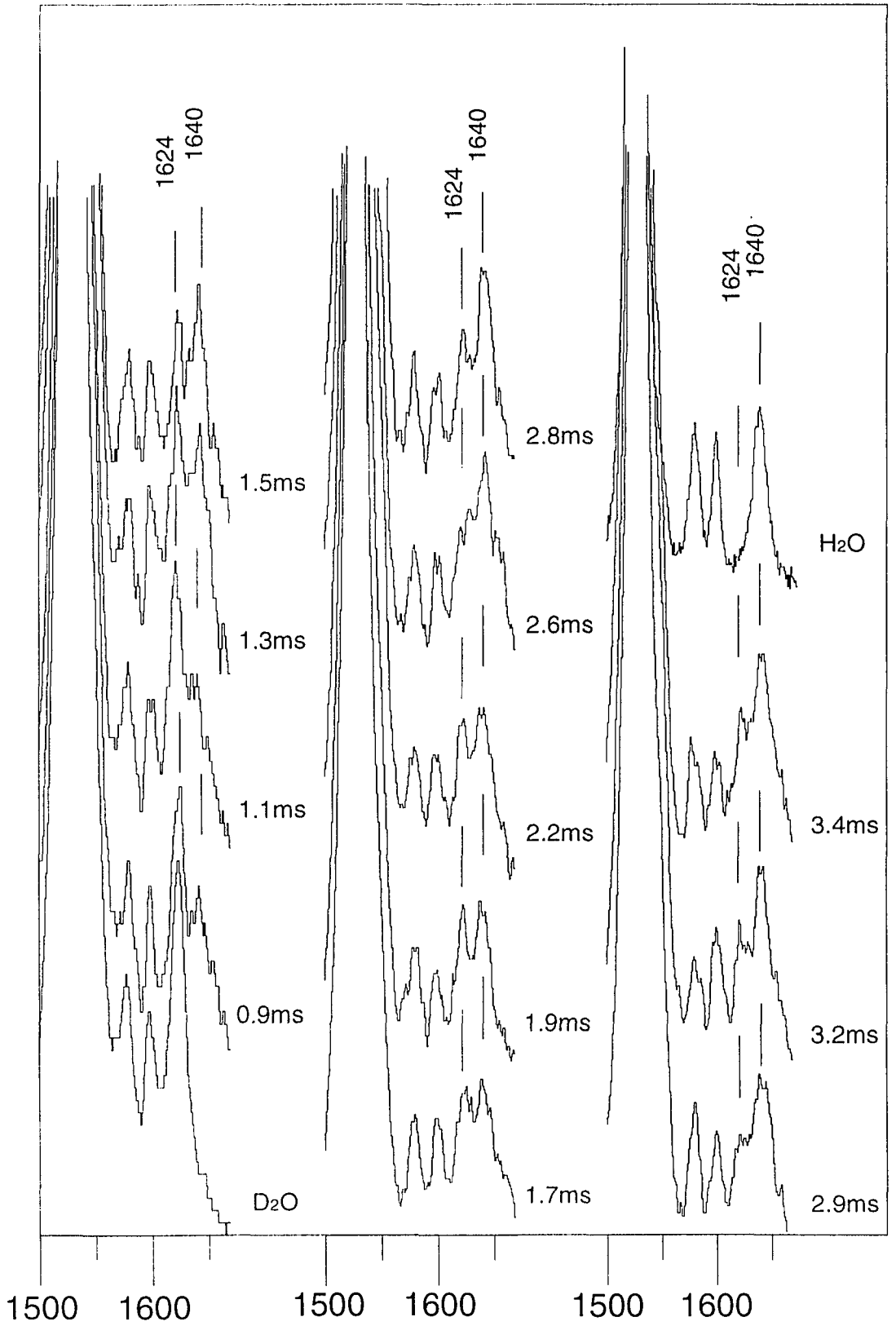
1624
1640
1.5ms
1.3ms
1.1ms
0.9ms
D2O
2.8ms
2.6ms
2.2ms
1.9ms
1.7ms
H2O
3.4ms
3.2ms
2.9ms
1500
1600
1500
1600
1500
1600

Figure 2.2: Kinetic plot of the deuterium-hydrogen exchange of the Schiff base nitrogen of bacteriorhodopsin with a jump from pD 6.5 to pH 6.5 (solid circle), to pH 2. 5 (open square), and to pH 10.5 (open circle). The straight line is a linear fit of the data obtained at pH 6.5. I_{1640} and I_{1624} are the band intensities (relative to the C=C stretching band intensities) of protonated and deuterated Schiff base, respectively, in the resonance Raman spectra of bR in H_2O and D_2O. $I_{1640}(t)$ and I_{1624} (t) are the band intensities of protonated and deuterated Schiff base of bR, respectively, as a function of time after mixing.

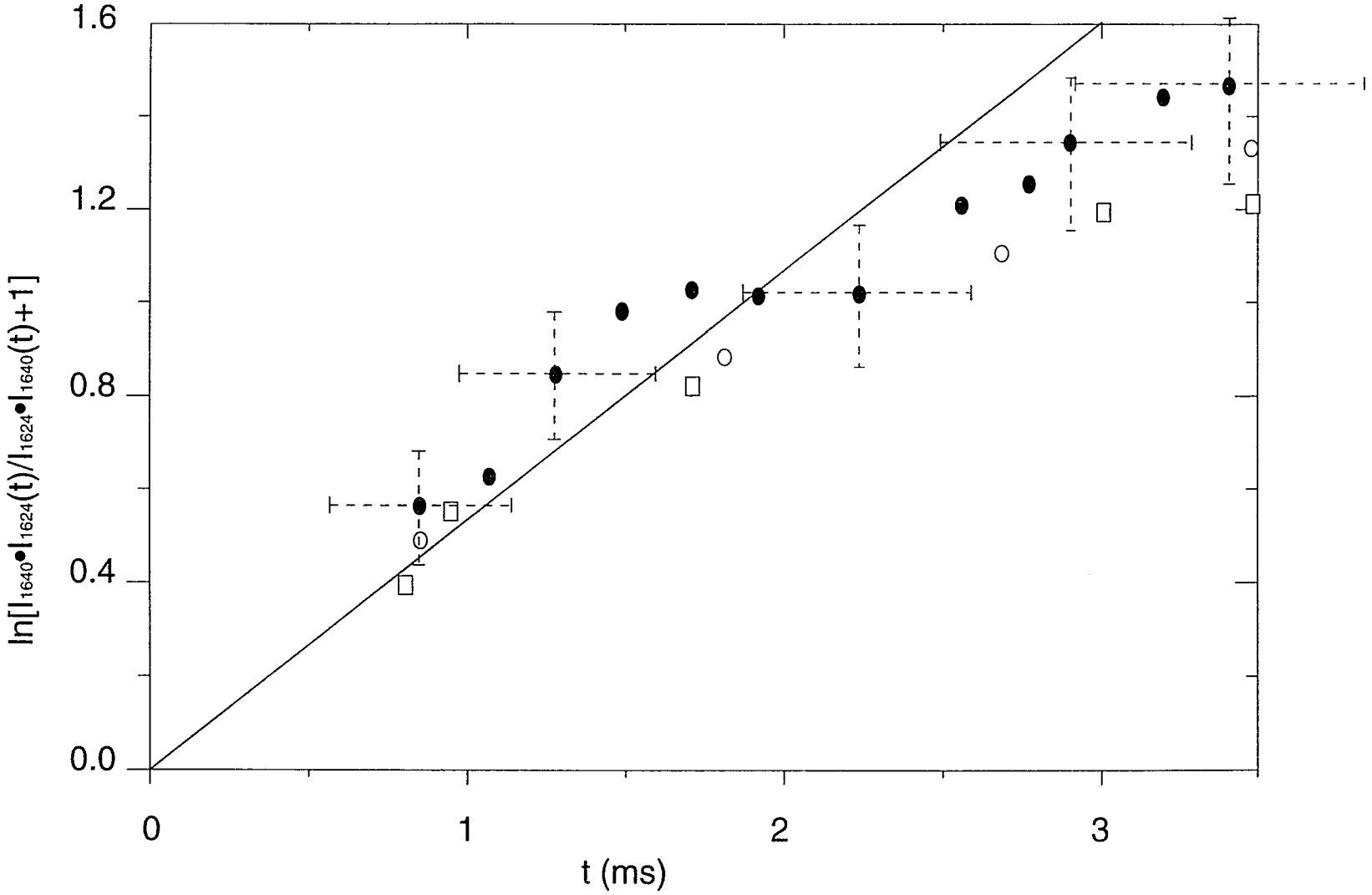
1.6
1.2
0.8
0.4
0.0
0
1
2
3
t (ms)
ln[I1640•I1624(t)/I1624•I1640(t)+1]

Figure 2.3: Resonance Raman spectra of rhodopsin at various delay times after mixing the rhodopsin sample in D_2O (dissolved with 10 mM CHAPSO) at pD 6.5 (pH meter reading) with 20 fold excess of H_2O at pH 3. The spectra of rhodopsin in H_2O and D_2 O are also shown for comparison. The spectra were obtained with 488.0 nm laser line from an argon laser at a power level of 40 mW; a cylindrical lens was used to reduce sample photolysis. The spectra had a resolution of 8 cm^{-1}.

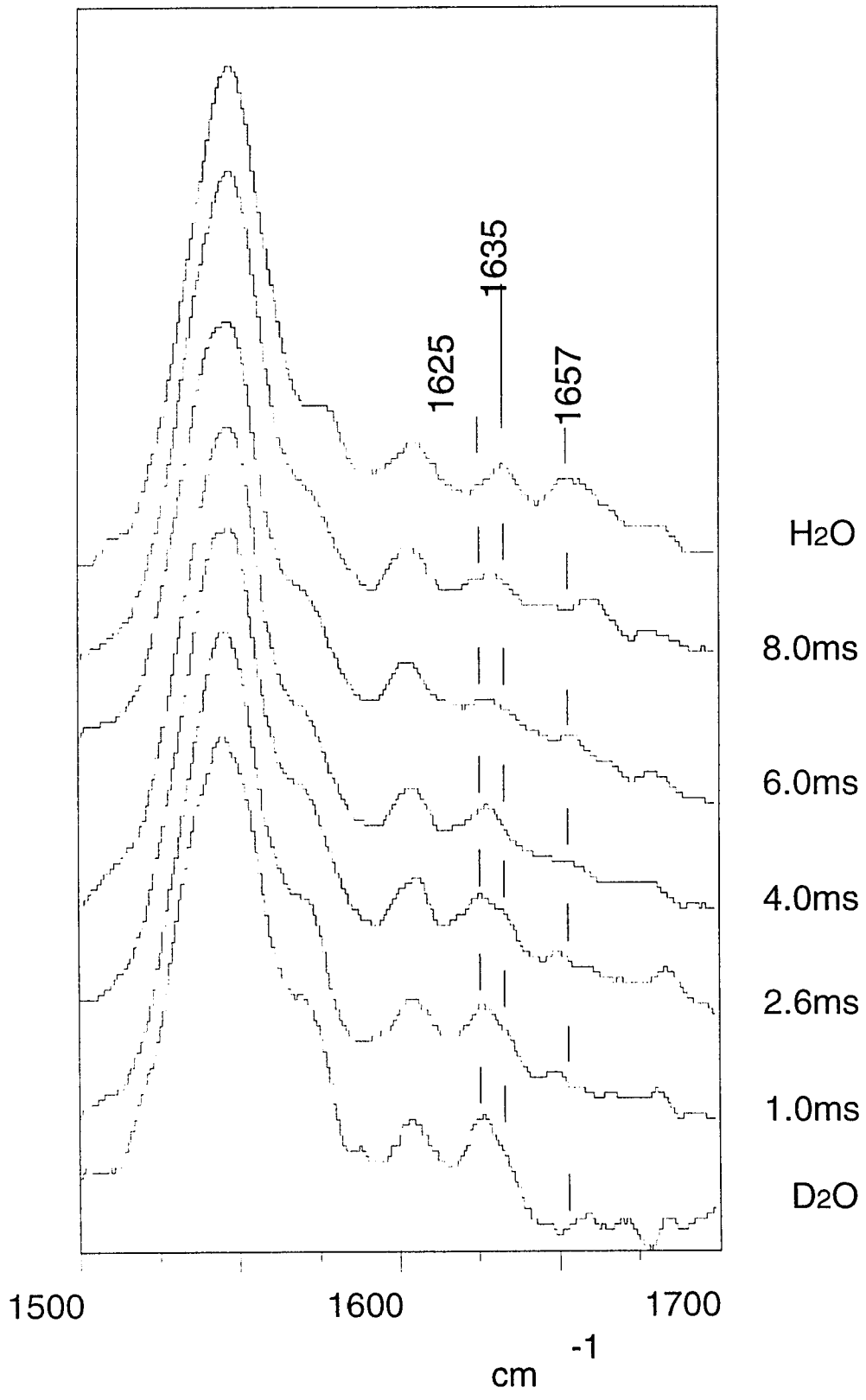
1625
1635
1657
H2O
8.0ms
6.0ms
4.0ms
2.6ms
1.0ms
D2O
1500
1600
1700
cm -1

Figure 2.4: Kinetic plot of the deuterium-hydrogen exchange of the Schiff base nitrogen of rhodopsin with the jump from pD=6.5 to pH 6.5 (solid circle), or to pH 3 (open square). The straight line is a linear fit of the data obtained at pH 6.5. I_{1657} and I_{1625} are the band intensities (relative to the C=C stretching band intensities) of protonated and deuterated Schiff base, respectively, in the resonance Raman spectra of rhodopsin in H_2O and D_2O. $I_{1657}(t)$ and $I_{1625}(t)$ are the band intensities of protonated and deuterated Schiff base of rhodopsin, respectively, as a function of time after mixing.

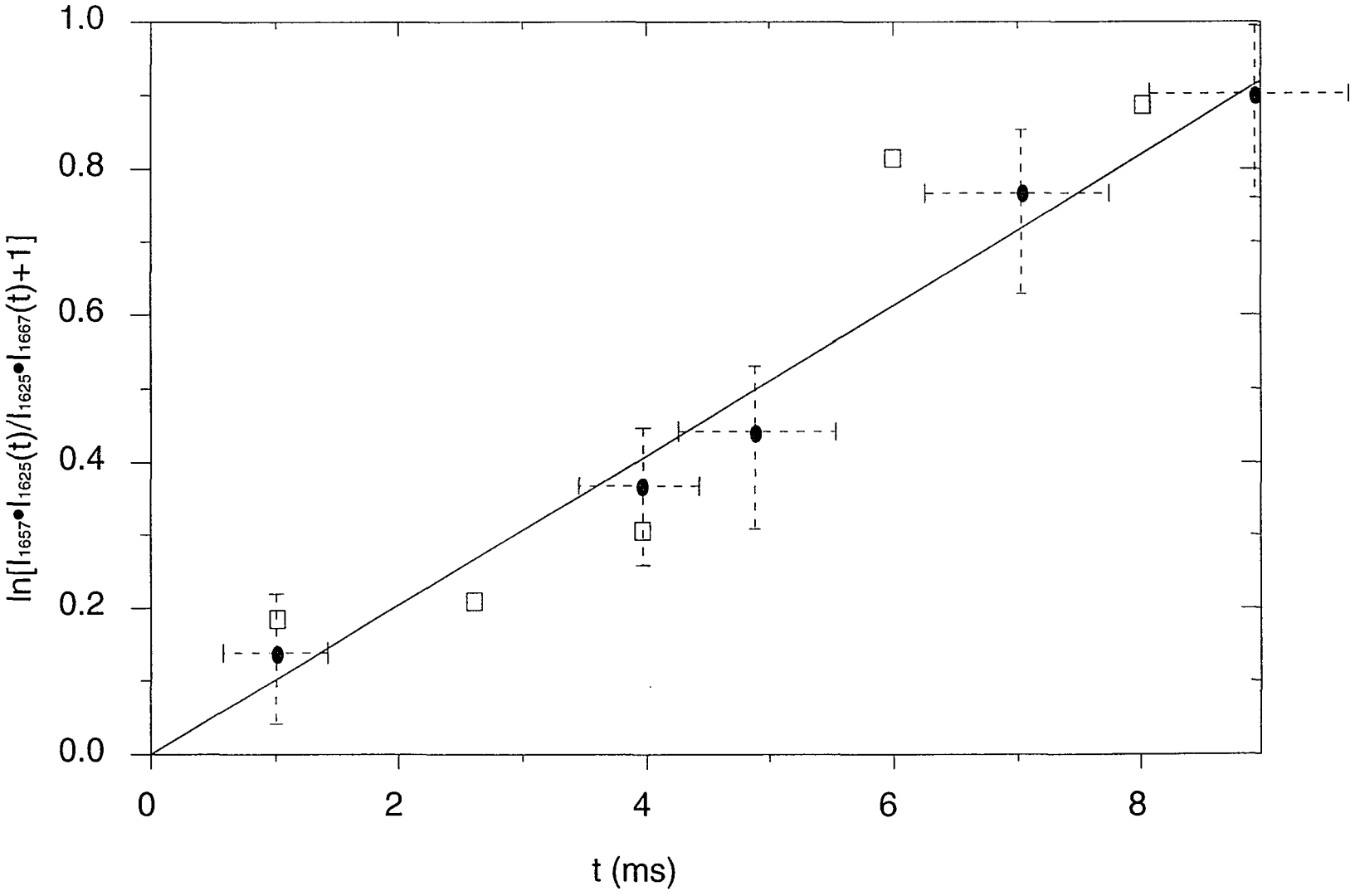
1.0
0.8
0.6
0.4
0.2
0.0
0
2
4
6
8
t (ms)
ln[I1657•I1625(t)/I1625•I1667(t)+1]

Figure 2.5: Raman spectra of Schiff base model compound (3-methyl-2-butene butylamine) at various delay times after mixing the Schiff base in D_2O at pD 2.5 (pH meter reading) with 20 fold excess of H_2O at pH 3 in the presence of 10 mM phosphate (series A) and 10 mM NaCl (series B), respectively. The spectra of the compound in H_2O and D_2O are also shown for comparison. The spectra were obtained with 514.5 nm laser line from an argon laser at a power level of 200 mW, with a resolution of 8 cm^{-1}.

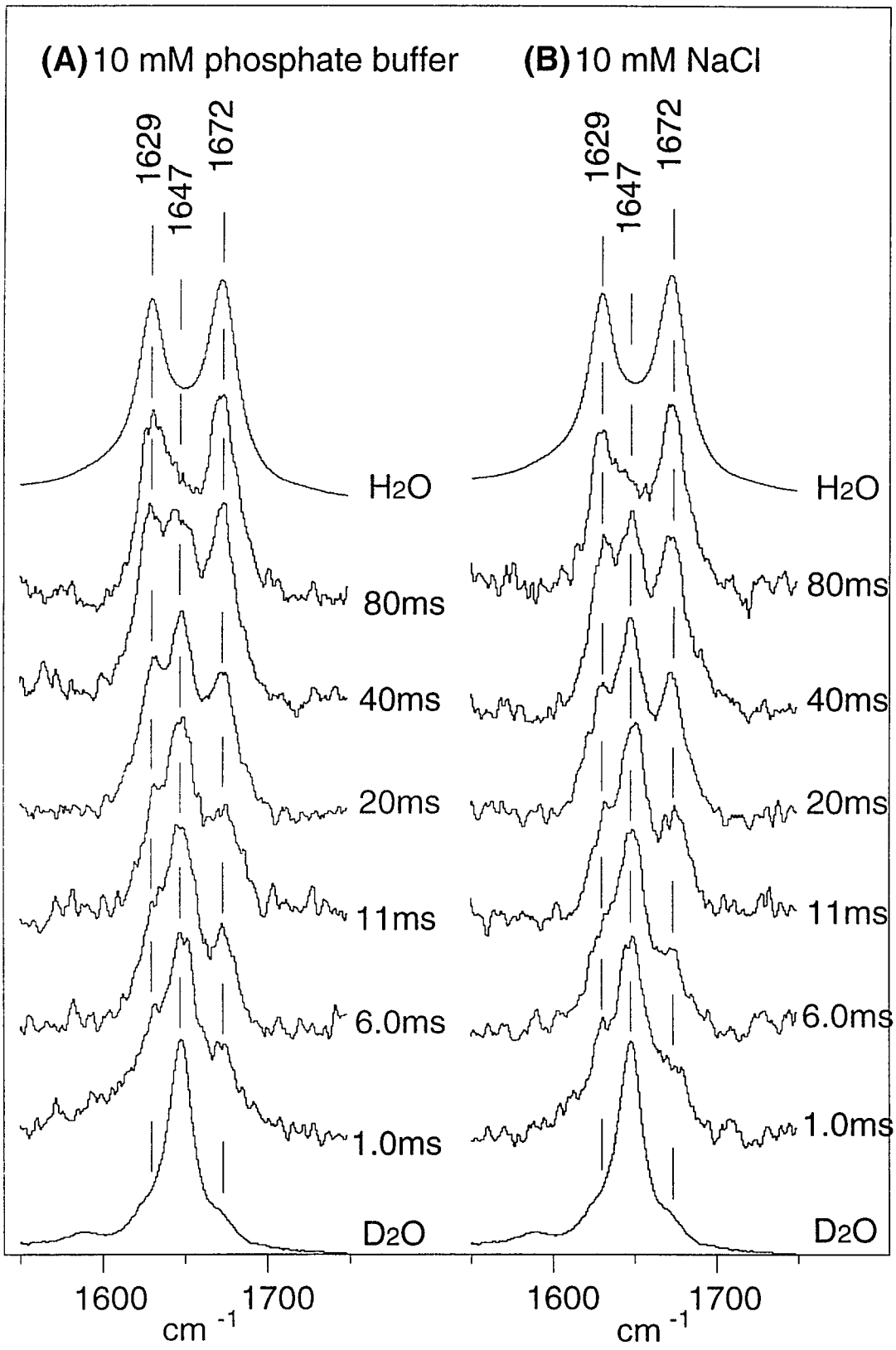
(A) 10 mM phosphate buffer
(B) 10 mM NaCl
1629
1647
1672
H2O
80ms
40ms
20ms
11ms
6.0ms
1.0ms
D2O
1600
1700
cm -1

Figure 2.6: The pH dependence of D-H exchange rate of the Schiff base model compound. The exchange rates (k) are obtained by the linear curve fitting procedure outlined in the legend of Figure 2.2 at various pHs (shown as solid circle). The line is a curve fit of equation 4 to the data points (less the pH = 0 point).

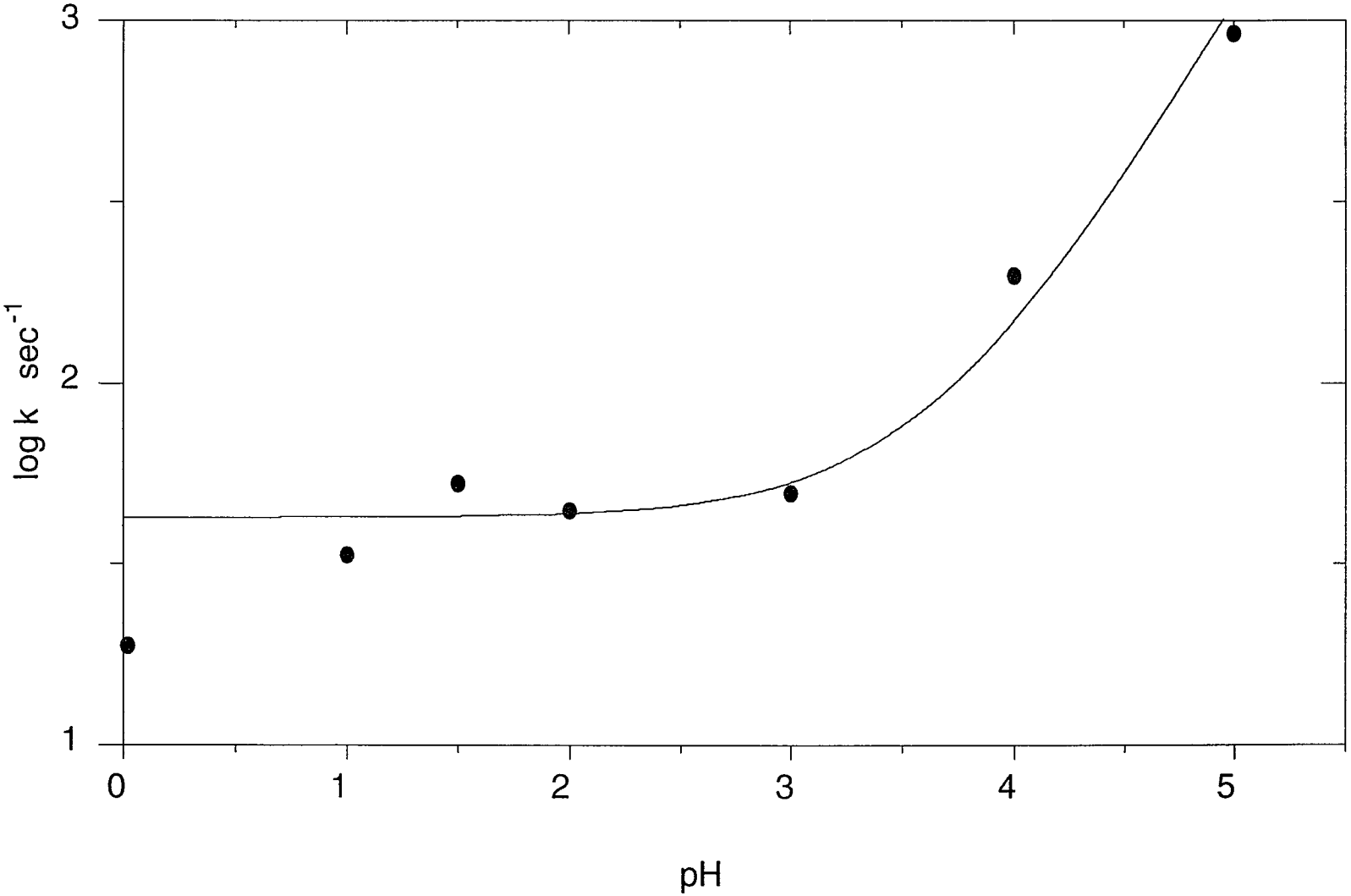
3
2
1
log k sec-1
0
1
2
3
4
5
pH

Chapter 3

VIBRATIONAL ANALYSIS OF A RETINAL PROTONATED SCHIFF BASE ANALOG*

I. ABSTRACT

A vibrational analysis of a retinal protonated Schiff base analog has been conducted by Raman measurements on this Schiff base and its isotopically labeled derivatives, and by calculations using *ab initio* methods. The calculated Raman spectra of the model and its isotopically labeled derivatives are in good agreement with the experimental data. Based on comparisons between the calculated Raman spectra of C=N *syn* and C=N *anti* Schiff base, a number of criteria to determine the Schiff base C=N configuration from Raman spectroscopy are developed. Two of these criteria have been previously proposed on the basis of empirical or semi-empirical calculations. The agreement between experiment and calculations suggests that *ab initio* methods are reliable enough to interpret the vibrational spectra of retinal protonated Schiff bases in various configurations and environments.

II. INTRODUCTION

---

* The content of this chapter has been published in the Journal of Physical Chemistry (Deng, H., L. Huang, M. Groesbeek, J. Lugtenburg, and R. H. Callender. (1994). Vibrational Analysis of a Retinal Protonated Schiff Base Analog. *JPC* **98**: 4776-4779)

Retinal isomerization reactions are functionally important in the proton pump cycle of bacteriorhodopsin (bR) and in the bleaching sequence of rhodopsin. Different models of retinal Schiff base isomerization reactions in rhodopsin and bR after absorbing a photon have been proposed (Warshel and Barboy, 1982; Liu and Asato, 1985; Tavan and Schulten, 1986; Fodor *et al.*, 1988a; Palings *et al.*, 1989; Grossjean *et al.*, 1990; Zhou *et al.*, 1993). For example, there are two suggestions on the configurational changes of the retinal Schiff base in bR upon absorbing a photon, one is from all-*trans* in bR to 13-*cis* in K, the first photoproduct, and other is from all-trans to 13,14-*dicis* (Fodor *et al.*, 1988a Zhou *et al.*, 1993). Interestingly, each of them appears to be consistent with certain experimental and theoretical studies. This is due to the fact that much of the experimental observation on the photoproduct of bR at the atomic scale are from vibrational spectroscopy, such as resonance Raman and FTIR, and theoretical analyses of the data have not achieved an agreed conclusion despite extensive vibrational analyses of the retinal Schiff base of a large amount of data from ^{13}C and deuterium labeled retinal Schiff bases, either free in solution or bound to pigments, which have been used to determine the conformation and double bond configuration of the retinal protonated Schiff base (RPSB) and its interactions with its protein environment (Smith *et al.*, 1984; Curry *et al.*, 1985; Smith *et al.*, 1985b; Tavan and Schulten, 1986; Deng and Callender, 1987; Smith *et al.*, 1987; Smith *et al.*, 1987; Fodor *et al.*, 1988a; Gilson *et al.*, 1988; Ames *et al.*, 1989; Palings *et al.*, 1989; Grossjean *et al.*, 1990; Cromwell *et al.*, 1992). Most analyses involve the use of Wilson FG method which relies heavily on empirical parameterization for each conformation or configuration of RPSB. Although this approach can provide the most accurate normal mode assignments to the vibrational spectrum of a Schiff base with a fixed configuration, it has rather limited value in predicting an unknown structure and/or external perturbation from a given

vibrational spectrum. Partly to overcome this limitation, semi-empirical quantum chemical methods, such as MINDO/3 and MNDO, have become more widely used (Tavan and Schulten, 1986; Fodor *et al.*, 1988a; Gilson *et al.*, 1988; Grossjean *et al.*, 1990; Cromwell *et al.*, 1992). These methods are capable of predicting values of force constants of a molecule with unknown structures and the changes of these force constants upon external perturbations. While the calculated normal modes, which can be evaluated by their frequencies and shifts upon isotopic labeling, are fairly good in some cases, they are rather poor in others, as has been shown before and will also be shown below.

In this paper, we probe the possibility of interpreting the vibrational spectra quantitatively by *ab initio* methods. This is done by performing *ab initio* and semi-empirical calculations on a protonated Schiff base (PSB) model compound (Scheme I; shown in the C=N *anti* configuration) with either C=N *anti* or C=N *syn* configuration and the accuracy of the theories is evaluated against Raman data of the model. This model is small enough so that calculations are feasible and yet retains many of the molecular features which, as a first step, allow the prediction of spectral changes with regard to the various configurations of RPSB. Besides, the configuration about the C=N bond of RPSB in pigments bears on a number of important pigment properties, including pigment color regulation and the dynamics and efficient conversion of light to chemical energy that occurs in the primary photophysical step (Smith *et al.*, 1984; Tavan and Schulten, 1986; Fodor *et al.*, 1988a; Ames *et al.*, 1989; Cromwell *et al.*, 1992; Livnah and Sheves, 1993). This is so because the charge distribution associated with the protonated Schiff base moiety and its environment is key to these issues (Honig *et al.*, 1979a; Honig *et al.*, 1979b; Birge, 1990). On the basis of our results, three experimental criteria are found which may be used as 'fingerprints' in the vibrational spectra of RPSB's for the C=N bond configuration. These criteria are

compared with those obtained in previous studies (Smith *et al.*, 1984; Smith *et al.*, 1987; Fodor *et al.*, 1988a; Ames *et al.*, 1989; Cromwell *et al.*, 1992; Livnah and Sheves, 1993).

III. RESULTS AND DISCUSSION

Figure 3.1 shows the Raman spectra of the PSB model and several isotopically labeled derivatives in aqueous solution. Most of the major bands observed in Figure 3.1A can be readily assigned on the basis of their isotopic shifts upon ^{13}C, ^{15}N or deuterium labeling. For example, the strong band at 1684 cm^{-1} is assigned to C=N stretch based on its 20 cm^{-1} shift when the Schiff base nitrogen is labeled by ^{15}N (Figure 3.1C). The 1632 cm^{-1} band, which is sensitive to the ^{13}C labeling (Figure 3.1E), but not to ^{15}N labeling (Figure 3.1C), is assigned to the C=C stretch mode. When the PSB nitrogen is deuterated, the C=N stretch mode at 1684 cm^{-1} shifts down to 1657 cm^{-1} due to its decoupling from the ND rock motion (Figure 3.1B). The 1497 cm^{-1} band in Figure 3.1A is assigned to the NH rock based on its disappearance upon Schiff base deuteration. The 1378 cm^{-1} band is very sensitive to the deuterium labeling on C_{15}, and thus can be assigned to the combination of $C_{14}H/C_{15}H$ rocks. In 15D labeled Schiff base spectrum (Figure 3.1G), the 979 cm^{-1} band is assigned to $C_{15}D$ rock, and the band at 1351 cm^{-1} is assigned to the $C_{14}H$ rock. Finally, the band at 1232 cm^{-1} can be assigned to the C_{14}-C_{15} stretch based on its 13 cm^{-1} shift when both C_{14} and C_{15} are labeled with ^{13}C (Figure 3.1E). It is interesting to note that upon Schiff base deuteration, this band apparently shifts up 15 cm^{-1} to 1247 cm^{-1} (Figure 3.1B), which also contains significant C_{14}-C_{15} stretch as shown by its 10 cm^{-1} shift in the spectrum of doubly ^{13}C labeled, deuterated Schiff base (Figure 3.1F).

Previous NMR studies on RPSB have shown that the chemical shift of the $C_{15}H$ proton is sensitive to C=N configuration: its chemical shift is >8.5 ppm

when C=N is *syn* and <8.5 ppm when C=N is *anti*. (Livnah and Sheves, 1993). The NMR spectrum of our PSB model compound in D_2O shows only one peak at 8.15 ppm in this region (data not shown). This indicates that PSB in aqueous solution has only one C=N configuration, and the $C_{15}H$ chemical shift suggests that the configuration is *anti*.

Figure 3.2 shows the calculated Raman spectra of fully optimized C=N *anti* PSB complexed with a chloride ion (Scheme I) at the *ab initio* HF/6-31g** level. Raman spectra of C=N *anti* PSB hydrogen bonded with a water molecule were also calculated (data not shown). It can be seen that the deviations of the calculated Raman frequencies are often significant from the experimental set (about 20 cm^{-1} after an uniform reduction of the frequencies by a factor of 0.9). On the other hand, the calculated isotopic shifts and Raman intensities of the major bands are in reasonable agreement with the experimental data. For example, the calculated shifts of C=N and C=C stretches upon ^{15}N; 14,15-^{13}C; and 15D labeling are all within 5 cm^{-1} or less of the observed shifts (Spectra A, C, E, G in Figure 3.1-2). The calculated C=N stretch shift upon nitrogen deuteration is 33 cm^{-1} (Figure 3.2B), which is somewhat larger than the observed 27 cm^{-1} shift (Figure 3.1B). This is because the calculation with the 6-31g** basis set over estimates the C=N stretch frequency more than the C=C stretch frequency so that the difference between C=N and C=C stretch is too large. Thus upon Schiff base deuteration, the calculated coupling between C=C and C=N stretches, which will push up the C=N stretch somewhat, is underestimated. In this particular case, better results were obtained with 3-21g basis set (data not shown). Our calculations also suggest that in the deuterated Schiff base, the C=N stretch couples strongly with C=C stretch to form a strongly Raman allowed in-phase mode and a weakly Raman allowed out-of-phase mode.

The calculations predict that the intense band at 1378 cm^{-1} in Figure 3.1A is the $C_{14}H/C_{15}H$ out of phase rocking mode. Upon 15D labeling, the $C_{14}H$ rock becomes slightly coupled with the NH rock according to our calculation, forming a mode at 1349 cm^{-1}, 36 cm^{-1} below the out of phase $C_{14}H/C_{15}H$ rock of the unlabeled Schiff base (compare Figure 3.2G with 2A). This $C_{14}H$ rock shifts up by 11 cm^{-1} upon additional deuteration of the Schiff base nitrogen (Figure 3.2H). These results are in reasonable agreement with our Raman experiments, in which the observed $C_{14}H$ rock in 15D PSB is at 1350 cm^{-1}, 28 cm^{-1} below the $C_{14}H/C_{15}H$ out of phase rock mode (compare Figure 3.1G with Figure 3.1A), and it shifts up by 6 cm^{-1} with further ND labeling (Figure 3.1H). The calculations predict that the $C_{15}D$ rock, which is observed at 978 cm^{-1} (Figure 3.1G), will shift up by 9 cm^{-1} upon further ND labeling (compare Figure 3.2G with 2H) due to its coupling with ND rock. The observed shift of this mode is 12 cm^{-1} (Figure 3.1H).

Upon 14,15-^{13}C labeling, the predicted down shift of the C_{14}-C_{15} single bond stretch mode, observed at 1232 cm^{-1} (Figure 3.1A), is 8 cm^{-1} (compare Figure 3.2E with 2A), compared with the observed shift of 13 cm^{-1} (Figure 3.1E). The predicted shift of this mode upon Schiff base nitrogen deuteration is 19 cm^{-1}, which is due to its decoupling with NH rock (Figure 3.2B). The observed shift of this mode is 15 cm^{-1} (Figure 3.1B). Upon 15D labeling, the observed upward shift of the C_{14}-C_{15} stretch mode is 25 cm^{-1} (Figure 3.1G), and the predicted shift of this mode is 14 cm^{-1} in PSB-chloride complex (Figure 3.2G) but is 29 cm^{-1} in PSB-water complex (data not shown). These results suggest that this mode is rather delocalized, and its mode composition is very sensitive to the Schiff base environment.

Another new mode in 15D PSB spectrum appears 23 cm^{-1} below the 1232 cm^{-1} mode (Figure 3.1G), and our calculations suggest that it is a combination of CH rocking and methyl vibrations. The predicted position of this mode is 21 cm^{-}

^{1} below the C_{14}-C_{15} stretch in the unlabeled spectrum (compare Figure 3.2G with 2A). The 15D labeling apparently removes most of the coupling between C_{14}-C_{15} stretch and NH rock so that in the 15D,ND labeled PSB, the C_{14}-C_{15} stretch is little shifted (< 3 cm^{-1}, Figure 3.1H), as predicted (Figure 3.2H). The results obtained by other basis sets (3-21g, 6-31g, and 4-31g*) and on PSB-water complex are in general agreement with that shown in Figure 3.2, although some differences, such as that mentioned above, are observed.

From above comparisons, we can see that the calculated isotope shifts of several major Raman bands of PSB are in very good agreement with experiment and the *ab initio* method used here should be accurate enough for the vibrational analysis on the PSB and similar compounds. Therefore, we extended our *ab initio* calculations to the less stable C=N *syn* PSB complexed with chloride ion (Figure 3.3), or hydrogen boned with a water molecule (data not shown). Based on comparisons between the calculated Raman spectra of C=N *syn* and C=N *anti* PSB, three criteria to determine the Schiff base C=N configuration based on vibrational signature become evident. Except for some relatively minor differences, these rules are independent of the basis set (3-21g, 6-31g, 4-31g* and 6-31g**) used in the calculations and are relatively insensitive to the strength of the hydrogen bonding on the Schiff base, and they are summarized below:

1. The C=N configuration of PSB can be determined by the C_{15}D rock mode frequency and its response upon deuteration of the Schiff base nitrogen. For the C=N *anti* configuration, the C_{15}D rock is quite localized and appears at about 980 cm^{-1} with moderate Raman intensity (see Figure 3.1G). This mode couples with the ND rock motion upon Schiff base deuteration and shifts up by about 10 cm^{-1} (Figure 3.1H; also compare Figure 3.2H with 2G). For the C=N *syn* configuration, the C_{15}D rock couples strongly with N-C stretch motion to form a weak C_{15}D rock mode about 50 cm^{-1} higher than that in the C=N *anti*

configuration (compare Figure 3.2G with 3G). The ND rock is predicted to appear as a separate band and is not coupled with the $C_{15}D$ rock when the Schiff base nitrogen is deuterated (compare 3H with 3G). In the PSB - water complex, there is no change of the predicted coupling except the ND rock appears at a lower frequency due to weaker hydrogen bonding on the N-D bond (data not shown). This behavior of the $C_{15}D$ rock was first found by Smith *et al.* (1987) in their empirical vibrational analysis of RPSB. Later it was found that the rule can be applied to unprotonated Schiff bases as well (Ames *et al.*, 1989; Cromwell *et al.*, 1992). However, since the $C_{15}D$ rock is rather weak, especially when C=N is *syn*, additional isotopic labeling may be necessary to identify this mode when this rule is applied to the retinal Schiff base under resonance conditions (Ames *et al.*, 1989).

2. The C=N configuration of PSB can be determined by the position of the C_{14}-C_{15} stretch frequency and its shift upon deuteration of the Schiff base nitrogen. For the C=N *anti* configuration, our data show that C_{14}-C_{15} stretch is at about 1230 cm^{-1} (Figure 3.1A). Upon Schiff base deuteration, this mode shifts up by about 15 cm^{-1} (observed, Figure 3.1B) or more (calculated, compare Figure 3.2B with 2A) and its intensity is reduced (Spectrum B, Figures 3.1-2). For the C=N *syn* configuration, the calculated C_{14}-C_{15} stretch is more delocalized as shown by the ^{13}C shifts of several bands in this region (Figure 3.3G). The most intense C_{14}-C_{15} stretch is about 85 cm^{-1} below the C_{14}-C_{15} stretch in C=N *anti* PSB (compare Figure 3.3A with 2A). The predicted shift of this mode in C=N *syn* PSB upon Schiff base deuteration is positive by ~50-60 cm^{-1} (Figure 3.3B), much larger than the predicted deuterium shift of the C_{14}-C_{15} stretch in C=N *anti* PSB. This rule is somewhat different from a similar rule obtained previously based on the empirical analysis of RPSB (Smith *et al.*, 1984; Livnah and Sheves, 1993). In that study, a much smaller change was predicted for the C_{14}-C_{15} stretch upon

deuteration of C=N *anti* RPSB. The discrepancy is explained by the delocalized nature of this mode. The C_{14}-C_{15} stretch may couple with motions several bonds away from the C_{14}-C_{15} bond in RPSB so that its response to the Schiff base deuteration is altered.

3. The C=N configuration of PSB can also be determined by the $C_{15}H$ rock mode frequency and its response to Schiff base deuteration. For the C=N *anti* configuration, the $C_{15}H$ rock couples strongly with the $C_{14}H$ rock to form an out-of-phase Raman band at about 1380 cm^{-1} (Figure 3.1A). This mode is insensitive to the Schiff base deuteration (Figure 3.1B; also compare Figure 3.2A with 2B). For the C=N *syn* configuration, the $C_{15}H$ rock couples with both $C_{14}H$ and NH rocks to form an intense Raman band. The frequency of this band is highly sensitive to the hydrogen bonding strength on the Schiff base nitrogen, and is predicted at about 7 cm^{-1} and 35 cm^{-1} below the out-of-phase $C_{14}H/C_{15}H$ rock mode for the C=N *anti* configuration in PSB - chloride complex (compare Figure 3.3A with 2A) and in PSB - water complex (data not shown), respectively. Upon Schiff base deuteration, this mode is disrupted in both types of complexes, resulting a large spectral change in this region. The difference in the Schiff base deuteration induced spectral changes of the $C_{15}H$ rock between the C=N *syn* and anti configurations has not been previously used to determine the C=N configuration, although it does exist. For example, in the Raman spectrum of the all-*trans* RPSB chromophore of light adapted bacteriorhodopsin, which is known to have a C=N *anti* configuration, no significant spectral change is observed upon Schiff base deuteration. On the other hand, in the Raman spectrum of 13-*cis* RPSB chromophore in dark adapted bacteriorhodopsin, which is known to have a C=N *syn* configuration and a weak hydrogen bonding to the Schiff base nitrogen, a strong band at about 1350 cm^{-1} disappears upon Schiff base

deuteration (Smith *et al.*, 1984). This is consistent with the results of our calculations, especially with that of the PSB - water complex.

We have also performed semi-empirical MNDO calculations on the PSB complexed with a chloride ion 2 Å away from the Schiff base hydrogen, with either C=N *anti* or *syn* configuration. The results show that in some cases, the calculated normal modes by MNDO method are rather poor, at least quantitatively. For example, in the C=N *anti* configuration, the calculated C_{14}-C_{15} stretch mode does not shift upon Schiff base deuteration (compared with 15 cm^{-1} shift observed in Raman experiment, Figure 3.1A, 1B). In addition, the calculated $C_{14}H/C_{15}H$ rock is higher than most of methyl bending modes, in contradictory to experimental observations. The predicted shift of $C_{14}H/C_{15}H$ rock upon $C_{15}D$ labeling is less than 10 cm^{-1} compared to the 28 cm^{-1} shift observed in the experiment, apparently because the coupling between $C_{14}H$ and $C_{15}H$ bending is underestimated. Besides, significant disturbance in the CH bending region upon Schiff base deuteration is also predicted due to overestimated coupling between NH bending and $C_{14}H/C_{15}H$ bending. These problems are generally absent in the *ab initio* calculations as shown above. Nevertheless, for many purposes, the semi-empirical methods are fine. The limitations of MNDO method and possible source of errors have been discussed in detail before (Grossjean *et al.*, 1990) and we will not repeat it here.

IV. CONCLUSION

We have shown that well defined spectral characteristics are present in the *ab initio* calculated spectra of native and labeled PSB which are sufficient to discern the configuration of the Schiff base. Since these results are in very good agreement with experimental data, it is reasonable to suggest that the *ab initio* methods used here, when combined with isotopic labeling studies, should

provide sufficient accuracy for the vibrational analysis on the RPSB in various environments.

Figure 3.1: Raman spectra of PSB in H_2O (A) and its ND (B), ^{15}N (C), ^{15}ND (D), 14,15-^{13}C (E), 14,15-^{13}C ND (F), 15D (G), and 15D,ND (H) derivatives. The spectra were measured with 514.5 nm laser line from an argon ion laser at a power level of 200-300 mW on an optical multichannel analyzer system, which has been described in detail elsewhere (Yue *et al.*, 1989). Solvent Raman bands was subtracted. Resolution of the spectrometer is 8 cm^{-1}. A spectral calibration is done for each measurement using the known Raman lines of toluene, and absolute band positions are accurate to within ± 3 cm^{-1}.

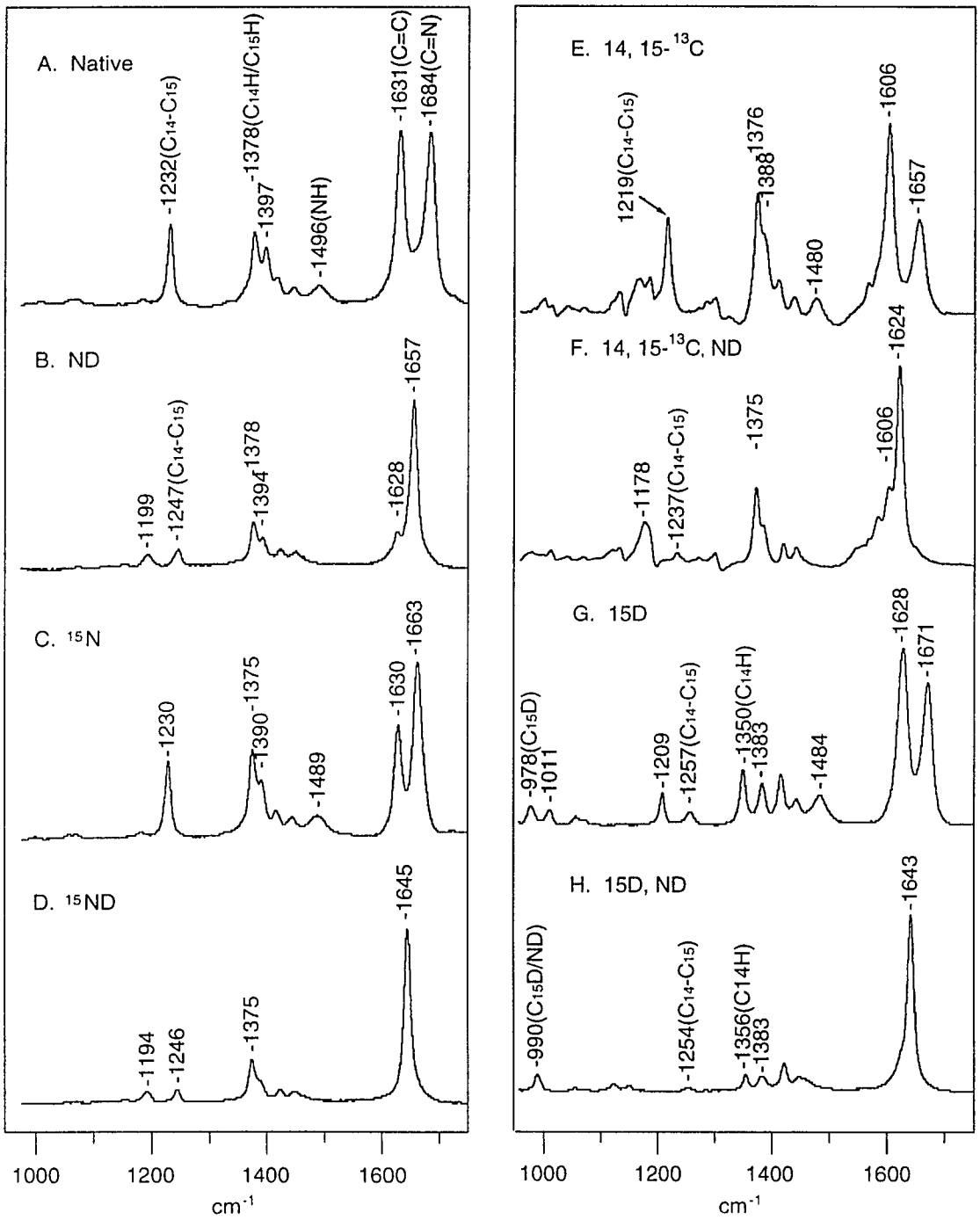
A. Native
-1232(C14-C15)
-1397
-1378(C14H/C15H)
-1496(NH)
-1631(C=C)
-1684(C=N)
B. ND
-1199
-1247(C14-C15)
-1394
-1378
-1628
-1657
C. 15N
-1230
-1390
-1375
-1489
-1630
-1663
D. 15ND
-1194
-1246
-1375
-1645
1000
1200
1400
1600
cm-1
E. 14, 15-13C
1219(C14-C15)
-1388
-1376
-1480
-1606
-1657
F. 14, 15-13C, ND
-1178
-1237(C14-C15)
-1375
-1606
-1624
G. 15D
-978(C15D)
-1011
-1209
-1257(C14-C15)
-1350(C14H)
-1383
-1484
-1628
-1671
H. 15D, ND
-990(C15D/ND)
-1254(C14-C15)
-1356(C14H)
-1383
-1643
1000
1200
1400
1600
cm-1

Figure 3.2 Calculated Raman spectra of C=N *anti* PSB complexed with a chloride ion (Scheme I) in H_2O (A) and its ND (B), ^{15}N (C), ^{15}ND (D), 14,15-^{13}C (E), 14,15-^{13}C, ND (F), 15D (G), and 15D,ND (H) derivatives. The geometry of PSB is fully optimized by Gaussian 92 (Frisch *et al.*, 1992) program. The vibrational frequencies with Raman intensities are then calculated by the methods as implemented in the Gaussian 92 program. All calculations have been done at HF/6-31g** level. The calculated frequencies are then multiplied by a factor of 0.9 to bring them closer to the observed values for an easier comparison. The distance between chloride ion and Schiff base hydrogen, r (Scheme I), is equal to 1.91 Å and the angle θ, as shown in Scheme I, is equal to 177 degrees.

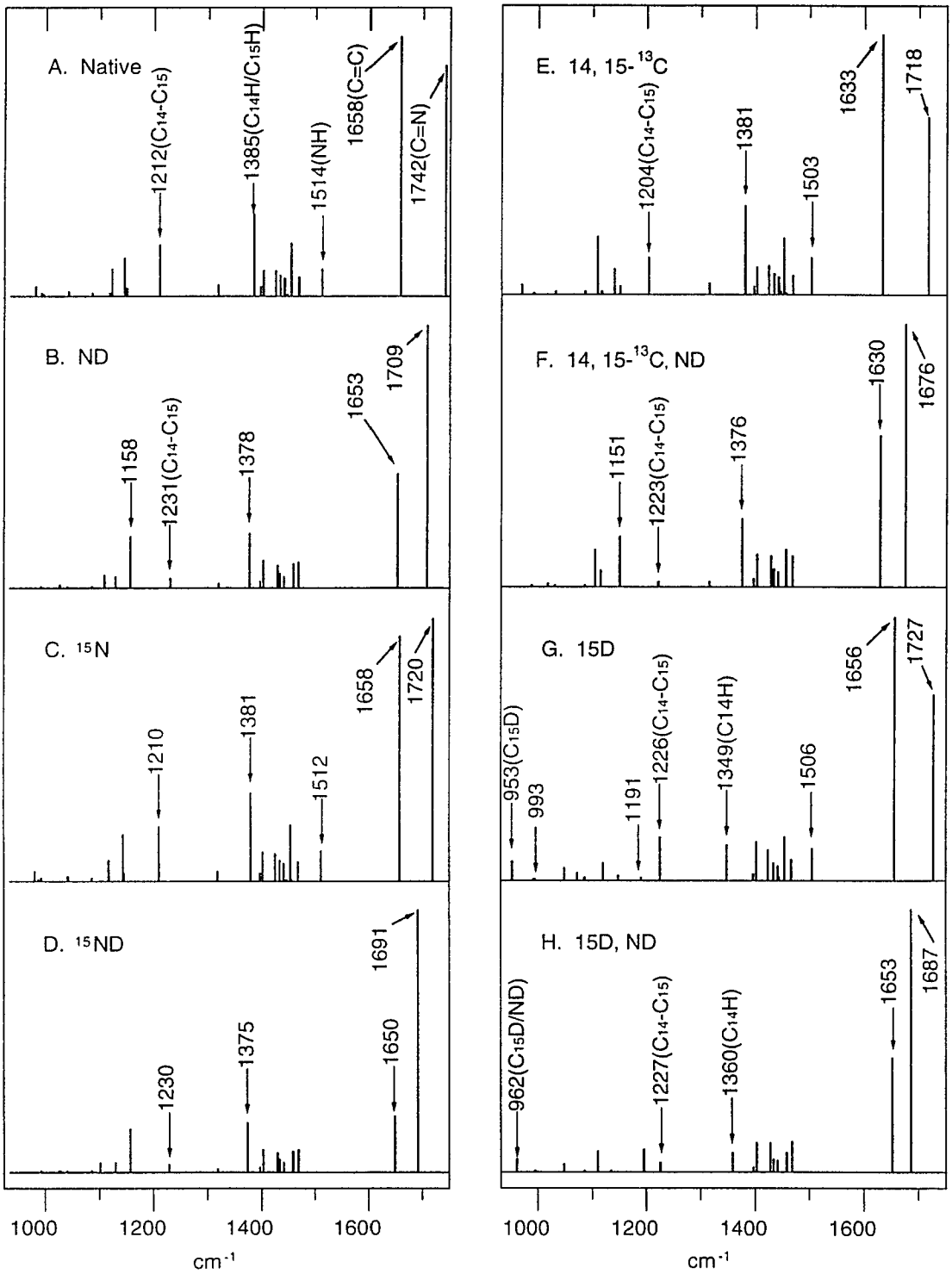
A. Native
1212(C14-C15)
1385(C14H/C15H)
1514(NH)
1658(C=C)
1742(C=N)
B. ND
1158
1231(C14-C15)
1378
1653
1709
C. 15N
1210
1381
1512
1658
1720
D. 15ND
1230
1375
1650
1691
E. 14, 15-13C
1204(C14-C15)
1381
1503
1633
1718
F. 14, 15-13C, ND
1151
1223(C14-C15)
1376
1630
1676
G. 15D
953(C15D)
993
1191
1226(C14-C15)
1349(C14H)
1506
1656
1727
H. 15D, ND
962(C15D/ND)
1227(C14-C15)
1360(C14H)
1653
1687
1000
1200
1400
1600
cm-1

Figure 3.3: Calculated Raman spectra of C=N *syn* PSB complexed with a chloride ion in H_2O (A) and its ND (B), ^{15}N (C), ^{15}ND (D), 14,15-^{13}C (E), 14,15-^{13}C, ND (F), 15D (G), and 15D,ND (H) derivatives. The geometry is fully optimized except the parameters r (= 1.91 Å) and θ (= 177°) are fixed because no optimum position of the chloride ion on the potential surface could be found for C=N *syn* configuration.

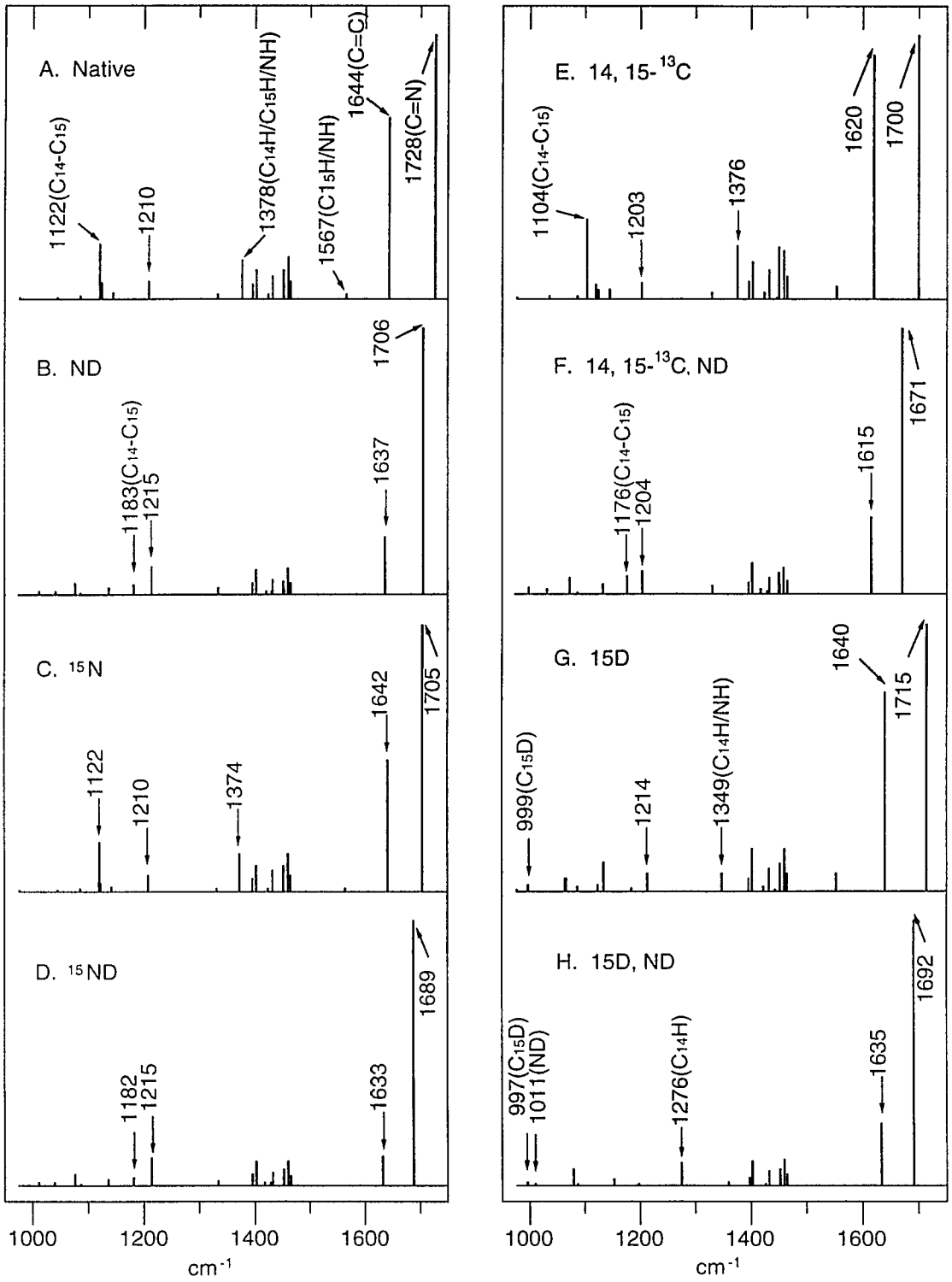
A. Native
1122(C14-C15)
1210
1378(C14H/C15H/NH)
1567(C15H/NH)
1644(C=C)
1728(C=N)
B. ND
1183(C14-C15)
1215
1637
1706
C. 15N
1122
1210
1374
1642
1705
D. 15ND
1182
1215
1633
1689
E. 14, 15-13C
1104(C14-C15)
1203
1376
1620
1700
F. 14, 15-13C, ND
1176(C14-C15)
1204
1615
1671
G. 15D
999(C15D)
1214
1349(C14H/NH)
1640
1715
H. 15D, ND
997(C15D)
1011(ND)
1276(C14H)
1635
1692
1000
1200
1400
1600
cm-1

V. SUPPLEMENTARY MATERIAL

3-methyl-2-butenal and methylamine HCl were purchased from Aldrich. ^{15}N labeled methylamine HCl was purchased from Cambridge Isotope Labs. Other labeled material were made by the procedure described in the following section. The Schiff base was formed by mixing equal molar ratios of 3-methyl-2-butenal, methylamine HCl, and NaOH in H_2O, and subsequently extracted by n-hexane. Protonation or deuteration of the Schiff bases was achieved by adding 1.0 equivalent of 37% HCl or DCl solution to hexane. The mixture was shaken vigorously and then centrifuged to remove hexane. Finally, the Schiff base was diluted to about 50 mM for Raman measurements.

The deuterated and ^{13}C-labeled 3-methyl-2-butenals were prepared as described here. The first step is the Horner-Emmons reaction of diethylphosphonoacetonitrile and acetone to form 3-methyl-2-butenenitrile. The nitrile function is reducted to the aldehyde with dibal, giving 3-methyl-2-butenal. The procedures are similar to those we used in the preparation of deuterated and ^{13}C-labeled retinals (M. Groesbeek, J. Lugtenburg, Photochem. Photobiol. vol. 56, 903- 908, 1992), but care has to be taken not to evaporate the volatile products. A ^{13}C label at C3 is introduced by using 2-^{13}C-acetone, a ^{13}C label at C2 and/or C1 is introduced by using 2-^{13}C and/or 1-^{13}C acetonitrile, respectively. A deuterium label at C2-D comes from deuterated acetonitrile and quenching of the reaction mixture with D_2O and a deuterium at C1-D comes from reduction of the nitrile function with diisobutyl aluminum deuteride (dibal-D) and work-up with D_2O.

Appropriately labeled acetonitrile (1.0 equivalent, usually 0.5 g) in diethylether was added to an ethereal solution of lithium diisopropylamine (2.0 equivalents) at -60°C. Then diethylchlorophosphate (1.0 equivalent) was added to form the corresponding anion of labeled diethylphosphonoacetonitrile. The

mixture was stirred for 1 hour and was allowed to warm to room temperature. Appropriately labeled acetone (1.0 equivalent) in diethylether was added and the mixture was stirred for an additional hour. Then H_2O or D_2O was added and the layers were separated. The water layer was extracted with diethylether and the combined organic layers were washed (brine) and dried ($MgSO_4$). The organic layer was diluted with two volumes of n-pentane and filtered over a layer of SiO_2. The filtrate was concentrated at room temperature in vacuo to 2 ml. The concentrate was diluted again with n-pentane and cooled to -60°C. Dibal-D or dibal-H (1.5 equivalents) was added and the mixture was stirred for 1 hour. Then a mixture of SiO_2 with D_2O or H_2O was added and the mixture was stirred for 2 hours. $MgSO_4$ was added and the solids were filtered off. The filtrate was concentrated in vacuo at room temperature. Purification was performed by SiO_2 flash column chromatography using 15% diethylether/n-pentane as eluent.

Chapter 4

A SUCCESSFUL WAY TO OBTAIN RESONANCE RAMAN SPECTRA OF OCTOPUS RHODOPSIN AND ISORHODOPSIN

I. ABSTRACT

Several facts demonstrate interesting differences between octopus and bovine visual pigments (Yoshizawa, 1972; Tsuda, 1979c; Tsuda *et al.*, 1980; Tsuda *et al.*, 1986; Pande *et al.*, 1987; Ovchinnikov *et al.*, 1988). Octopus rhodopsin is dramatically different from bovine rhodopsin as well as 11-cis protonated Schiff base retinal in the finger print region (Pande *et al.*, 1984; Pande *et al.*, 1987; Deng *et al.*, 1991a; Deng *et al.*, 1991b). For a more detailed study, it is necessary to perform a resonance Raman experiment of octopus pigments regenerated with deuterium and ^{13}C labeled chromophore. Flow experiments, which need a relatively large amount of sample, are not practical for labeled octopus, due to the rarity of native octopus samples (Callender *et al.*, 1976; Mathies *et al.*, 1976). This chapter introduces a successful method of obtaining octopus rhodopsin and isorhodopsin spectra which need only limited sample. This method allows the isotopic study of octopus rhodopsin and isorhodopsin, as well as other scarce opsins.

II. INTRODUCTION

Rhodopsin, a functional molecule in visual pigments of animals, usually contains an 11-cis retinal bonded to apoprotein via a Schiff base, will undergo a cis to trans convertion after exposure to light (Wald, 1968). The trans form, which is called bathorhodopsin, will thermal decay to a series of meta forms (Yoshizawa and Wald, 1963). At liquid nitrogen temperature, the thermal decay will be blocked (Wald *et al.*, 1950). An equilibrium mixture of rhodopsin, bathorhodopsin and isorhodopsin, which contains 9-cis retinal and apoprotein, will be formed and the composition of the mixture is determined by the wavelength of the irradiating beam (Yoshizawa and Wald, 1963; Yoshizawa, 1972).

Owing to the light sensitivity, the spectrum of rhodopsin cannot be taken directly without special condition (Rimai *et al.*, 1970; Oseroff and Callender, 1974). Some methods have been developed specifically to obtain spectra of rhodopsin, bathorhodopsin and isorhodopsin (Callender and Honig, 1977). The first method is a flow experiment which was independently developed by two groups (Callender *et al.*, 1976; Mathies *et al.*, 1976). The basic idea is to have the sample flow through a capillary in the path of the probing laser beam at a high enough flow to insure the possibility of photon absorption of any individual rhodopsin molecule is very small within the laser-sample interaction region. While this method is simple its disadvantage lies in its requirement of large amounts of sample, usually dozens of $OD \bullet cm^3$. This becomes impractical when limited sample is available, for instance, in the case of doing experiment for some scarce opsins. The other method is pump-probe experiment which was first developed by Oseroff and Callender (1974). The primary concept is that thermal decay would be blocked at low temperature (Wald *et al.*, 1950). For example, if the temperature is about 120K, only three species, rhodopsin, bathorhodopsin and

isorhodopsin would be present. The frequency of the irradiating laser determines the composition these three photospecies (Hurley *et al.*, 1977). The resonance Raman spectra is taken by a weak "probe" laser beam while the sample composition of these three species is controlled by a strong "pump" laser beam. Three spectra of different sample compositions are collected, then computing with knowledge of composition by chemical extraction, pure spectra of rhodopsin, bathorhodopsin and isorhodopsin may be obtained. This method's main advantage is the diminished amount of sample required for an experiment, usually less than 1 OD•cm^3. The disadvantage of this technique lies in the difficulty in choosing the wavelengths of the pump beams. Additionally the chemical extraction method requires large amounts of sample and the result is seldom accurate enough for a perfect subtraction. Obviously, the choice of the pump beam's wavelength in order to maximize the differences among the species-mixture spectra is very important, and depends upon the Raman cross-sections of rhodopsin, bathorhodopsin and isorhodopsin, and their quantum yield. If the absorption maxima are well separated, it is usually easy to find the optimum laser beam because of the ease in "pumping" one species into the other two or making the ratios very different, provided the effect of quantum yield can be neglected here. For example, for bovine pigments, the absorption maximum of bathorhodopsin is in 540 nm, rhodopsin 498 nm, and isorhodopsin 485 nm. By using a 488 nm beam from an Ar+ laser as a probe, a bathorhodopsin-rich spectra can be obtained. Again using a weak 488 nm as a probe, but irradiating the sample with a much stronger (30~50 times) "pump" laser beam with wavelength of 568 and 647 nm (both from Ar+), two more batho-poor spectra with different rhodopsin/isorhodopsin ratios are obtained. By this techniques the spectral differences are large enough to assure successful subtraction to three pure

spectra (Deng and Callender, 1987). The situation different in the case of octopus rhodopsin. Here the absorption maximum of bathorhodopsin is 545 nm, rhodopsin 472 nm, isorhodopsin 462 nm (Yoshizawa, 1972; Tsuda *et al.*, 1980). The difference between rhodopsin and isorhodopsin in only 10 nm, by contrast to 20 nm in the bovine case. A small difference causes difficulty in choosing pump beams. Possible lines from K+ lasers, 530 and 568 nm, have been tested. None of them, however, leads to a successful subtraction that yield pure rhodopsin and isorhodopsin, due to the small rhodopsin/isorhodopsin difference. In this study, a dye laser must be employed to provide a pump beam with another wavelength.

III. MATERIAL AND METHOD

Octopus rhodopsin is prepared as previously described (Tsuda, 1979c; Tsuda *et al.*, 1986; Koutalos *et al.*, 1989). The configuration of the pump-probe experiment has been described previously (Oseroff and Callender, 1974). The 457.9 nm Ar+ line is used as probe for resonance Raman spectra. Figure 4.1 displays a probe only spectra.

Characteristic Bands

The spectrum in Figure 4.1 contains all three species, rhodopsin, bathorhodopsin and isorhodopsin species. However, specific markers bands can be assigned to a specific species. From IR experiments, the 887 and 940 cm^{-1} peaks are assigned to bathorhodopsin, the 1325 cm^{-1} peak arises from isorhodopsin, and the 1017 cm^{-1} peak from rhodopsin (Bagley *et al.*, 1989; Deng *et al.*, 1991a). We make the assumption that those assignment are correct to isolate the spectra of the three species. Below, it will be seen that this yields the correct rhodopsin spectrum (brown from flow results) and the

correct chemical composition as measured from chemical extraction measurements. Knowledge of the characteristic bands of each species is important. The relative heights of their bands are the criterion needed to indicate difference in constituent ratios.

Choosing the Pump Beams from a Dye Laser

A dye laser (Model 700R, Lexel) was employed for the purpose of providing continuous wavelength laser beam to "pump" the sample, that is, to change the compositions of rhodopsin, bathorhodopsin and isorhodopsin. Figures 4.2 - 4.7 show the method choosing two pump beams. Figure 4.2 displays spectra taken with the same probe but different pumps (from 540 to 580 nm). Visual inspection of these shows little difference. Figure 4.3 shows an expanded part of Figure 4.2, displaying the 968 and 956 cm^{-1} bands. These are the characteristic bands of rhodopsin and isorhodopsin, respectively. Figure 4.4 shows the bands at 968 nm in Figure 4.3 normalized, leaving the 956 cm^{-1} band to vary from one pump beam to the other. The bands in 956 cm^{-1} in Figure 4.4 are expanded in Figure 4.5. Table 4.1 shows the relative rhodopsin/isorhodopsin ratio varies with different wavelengths of pump beam. Figure 4.6 plots the magnitudes of the band at 956 cm^{-1} in Figure 4.5 as function of the wavelengths of the pump beams. Thus, from Figure 4.5, spectra obtained with a pump in the range of 550 to 554 nm, and the other over 573 nm (in case of using Rhodamine 560 as dye) as pumps have the largest rhodopsin/isorhodopsin ratio difference. Similar experiments are performed for octopus pigment regenerated with an isotopically labeled retinal chromophore (10,11-$^{13}C_2$). These results, shown in Table 4.2 and Figure 4.7, confirms previous results obtained from native rhodopsin. Thus, these two beams, 553 and 575 nm, are used in further experiments.

Computer Subtraction

Figures 4.8-10 show how the pure rhodopsin , isorhodopsin and bathorhodopsin may be obtained from three species-mixture spectra. Displayed are: 457 nm probe only [Figure 4.8(a)], weak 457 nm probe (5 mW) plus strong 553 nm pump (250 mW) [Figure 4.8(b)], and weak 457 nm probe plus strong 575 nm pump [Figure 4.8(c)]. From the above discussions of the characteristic bands, we may assure that the spectrum in Figure 4.8(a) is a bathorhodopsin-rich one, (bands in 940 and 887 cm^{-1} are intense), while spectra in Figure 4.8(b) and Figure 4.8(c) are bathorhodopsin-poor spectra (the bands in 940 and 887 cm^{-1} are small). Careful examination shows the spectrum in Figure 4.8(b) has more isorhodopsin and less rhodopsin than the one shown in Figure 4.8(c) (by observing the characteristic bands of rhodopsin and isorhodopsin). Thus, by subtracting the spectrum in Figure 4.8(a) from the spectrum in Figure 4.8(b) eliminating the 887 and 940 cm^{-1} bands, a bathorhodopsin-free spectrum is obtained [Figure 4.9(a)]. Similarly, by subtracting the spectrum in Figure 4.8(a) from that in Figure 4.8(c), another bathorhodopsin-free spectrum is also obtained (Figure 4.9(b)). Note that although both spectra in Figure 4.9(a) and Figure 4.9(b) are bathorhodopsin-free, the rhodopsin/isorhodopsin ratios of each one are different. The spectrum in Figure 4.9(a) has more isorhodopsin and less rhodopsin than the spectrum in Figure 4.9(b). Thus, by subtracting the spectrum in Figure 4.9(a) from the one in Figure 4.9(b), a pure rhodopsin spectrum is obtained [Figure 4.9(c)], which is identical to the spectrum obtained from the flow experiment at ambient temperature (see Figure 4.11). Also, by subtracting the spectrum in Figure 4.9(b) from the one in Figure 4.9(a), a pure isorhodopsin spectrum is obtained [Figure 4.10(a)]. This is the first example of a resonance Raman

spectrum of octopus isorhodopsin, therefore it can only be compared with the IR spectrum that it confirms (Bagley *et al.*, 1989).

It may be noted that Figure 4.8(a) is a bathorhodopsin-rich spectrum. An isorhodopsin-free spectrum [Figure 4.10(b)] is obtained by the subtraction of the spectrum in Figure 4.10(a) (pure isorhodopsin) from that in Figure 4.8(a). A pure bathorhodopsin spectrum [Figure 4.10(c)] is obtained by subtraction of the spectrum in Figure 4.9(c) (pure rhodopsin) from that in Figure 4.10(b). The spectrum in Figure 4.10(c) has been published previously (Deng *et al.*, 1991a; Deng *et al.*, 1991b).

From the parameters which are used to perform the subtractions, we conclude that the first 457.9 nm probe only spectrum shows 57% bathorhodopsin, 22% rhodopsin, and 21% isorhodopsin; the second spectrum, 457.9 nm probe plus 553 nm pump, shows 22% bathorhodopsin, 28% rhodopsin, and 50% isorhodopsin; and the third, 457.9 nm probe plus 575 nm pump spectrum shows 22% bathorhodopsin, 40% rhodopsin, and 38% isorhodopsin. The composition of the probe only spectrum consists with the chemical extraction result (Tsuda, 1979a; Kitagawa and Tsuda, 1980; Pande *et al.*, 1987), of 58% bathorhodopsin, 22% rhodopsin, and 20% isorhodopsin.

IV. DISCUSSION

Usually, except for bovine pigments that are commercially obtainable, visual pigments from animals are very rare. Low temperature "pump and probe" experiment can defeat this difficulty because it only requires a small amount of sample. The difficult task in determining the wavelengths of pump-beams is, first finding two close characteristic bands. Their relative intensity is more helpful in distinguishing the different photochemical species compositions than is the absolute intensity.

Table 4.1 Relative Rhodopsin/Isorhodopsin Ratios (in arbitrary units) vs. Different Wavelengths of Pump Beam for Native Octopus

pump beams (nm)	I_{956}/I_{968}
574	0.935
570	0.943
566	0.949
562	0.959
558	0.966
554	0.977
550	0.976
546	0.978
542	0.973
538	0.963
534	0.956

Table 4.2 Relative Rhodopsin/Isorhodopsin Ratios (in arbitrary units) vs. Different Wavelengths of Pump Beam for 10,11-$^{13}C_2$ labeled Octopus

pump beams (nm)	relative rhodopsin/isorhodopsin
576	0.958
572	0.9590
568	0.9618
564	0.9693
560	0.9727
556	0.9788
552	0.9791
548	0.9785
544	0.9751
540	0.9679

Figure 4.1: Resonance Raman spectrum of native octopus pigment at 120 K with a probe beam of 457.9 nm from an Ar+ laser. It is a mixture of bathorhodopsin, rhodopsin, and isorhodopsin. The 887 and 940 cm^{-1} peaks are characteristic bands of bathorhodopsin, while 956 and 1325 cm^{-1} peaks arise from isorhodopsin, and 968 and 1017 cm^{-1} peaks from rhodopsin.

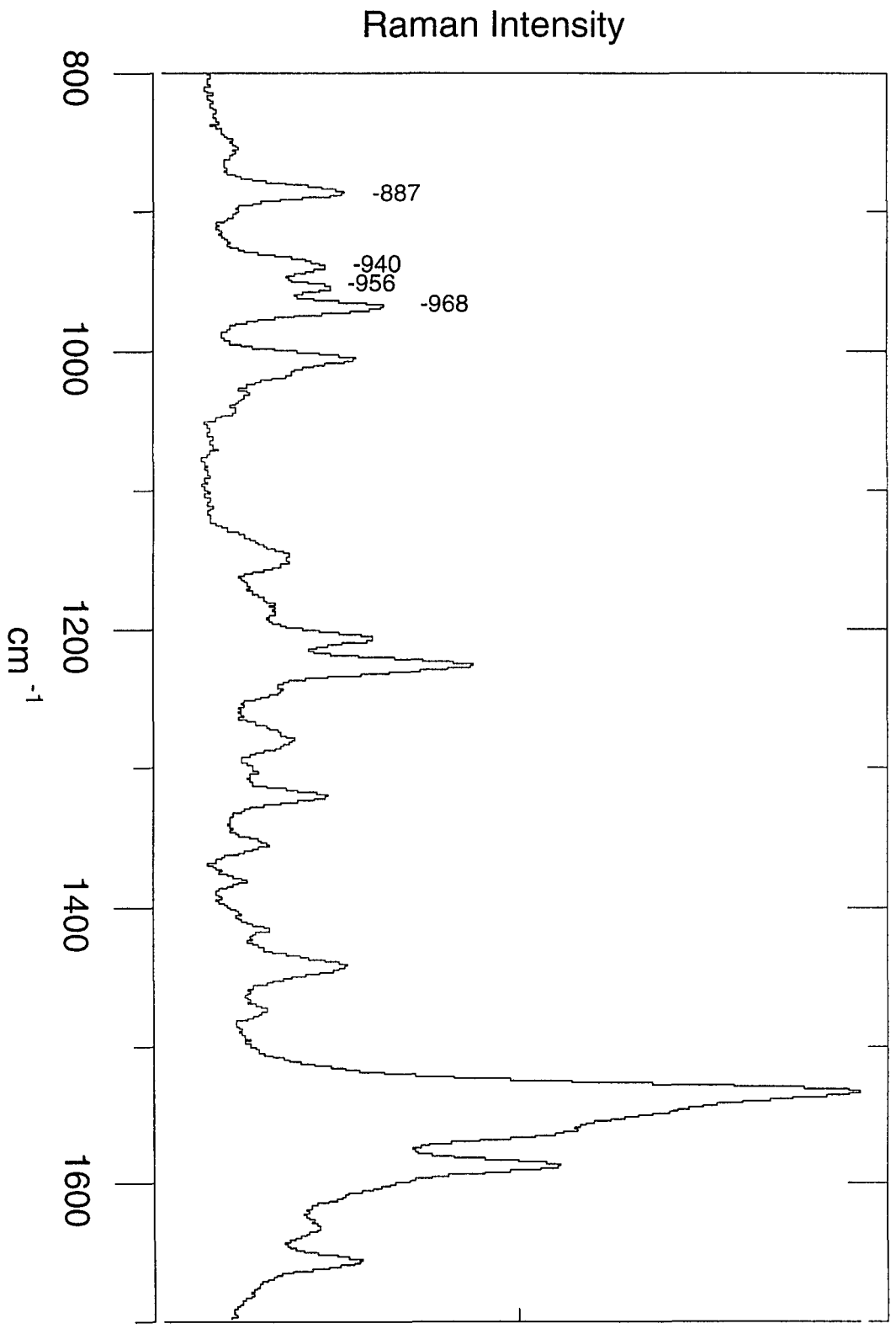
Raman Intensity
800
1000
1200
1400
1600
cm -1
-887
-940
-956
-968

Figure 4.2: Resonance Raman spectrum of native octopus pigment at 120 K with a weak (~5 mW) probe beam of 457.9 nm from an Ar+ laser, and different strong (~250 mW) pump beams, from 540 to 580 nm, from a dye laser. It is not easy to see the differences among different pump beams.

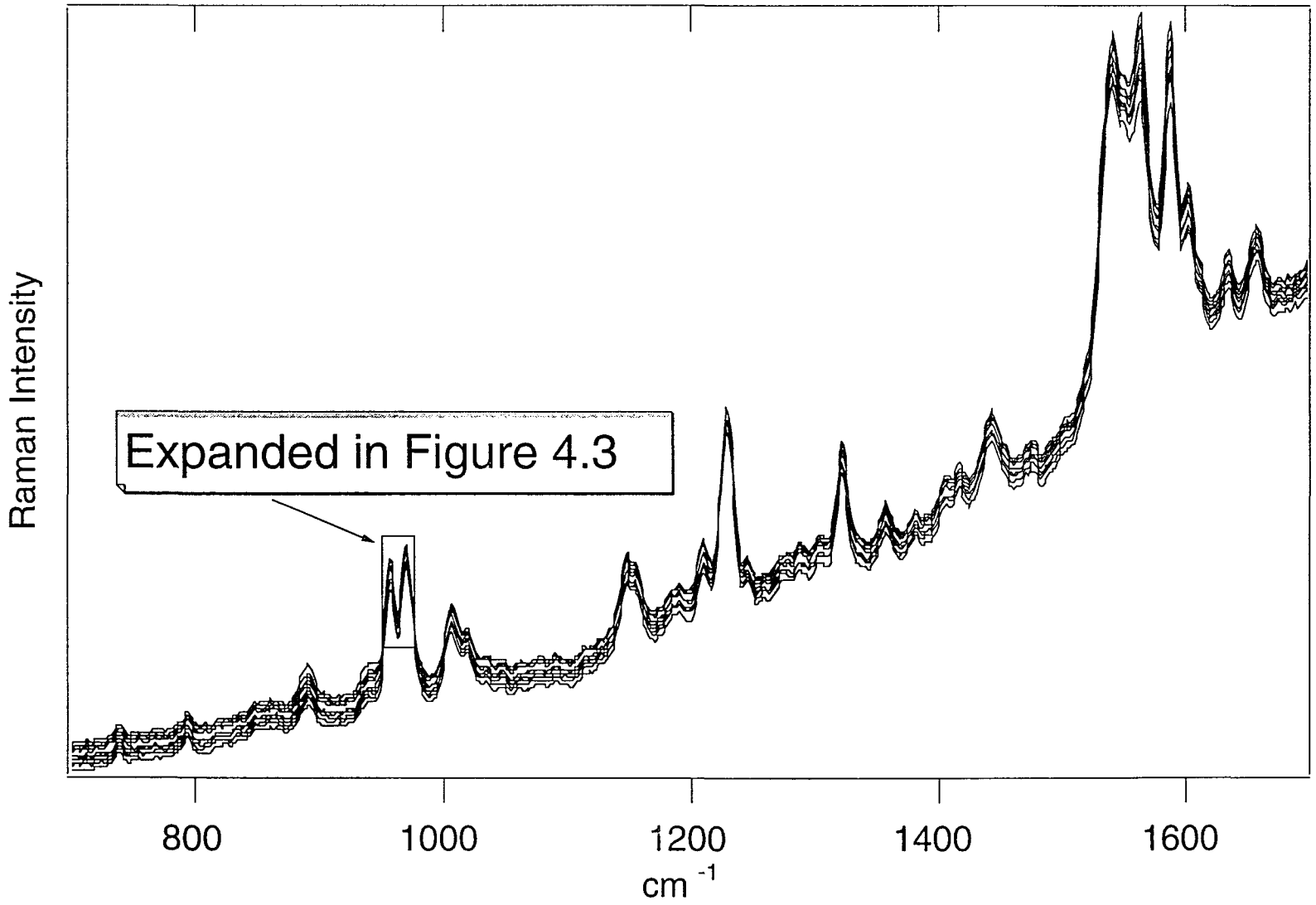
Raman Intensity
Expanded in Figure 4.3
800
1000
1200
1400
1600
cm -1

Figure 4.3: An expanded part of Figure 4.2, displaying the 968 and 956 cm^{-1} bands. These are the characteristic bands of rhodopsin and isorhodopsin, respectively. Their relative intensities slightly change with different pump beams.

Raman Intensity
950
955
960
965
970
975
cm-1

Figure 4.4: The bands at 968 nm in Figure 4.3 has been normalized, leaving the 956 cm^{-1} band to vary from one pump beam to the other. It is more clear to see the rhodopsin/isorhodopsin ratios are different.

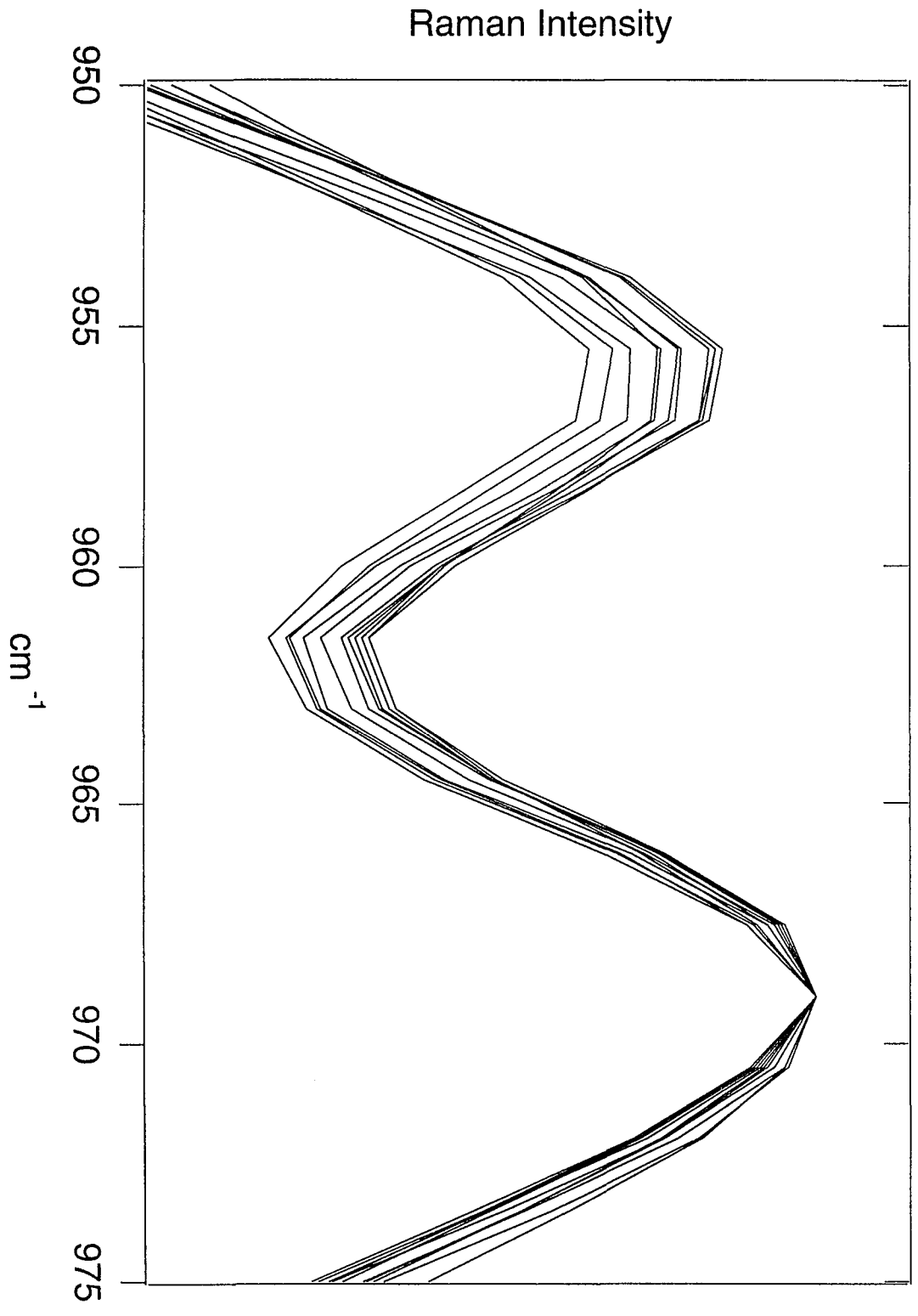
Raman Intensity
950
955
960
965
970
975
cm -1

Figure 4.5: The bands in 956 cm^{-1} in Figure 4.4 are expanded again for the purpose to show the spectra with different pump beams. Note the unit of the Raman intensities here are arbitrary. Numbers with arrow are the wavelength of pump beams.

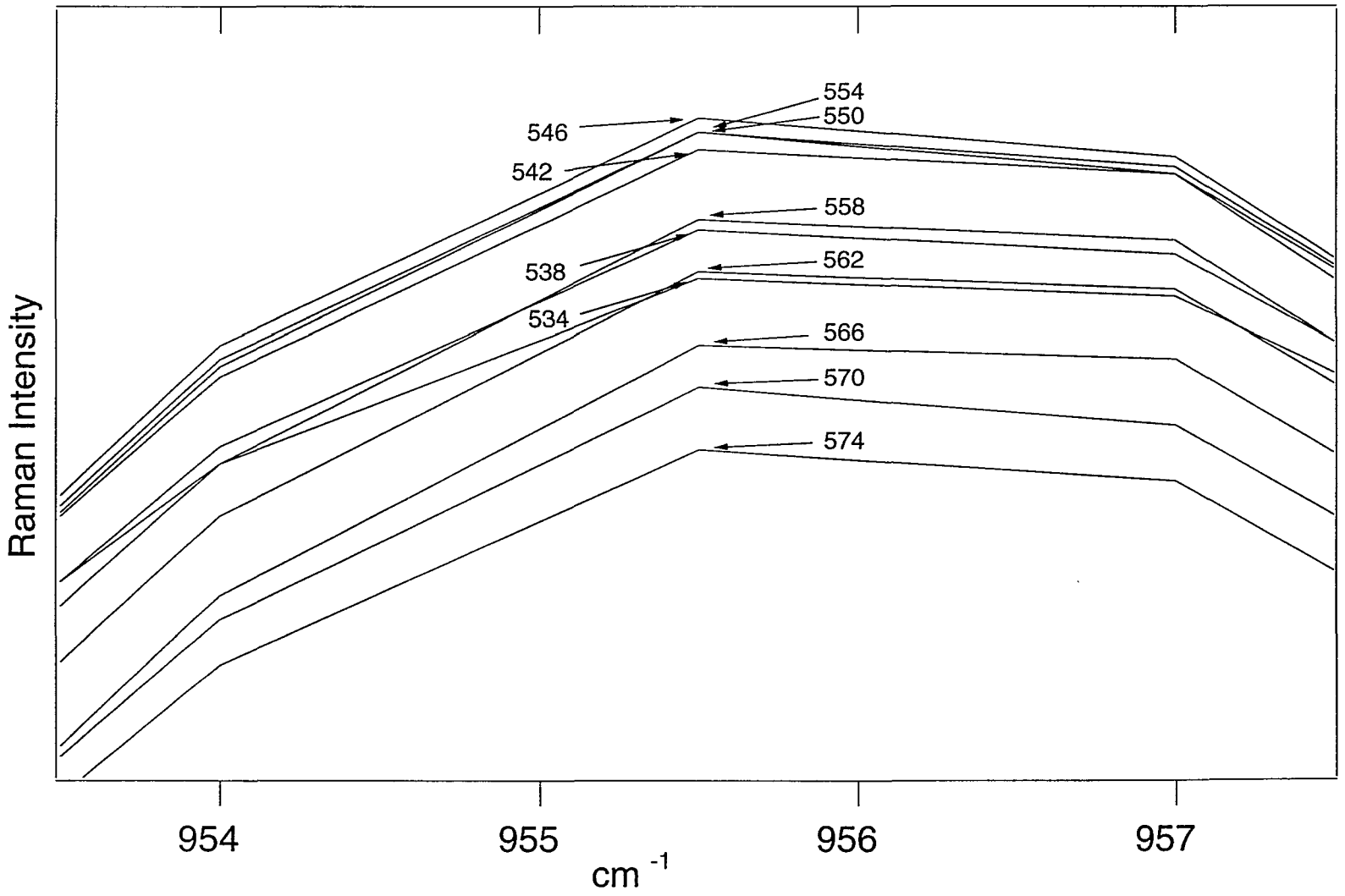
554
550
546
542
558
538
562
534
566
570
574
Raman Intensity
954
955
956
957
cm -1

Figure 4.6: The intensity ratios, I_{956}/I_{968}, vs. wavelengths of the pump beam. It shows that if the wavelength of one pump beam is at the range of 550 to 554 nm and the other over 575 nm, the difference of the rhodopsin/isorhodopsin ratios of the two spectra collected with these two pump beams will be maximized.

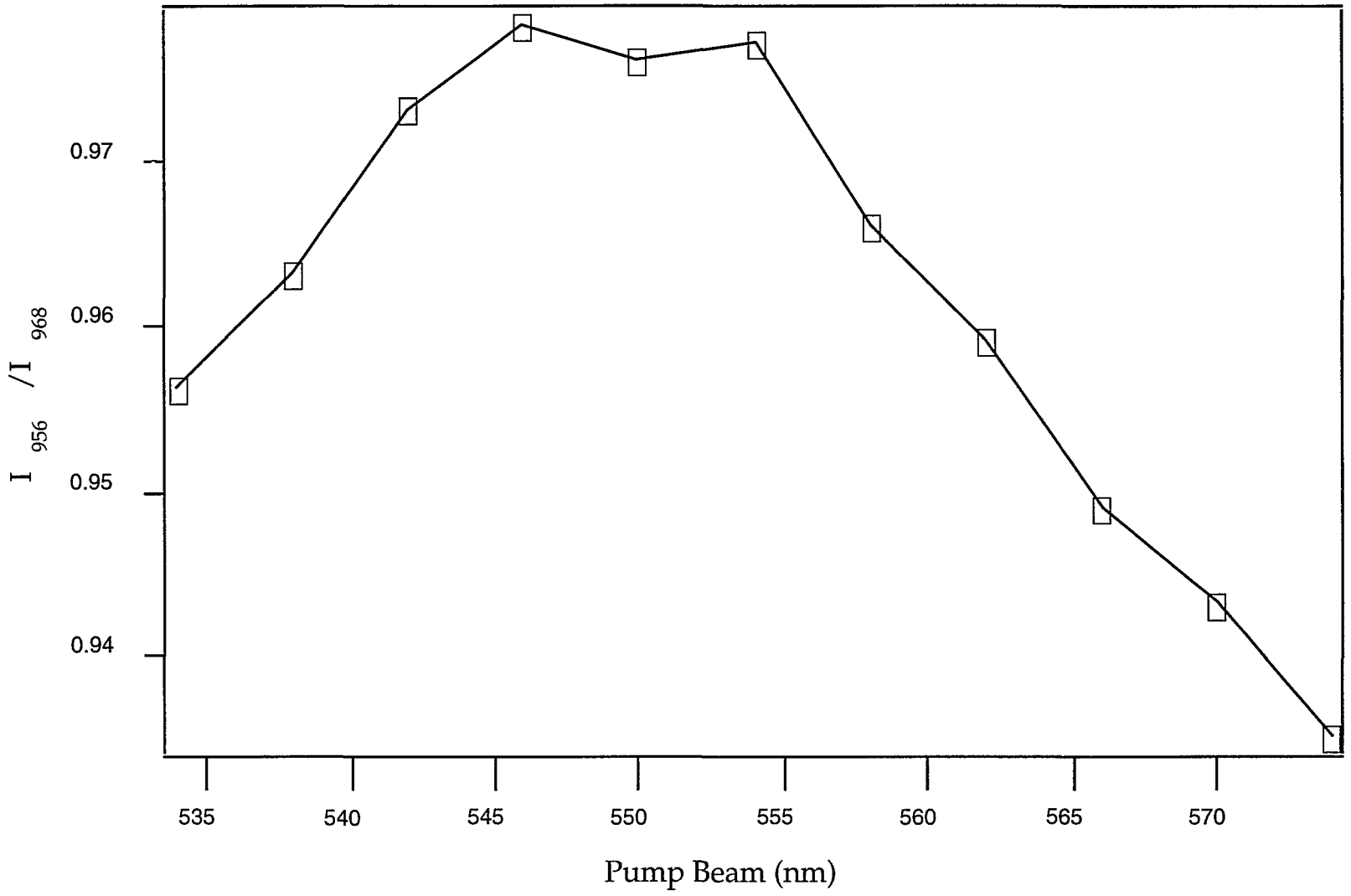
0.97
0.96
0.95
0.94
I 956 /I 968
535
540
545
550
555
560
565
570
Pump Beam (nm)

Figure 4.7: Obtained with identical process as the result in Figure 4.6, but it is for octopus pigment regenerated with 10,11-$^{13}C_2$ labeled retinal chromophore. They are very similar, as expected. Two wavelengths, 553 and 575 nm, are chosen to used in later experiments.

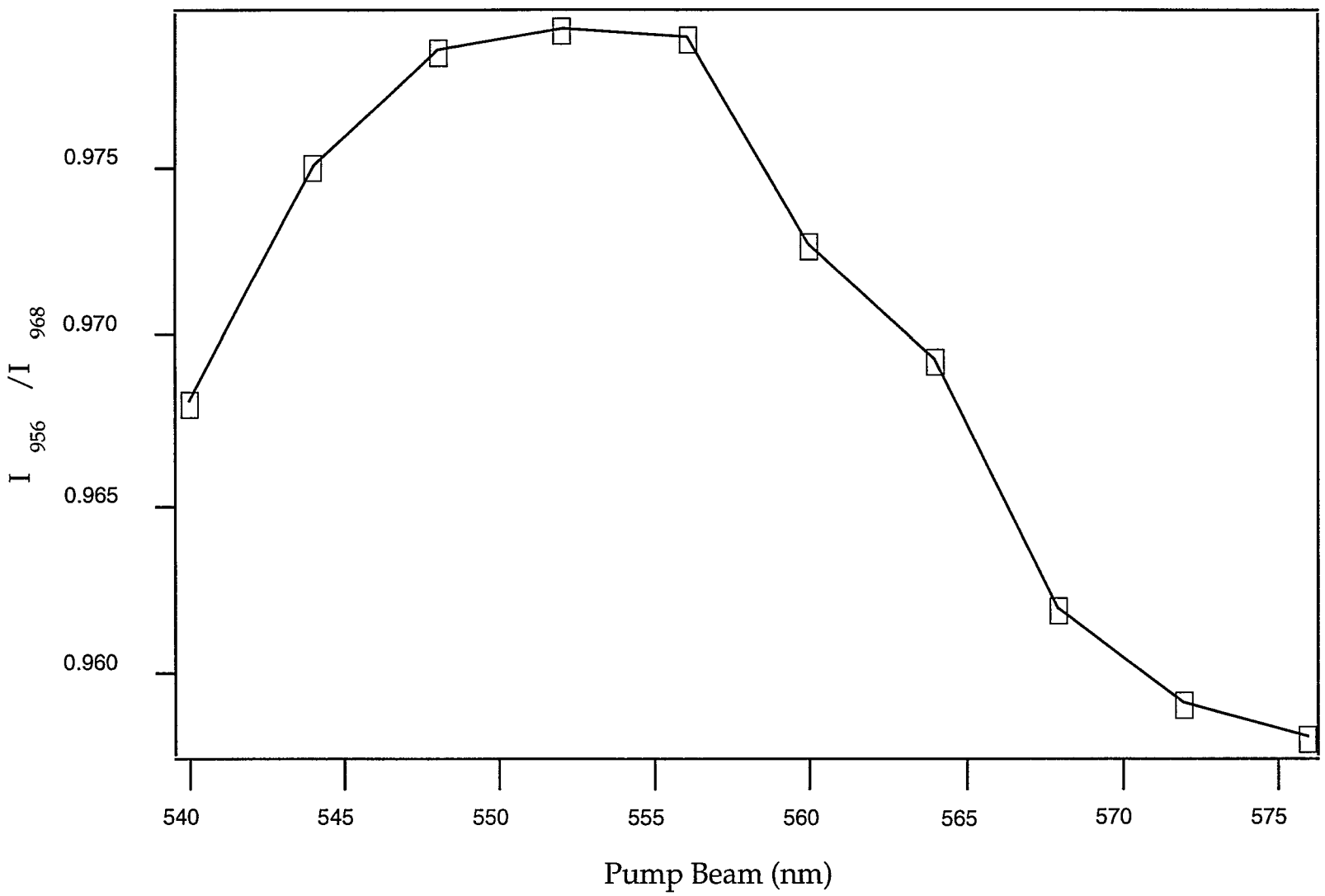
0.975
0.970
0.965
0.960
I 956 /I 968
540
545
550
555
560
565
570
575
Pump Beam (nm)

Figure 4.8: (a) resonance Raman spectrum of octopus rhodopsin with 457.9 nm probe only at 120 K.
(b) resonance Raman spectrum of octopus rhodopsin with 457.9 nm probe plus 553 nm pump at 120 K.
(c) resonance Raman spectrum of octopus rhodopsin with 457.9 nm probe plus 575 nm pump at 120 K.

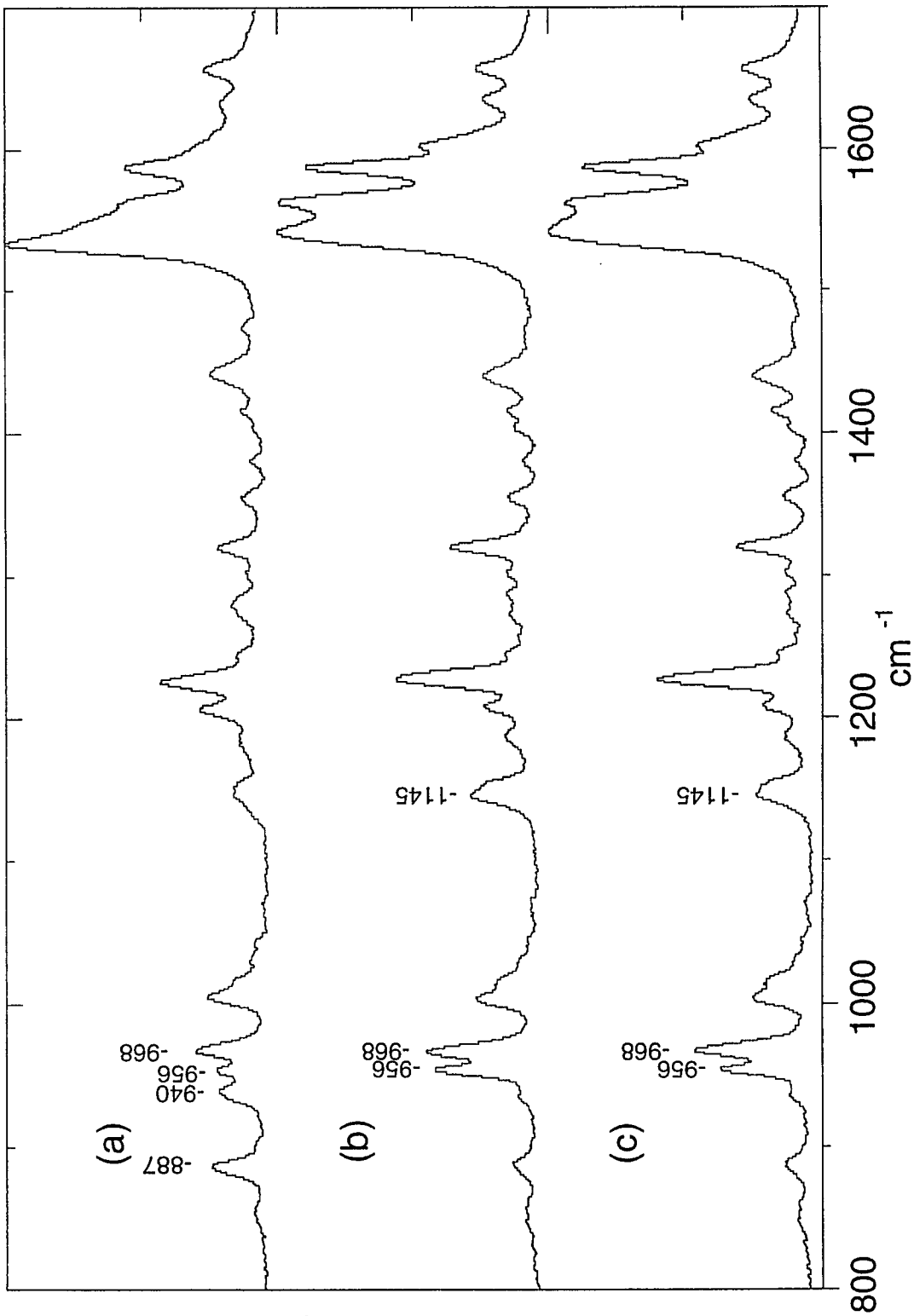
Raman Intensity
800
1000
1200
1400
1600
cm -1
(a)
-887
-940
-956
-968
(b)
-956
-968
-1145
(c)
-956
-968
-1145

Figure 4.9: (a) Figure 4.8(b) - Figure 4.8(a). Free of bathorhodopsin
(b) Figure 4.8(c) - Figure 4.8(a). Free of bathorhodopsin, with a different rhodopsin/isorhodopsin ratio from the spectrum in Figure 4.9(a) See text.
(c) Figure 4.9(b) - Figure 4.9(a). Pure rhodopsin.

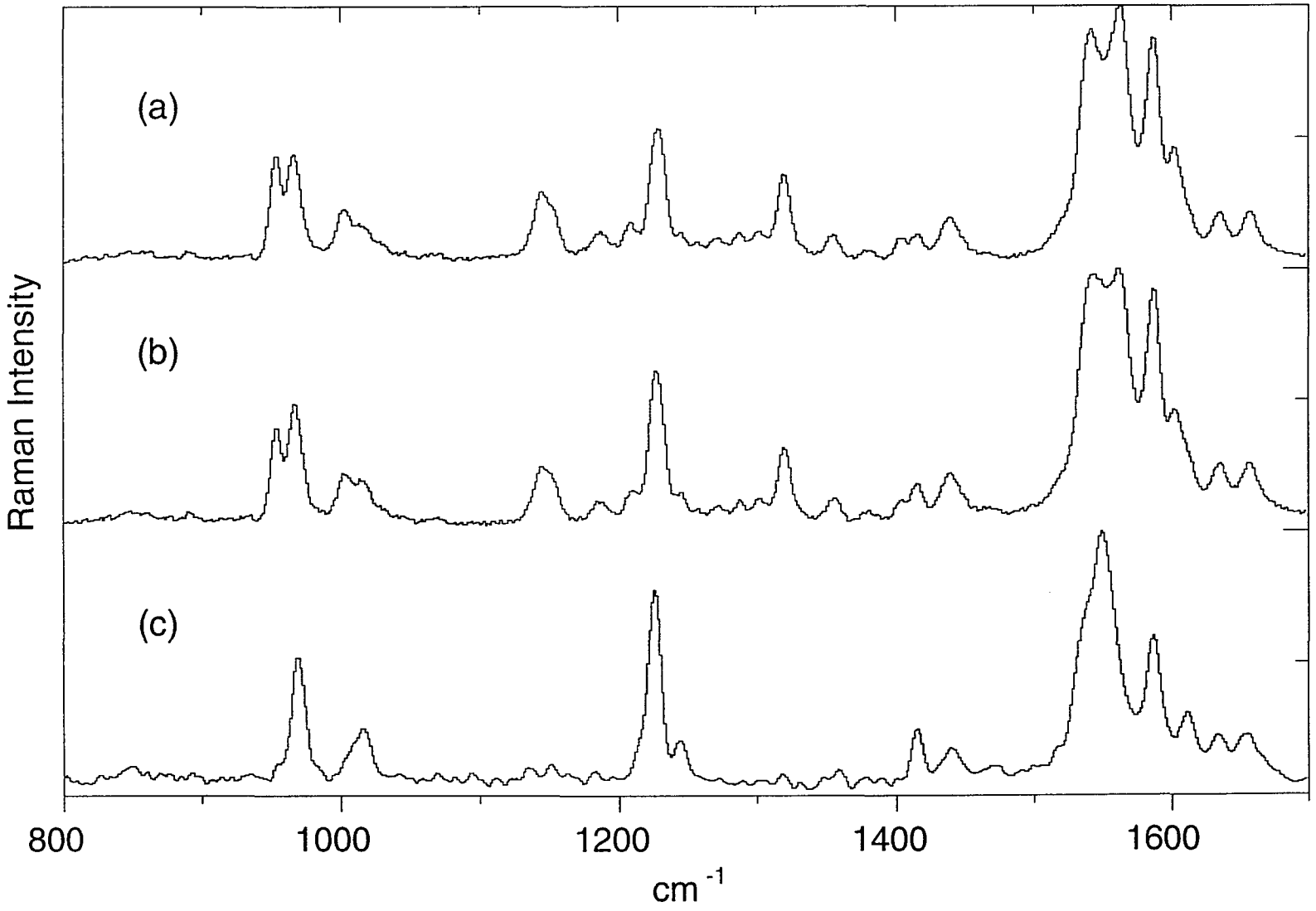
(a)
(b)
(c)
Raman Intensity
800
1000
1200
1400
1600
cm -1

Figure 4.10: (a) Figure 4.9(a) - Figure 4.9(b). Pure isorhodopsin.
(b) Figure 4.8(a) - Figure 4.10(a). Free of isorhodopsin.
(c) Figure 4.10(b) - Figure 4.9(c). Bathorhodopsin.

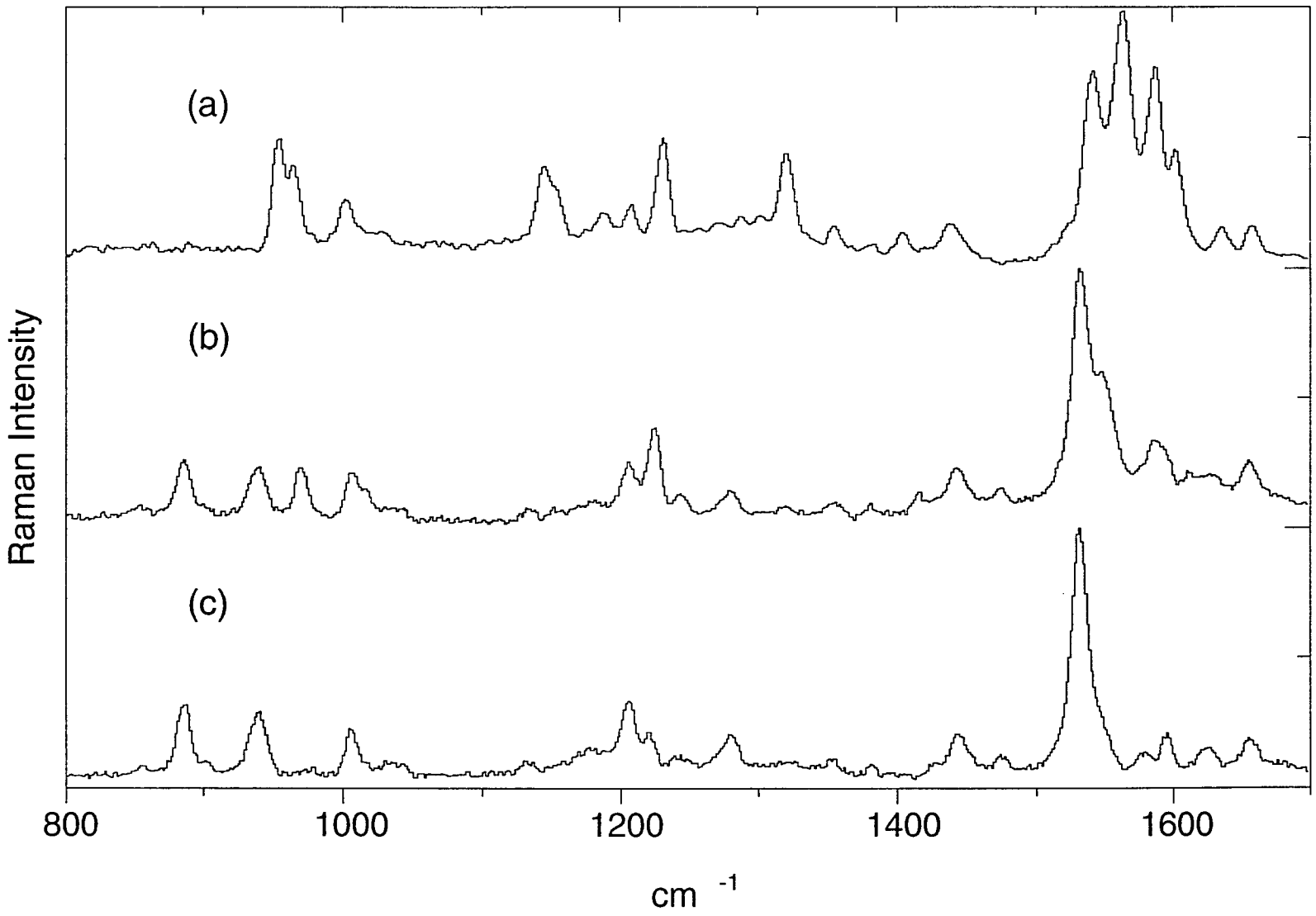
(a)
(b)
(c)
Raman Intensity
800
1000
1200
1400
1600
cm -1

Figure 4.11: Comparison of Resonance Raman spectra of octopus rhodopsin from (a) flow experiment at 10°C.
(b) pump-probe experiment at 120K (same as Figure 4.9(c)).
They are consistent to each other.

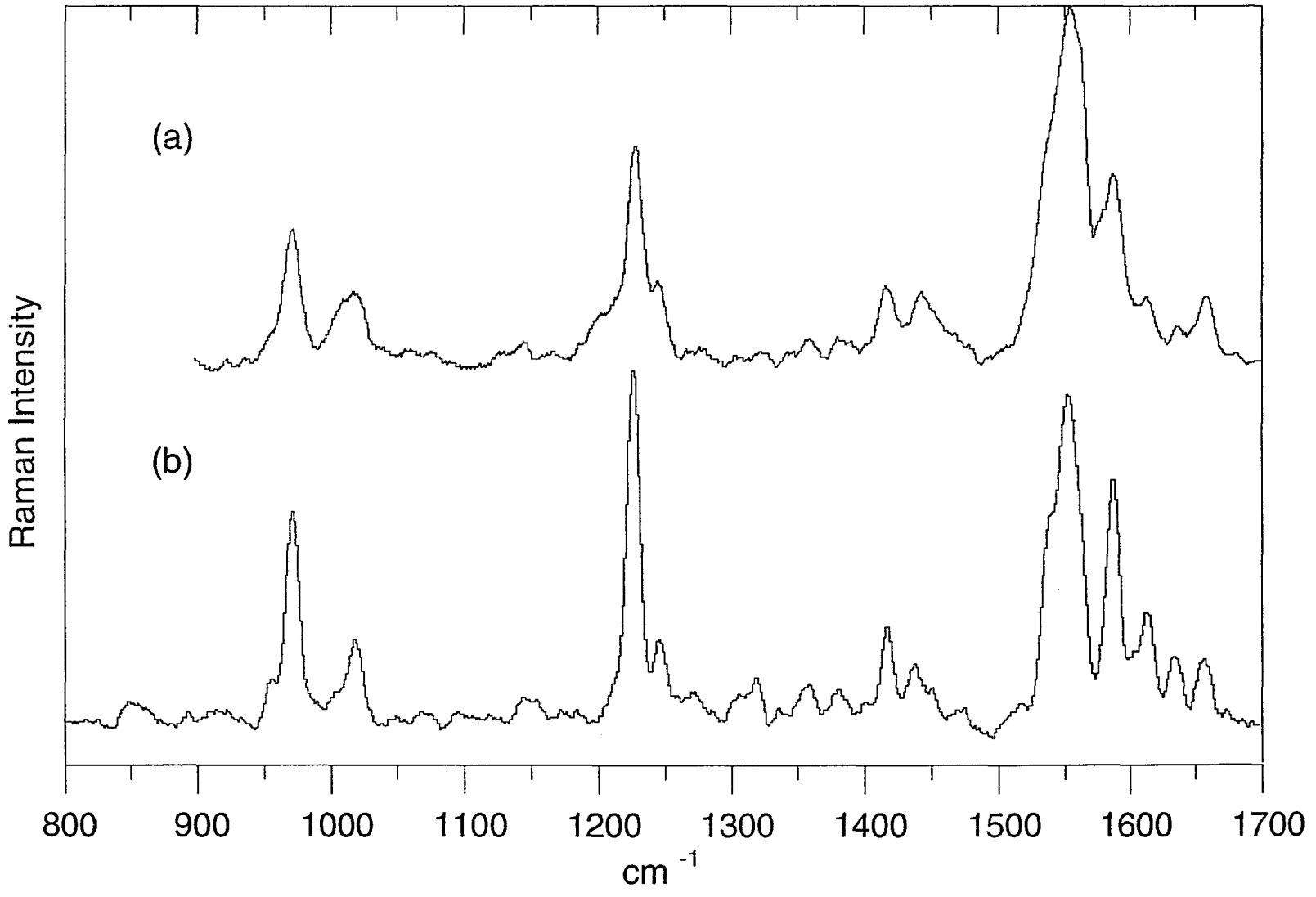
(a)
(b)
Raman Intensity
800
900
1000
1100
1200
1300
1400
1500
1600
1700
cm -1

Chapter 5

RESONANCE RAMAN STUDIES OF ^{13}C- AND ^{2}H- LABELED OCTOPUS RHODOPSIN, ISORHODOPSIN AND BATHORHODOPSIN FOR FINGERPRINT VIBRATIONS AND THE CHROMOPHORE STRUCTURE AND ENVIRONMENT

I. ABSTRACT

The resonance Raman spectrum of octopus rhodopsin in both the C-C stretch and CH bending region has been found to be very different from that found in either bovine rhodopsin or free 11-*cis* retinal Schiff base (Pande *et al.*, 1987; Deng *et al.*, 1991a; Deng *et al.*, 1991b). Recently, our laboratory has also found the fingerprint spectral region in octopus rhodopsin is changed substantially upon Schiff base deuteration in clear contrast to that in bovine rhodopsin. This suggests the 11-*cis* retinal chromophore in octopus rhodopsin has an unusual configuration and/or environment. In order to study the nature of the chromophore-opsin interaction in more detail, we have obtained the spectra of octopus rhodopsin and its 9-^{13}C, 10-D, 10,11-$^{13}C_2$, 12,13-$^{13}C_2$, 13-^{13}C, 14-D, 14,15-$^{13}C_2$, 14,15-$^{13}C_2$-N-D, and N-D isotopically labeled derivatives at 120 K using the 'pump-probe' technique. Our detailed analysis suggest that the retinal Schiff base C=N bond is anti, despite deuteration of the Schiff base inducing large changes in the finger print region of octopus resonance Raman

data. The Raman bands in the fingerprint region have been assigned on the basis of their isotopic shifts upon ^{13}C or deuterium labeling.

II. INTRODUCTION

The visual pigment, rhodopsin, consists of a single chromophore, 11-*cis* retinal, covalently bound in the form of a protonated Schiff base to the ε-amino group of lysine in the apoprotein opsin (e.g. Wald, 1968; Spiro, 1987; Birge, 1990). Vision is initiated when the chromophore absorbs a photon, and rhodopsin is isomerized to its primary photoproduct, bathorhodopsin. The transition of rhodopsin to bathorhodopsin is of primary concern in understanding the photophysics of vision, since it involves the conversion of the photon energy to the chemical energy responsible for visual transduction (Cooper, 1979; Honig *et al.*, 1979b; Cooper *et al.*, 1986). Our understanding of visual photochemistry results mostly from studies on bovine rhodopsin (Palings *et al.*, 1987; Palings *et al.*, 1989).

It was suggested that the separation of the positively charged chromophore Schiff base, $C_{15}=NH^+$, from its counterion in the isomerization process plays a key role in the primary photochemical event (Honig *et al.*, 1979b; Birge, 1990). The configuration of the $C_{15}=NH^+$ double bond, that is, whether it is cis or trans, is quite relevant to understand the energy conversion. Based on the resonance Raman study and normal mode calculation on bacteriorhodopsin, Smith *et al.* (1984) has suggested that the shift of the C_{14}-C_{15} stretching frequency upon deuteration on the Schiff base is an indicator of the C=N configuration, that is, this shift will be a small one (<5 cm^{-1}) if the C=N configuration is trans, while a large upshift from ~1144 to ~1206 cm^{-1} if the configuration is cis.

Regardless the frequency of the C_{14}-C_{15} stretch, this criterion may imply that the chromophore has a trans C=N configuration if no significant changes are

observed in the fingerprint region of the Raman spectrum upon the deuteration of the nitrogen in the Schiff base.

There are some interesting differences in the photochemical behavior of vertebrate and invertebrate pigments (Yoshizawa, 1972). Structural details of chromophore are now known for almost all the intermediates, including rhodopsin, bathorhodopsin and metarhodopsin, that are involved in the bovine bleaching process (Palings *et al.*, 1987; Palings *et al.*, 1989). In comparison, relatively little is known about invertebrate pigments and their intermediates.

Squid and octopus rhodopsin are conceivably the best characterized invertebrate pigments (Yoshizawa, 1972; Tsuda, 1979c; Tsuda *et al.*, 1980; Pande *et al.*, 1984; Tsuda *et al.*, 1986; Pande *et al.*, 1987; Ovchinnikov *et al.*, 1988; Deng *et al.*, 1991a; Deng *et al.*, 1991b). A comparative study of octopus and bovine rhodopsin is of importance because of the interesting similarities and differences between these two pigments. In general, both bovine and octopus rhodopsins contain 11-*cis* chromophores and the meta products of both species contain *trans* chromophores (Pande *et al.*, 1987). The bathorhodopsins of both species absorb at fundamentally the same wavelength (540 nm for octopus bathorhodopsin and 543 nm for bovine bathorhodopsin) (Tsuda *et al.*, 1980; Tsuda *et al.*, 1982). Both pigment systems absorb the energy of a single photon, at ca 55 kcal/mol, and convert the same fraction of this light energy, about 60%, to form the high-energy bathorhodopsin protein. However, there is a lager difference between the λ_{max}'s of octopus rhodopsin (λ_{max} = 472 nm) and bathorhodopsin (λ_{max} = 540 nm) compared to the bovine counterparts (500 and 543 nm, respectively). Also, unlike that of bovine, the chromophore-protein complex of octopus never dissociates (Tsuda, 1979c; Tsuda, 1982).

Resonance Raman spectroscopic studies have contributed more to our understanding of the geometry of the protein-bound chromophores than any

other spectroscopic investigations (Birge, 1990). The visual sequence of changes has been studied both by kinetic methods and by trapping the various intermediates at low temperatures. Our previous work has shown that the resonance Raman spectra of the two rhodopsins are very different as are the spectra of the two batho products (Pande *et al.*, 1987; Deng *et al.*, 1991a; Deng *et al.*, 1991b). In order to understand how those differences in spectra relate to chromophore structure, we performed a series of resonance Raman measurements of octopus bathorhodopsin where the chromophores have been isotopically labeled by deuterium at virtually every chromophore hydrogen position one by one. This has led to an understanding of bathorhodopsin's HOOP modes showing that the (presumably *trans*) chromophore is twisted differently in octopus bathorhodopsin than in bovine bathorhodopsin and suggesting that the specific active site interactions between chromophore and protein are quite different for the two species (Deng *et al.*, 1991a).

The fingerprint region of octopus rhodopsin spectrum of the N-D derivative is very different from the that of native sample [see Figure 5.2(b)]. Based on the above discussion about the C=N configuration, at first we jumped to the conclusion that octopus rhodopsin has a cis C=N configuration which is different from bovine rhodopsin. However, there are two contradicts with this assignments. First, if the upshift band observed in the N-D derivative is really the C_{14}-C_{15} stretching mode, it is too high because it is supposed at about 1150 cm^{-1}. Second, the shift is only 20 cm^{-1} which is too small compared to the expected ~50 cm^{-1}.

In this chapter we continue this work by reporting on how the resonance Raman bands of octopus rhodopsin, bathorhodopsin and isorhodopsin in the fingerprints region are affected by deuterium and ^{13}C labeling of chromophore backbone at: 9-^{13}C, 10-D, 10,11-$^{13}C_2$, 12,13-$^{13}C_2$, 13-^{13}C, 14-D, 14,15-$^{13}C_2$,

14,15-$^{13}C_2$-N-D, and N-D. Analysis of these data allows us to tentatively assign some bands to vibration modes and obtain some conclusions of the chromophore structure, based on the assignments. Along with the result of the recent vibrational analysis of a retinal protonated Schiff base analog (Deng *et al.*, 1994b), we conclude that the C=N configuration of octopus rhodopsin is trans despite the changes in the fingerprint region of the resonance Raman spectrum upon nitrogen deuterated.

III. MATERIALS AND METHODS

The synthesis and characterization of the 9-^{13}C, 10-D, 10,11-$^{13}C_2$, 13-^{13}C, 14-D, 14,15-$^{13}C_2$, 14,15-$^{13}C_2$-N-D, and N-D retinals of either 11-*cis* or 9-*cis* configurations were described by Lugtenburg *et al.* (1988). Octopus microvillar membranes were prepared and bleached as previously described (Koutalos *et al.*, 1989; Deng *et al.*, 1991a).

The labeled chromophores in ethanol were added to 10 mL opsin suspension with a retinal/opsin molar ratio of 1.2:1. After incubation for 60 min. at room temperature, 50 µl of 2.0 M hydroxylamine, pH 6.5, was added to the suspension. The regenerated membranes were washed once with 5 mM Tris buffer, pH 7.2, then twice with 4% bovine serum albumin (fatty acid free, Sigma Chemical Co., St. Louis, MO) in 5 mM Tris, pH 7.2, to remove excess chromophore. After a final wash with 5 mM Tris, pH 7.2, the membranes were stored at -60°C until further use. Approximately 60% of the opsin was regenerated using this procedure. No difference was observed in the Raman spectra of the native pigment and that regenerated with 11-*cis* or 9-*cis* unlabeled retinals. All operations are carried out in dim red light.

Resonance Raman spectroscopy has been widely used to obtain direct information on the chromophore structures of visual pigments. The use of low-

temperature studies, coupled with the pump-and-probe technique, allows the studies of the rhodopsin, isorhodopsin and bathorhodopsin. The resonance Raman experiments were performed at 120K in a liquid nitrogen coldfinger Dewer, as previously described (Oseroff and Callender, 1974; Deng *et al.*, 1991a), with the dual-beam pump-probe technique. The native or deuterated membranes were centrifuged to a thick pellet that was applied to the sample tip of the coldfinger and then cooled down to 120 K. The photostationary mixtures of rhodopsin (λ_{max} = 472 nm), isorhodopsin (λ_{max} = 462 nm), and bathorhodopsin (λ_{max} = 540 nm) at 120K were obtained and their Raman spectra taken with the "probe" beam (457.9 nm line from an Ar+ laser). The composition of the mixture can be changed by simultaneously irradiating the sample with the second high-intensity "pump" laser beams (e.g. in the experiments described here, 553 nm or 575 nm from a dye laser). For each sample, three Raman spectra were taken: The first was a probe-only spectrum with 57% bathorhodopsin, 22% rhodopsin and 21% isorhodopsin (Pande *et al.*, 1987). The second was a pump-probe (457.9 nm - 553 nm) with a pump/probe intensity ratio of 40:1. According to the analysis in Chapter 4, this pump will give a composition of 22% bathorhodopsin, 28% rhodopsin and 50% isorhodopsin. The third was also a pump-probe (457.9 nm - 575 nm) with a pump/probe intensity ratio of 50:1, determining the composition with 22% bathorhodopsin, 40% rhodopsin and 38% isorhodopsin. The above percentages are with about 3% deviation from estimation. Therefore, it is possible to obtain almost pure bathorhodopsin by subtracting the appropriate amount of the second spectrum from the first spectrum. And by subtracting the appropriate amount of bathorhodopsin from the second and the third spectrum. Two rhodopsin/isorhodopsin mixed spectra with different rhodopsin/isorhodopsin ratios were obtained. Rhodopsin and

isorhodopsin spectra were finally obtained by subtracting the mixture spectra each from the other.

IV. RESULTS AND DISCUSSION

The bands in the fingerprint region of octopus bathorhodopsin, rhodopsin and isorhodopsin Raman spectra can be assigned to specific C-C stretching modes based on its isotopic shift described in detail as following.

Bathorhodopsin

Figure 5.1 shows the resonance Raman spectra of octopus (a) bathorhodopsin and its (b) ND, (c) 9-^{13}C, (d) 10-D, (e) 10,11-$^{13}C_2$, (f) 13-^{13}C, (g) 14-D, (h) 14,15-$^{13}C_2$ and (i) 14,15-$^{13}C_2$ ND derivatives. In the 1100-1250 cm^{-1} fingerprint region, the isotopic shifts of the modes are presented in Table 5.1. The band of 1151 cm^{-1} in the spectrum of 10,11-$^{13}C_2$ derivative can be assigned to the $^{13}C_{10}$-$^{13}C_{11}$ stretch on the basis isotopic shift. In bovine bathorhodopsin, this stretch is at 1166 cm^{-1} in the native sample, and 1154 cm^{-1} in 10,11-$^{13}C_2$ derivative (Palings *et al.*, 1987). The C_{10}-C_{11} stretch may be then assigned to 1179 cm^{-1} in the native octopus bathorhodopsin, since it is not very clear to see intensity loss in the spectra. The C_{14}-C_{15} stretch is assigned to 1205 cm^{-1} due to the 19 cm^{-1} shift in the 14,15-$^{13}C_2$ derivative. The 12 cm^{-1} downshift of the 1222 cm^{-1} band can be interpreted as this band is coupled with the C_{14}-C_{15} stretch in the native bathorhodopsin, "pushed up" about 10 cm^{-1}. The ^{13}C- induced shifts may also be small and delocalized over several normal modes, e.g. C_8-C_9 (or C_{12}-C_{13}) where the stretching character is delocalized(Palings *et al.*, 1987). In this case, the strong characteristic coupling of the $C_{10}H$ (or $C_{14}H$) rock with the C_8-C_9 (or C_{12}-C_{13}) stretching coordinate will be used to assign the "C_8-C_9 mode" (or "C_{12}-C_{13} mode") (Palings *et al.*, 1987). By this method, explained previously, it

has been tentatively suggested that the C_{10}-C_{11}, C_{14}-C_{15}, C_8-C_9 and C_{12}-C_{13} stretches are assigned to 1179, 1206, 1206 (unresolved) and 1241 cm^{-1}, respectively, based on the spectra of deuterium substituted derivatives (Deng *et al.*, 1991b). Here we find that the new data obtained from ^{13}C labeled chromophores can confirm the first two assignments, but cannot give new information about the latter two ones. For the coupling consideration, the C_8-C_9 stretch is assigned to 1243 cm^{-1} on the basis of 75 cm^{-1} upshift in 10-D derivative. Since the C_8-C_9 stretch mode upshifts, the coupling between the C_{14}-C_{15} stretch and the C_8-C_9 is removed, resulting a upshift of the C_{14}-C_{15} stretch to 1212 cm^{-1}. The C_{12}-C_{13} stretch is assigned to 1222 cm^{-1} on the basis of its 87 cm^{-1} upshift in 14-D derivative.

Rhodopsin

The resonance Raman spectra of octopus (a) rhodopsin and its (b) ND, (c) 9-^{13}C, (d) 10-D, (e) 10,11-$^{13}C_2$, (f) 13-^{13}C , (g) 14-D, (h)14,15-$^{13}C_2$ and (i) 14,15-$^{13}C_2$ ND derivatives are shown in Figure 5.2. The isotopic shifts in the fingerprint region are presented in Table 5.2. The C_8-C_9 stretch is delocalized at 1226 and 1245 cm^{-1} demonstrated by the loss intensity of the band at 1226 cm^{-1} and the disappearance of 1245 cm^{-1} in the 10-D derivative. There are no significant changes observed in the fingerprint regions of 9-^{13}C, 10,11-$^{13}C_2$, 12,13-$^{13}C_2$ (data not shown) derivatives. A moderate band appears at 1146 cm^{-1} and a small band at 1189 cm^{-1} in the 13-^{13}C derivative. The 1146 cm^{-1} band is interpreted to be the C_{10}-C_{11} stretch which is decoupled from the C_{12}-C_{13} stretch. The C_{10}-C_{11} stretch should be in the range of 1146-1150 cm^{-1} in the native spectrum, if the coupling between the C_{10}-C_{11} and the C_{12}-C_{13} is small. This assumption may be true since the spectra of 10,11-$^{13}C_2$ and 12,13-$^{13}C_2$ are very similar to that of native in the fingerprint region. The 14-D derivative spectrum

clearly indicates that the C_{12}-C_{13} stretch is located in the 1226 cm^{-1} band since some intensity of this band shifts to 1293 cm^{-1}. The C_{14}-C_{15} stretching character is localized in the 1226 cm^{-1} mode as indicated by the 18 cm^{-1} shift of this line in the 14,15-$^{13}C_2$ derivative. The 1243 cm^{-1} line can be characterized as the C_8-C_9 stretch on the basis of the 69 cm^{-1} upshift in the 10-D derivative.

Isorhodopsin

Figure 5.3 shows the resonance Raman spectra of octopus (a) isorhodopsin and its (b) ND, (c) 9-^{13}C, (d) 10-D, (e) 10,11-$^{13}C_2$, (f) 13-^{13}C, (g) 14-D, (h)14,15-$^{13}C_2$ and (i) 14,15-$^{13}C_2$ ND derivatives. Table 5.3 presents the isotopic shifts in the fingerprint region of octopus isorhodopsin. The C_{10}-C_{11} stretch is assigned to 1144 cm^{-1} on the basis of the 14 cm^{-1} shift in the 10,11-$^{13}C_2$ derivative. A new band appears at 1280 cm^{-1}, with some band intensity losses at 1186 cm^{-1} in the 10-D derivative. Thus the band at 1186 cm^{-1} is assigned to C_8-C_9 stretch. The new band appearing at 1307 cm^{-1} in the 10D derivative can be interpreted as coupling with the upshifted C_8-C_9 stretch and "pushed up" from 1288 or 1300 cm^{-1}. The C_{14}-C_{15} stretch is assigned to the 1209 cm^{-1} mode as indicated by the 13 cm^{-1} shift of this line in the 14,15-$^{13}C_2$ derivative, whose spectrum also shows the C_{14}-C_{15} stretch to have some contribution to the band at 1229 cm^{-1}, owing to the loss of intensity. The C_{12}-C_{13} stretch is assigned to 1229 cm^{-1} on the basis of the 58 cm^{-1} upshift in 14-D derivative.

C=N Configuration

It has been reported that C_{14}-C_{15} stretch mode frequency and its shift upon Schiff base deuteration is sensitive to the C=N configuration (Smith *et al.*, 1984). Empirical and semi-empirical normal mode calculations have shown that a trans C=N configuration results in a small shift (~5 cm^{-1}) of the C_{14}-C_{15} stretch

(~1200 cm^{-1}) upon N-deuteration, whereas a large (~50 cm^{-1}) shift (from ~1150 cm^{-1}) is observed when the C=N configuration is syn (Smith *et al.*, 1984). Based on this rule, we can easily conclude that C=N configurations of both bathorhodopsin and isorhodopsin are *anti* because of the invariance of the C14-C15 stretch upon N-deuteration. This rule, however, can not apparently cover the case observed in octopus rhodopsin in which the C_{14}-C_{15} frequency and its deuteration shift in octopus rhodopsin Raman spectra are anomalous.

Recently, a vibrational analysis of a retinal protonated Schiff base analog has been conducted using Raman measurements to characterize this Schiff base and its isotopically labeled derivatives, and by calculations using *ab initio* methods (Deng *et al.*, 1994b). This analog contains one C=C double bond which is in conjugation with the C=N bond. Our results show that for the C=N *anti* configuration, the C_{14}-C_{15} stretch is at about 1230 cm^{-1} and upon Schiff base deuteration, this mode shifts up by 15 cm^{-1} or more, with its intensity reduced. For the C=N *syn* configuration, the calculated C_{14}-C_{15} stretch is about 85 cm^{-1} below the C_{14}-C_{15} stretch in C=N anti configuration, and the predicted shift of this mode upon Schiff base deuteration is positive by ~50-60 cm^{-1}. The observed C_{14}-C_{15} stretch frequency and its shift upon Schiff base deuteration in the octopus rhodopsin spectra are analogous to that observed in this Schiff base model compound. This suggests that the coupling among C-C stretches are greatly disturbed, so that C_{14}-C_{15} stretching mode becomes much more localized. On the basis of this study, we suggest that the C=N configuration in octopus rhodopsin is *anti*.

Single Bond Conformations in Bathorhodopsin

The frequency of a C-C stretching mode in an s-*cis* structure is expected to be ~100 cm^{-1} below that of its s-trans conformer (Smith *et al.*, 1986). Since the

C10-C11 (1179 cm^{-1}) and C14-C15 (1206 cm^{-1}) stretches of bathorhodopsin are 20 and 1 cm^{-1} above their frequencies in the all-trans PSB (1159 cm^{-1} and 1205 cm^{-1}, see Palings *et al.*, 1987), respectively, it is easily concluded that both C_{10}-C_{11} and C_{14}-C_{15} are s-*trans*.

Comparison to the C-C stretching modes of PSB retinals

The fingerprint correlation diagrams for bathorhodopsin, rhodopsin and isorhodopsin with their counterpart PSB retinals are displayed in Charts 5.1 - 5.3, respectively. Data of PSB retinals are from Palings *et al.*, 1987. We would like to stress that the above assignments are mostly tentative because of the lack of normal modes calculation. The data shown in Charts 5.1 - 5.3 suggest that either the force constants of C-C stretch in octopus are very different from that of free PSB retinals, or the assignments need to be confirmed by further data.

Conformation of Rhodopsin

One of the most interesting characteristics of octopus rhodopsin is the intense band in the fingerprint region. Without the help of normal mode calculations, we have tentatively assigned it to the mixing of C_{14}-C_{15} and C_{12}-C_{13} stretches, with some probable contribution from the C_8-C_9 stretch. Based on these data, combined with other resonance Raman data using deuterium and ^{13}C labeled retinal chromophore, we propose that the portion from β-ionyl ring to C_{12} of the ethylenic chain with the methyl group of octopus rhodopsin is somewhat tightly embedded in the protein binding pocket. This proposal has some support. First, almost no changes are observed in the fingerprint region of the rhodopsin spectra of 9-^{13}C, 10,11-$^{13}C_2$, 12,13-$^{13}C_2$ derivatives. Low resonance Raman intensity indicates that the relaxation of the rhodopsin vertically excited state does not involve the displacement of the equilibrium

points of those atoms. This will probably happen if there are some nonbonding interaction between the chromophore and the environment apoprotein. Second, the similarity of the frequency and Schiff base deuteration behavior of the C_{14}-C_{15} stretch mode of the octopus rhodopsin to that of the model compound which only contains one C-C single bond and one C=C double bond may hint that only the C_{13}=C_{14}-C_{15}=N part of the octopus rhodopsin chromophore is relatively free. Third, the frequency of the C_{14}-C_{15} stretch of octopus rhodopsin (1226 cm^{-1}) is much higher than that of the PSB and bovine rhodopsin, both 1190 cm^{-1} (Palings *et al.*, 1987). The reason for a high frequency of a single bond would be a large force constant which could be introduced by the changes of the CCC angles. Part of the chromophore embedment will usually procure this CCC angle changes. Fourth, the spectrum of octopus rhodopsin regenerated with 15-D labeled retinal chromophore shows that most of the intensity of the 1226 cm^{-1} band upshifts 12 cm^{-1} after the 15-D substitution (data not shown). This would be hard to understand if no part of the chromophore is tightly embedded. Finally, the flexibility in C6-C7 single bond allows this embedment (Honig *et al.*, 1971).

We wish to stress that the above proposal about the chromophore of octopus rhodopsin is qualitatively tentative because the lack of the calculation of the normal mode owing to the limitations of the calculation speed and the disk space. We propose to do the calculation first on a model compound. This work is currently in progress. We have hopes the specific model obtained after normal mode calculation will fit the experimental data and explain the cause of the anomalous 1226 cm^{-1} band and low λ_{max} by comparison to that of bovine.

Table 5.1 Bathorhodopsin Vibrational Frequencies

derivative	fingerprint frequency (cm^{-1})			
native	1179	1206	1222	1243
9-^{13}C	1177(-2)	1204(-2)	1225(+3)	1243(0)
10,11-$^{13}C_2$	1151(-28)	1204(-2)	1223(+1)	1240(-3)
12,13-$^{13}C_2$	1167(-12)	1205(-1)	1221(-1)	1238(-5)
13-^{13}C	1168(-11)	1207(+1)	1222(0)	1239(-4)
14,15-$^{13}C_2$	1169(-10)	1187(-19)	1210(-12)	1246(+3)
10-D	1168(-11)	1227(+21)	-	1318(+75)
14-D	1155(-24)	1213(+7)	1309(+87)	1244(+1)

Table 5.2 Rhodopsin Vibrational Frequencies

derivative	fingerprint frequency (cm^{-1})			
native		1226	1226	1243
9-^{13}C		1228(+2)	1228(+2)	1247(+4)
10,11-$^{13}C_2$		1226(0)	1226(0)	1243(0)
12,13-$^{13}C_2$		1224(-2)	1224(-2)	1245(+2)
13-^{13}C	1146	1225(-1)	1206(-20)	1239(-4)
14,15-$^{13}C_2$	1171	1208(-18)	1223(-3)	1243(0)
10-D	1140	1221(-5)	1221(-5)	1295(+69)
14-D	1176	1223(-3)	1293(+67)	1244(+1)

Table 5.3 Isorhodopsin Vibrational Frequencies

derivative	fingerprint frequency (cm^{-1})			
native	1144	1186	1209	1229
9-^{13}C	1144(0)	1183(-3)	1211(+2)	1234(+5)
10,11-$^{13}C_2$	1130(-14)	1186(0)	1208(-1)	1232(+3)
12,13-$^{13}C_2$	1142(-2)	1187(+1)	1206(-3)	1230(+1)
13-^{13}C	1143(-1)	1185(-1)	1207(-2)	1231(+2)
14,15-$^{13}C_2$	1143(-1)	1186(0)	1196(-13)	1228(-1)
10-D	1140(-4)	1280(+94)	1221(-5)	1228(+1)
14-D	1143(0)	1226(+30)	1209(0)	1287(+58)

Table 5.4 Schiff Base Frequencies in H_2O and D_2O

	C=NH	C=ND	
pigment	(cm^{-1})	(cm^{-1})	shift (cm^{-1})
rhodopsin	1656	1632	24
bathorhodopsin	1656	1626	30
isorhodopsin	1659	1637	22

Figure 5.1: The resonance Raman spectra of octopus (a) bathorhodopsin and its (b) ND, (c) 9-^{13}C, (d) 10-D, (e) 10,11-$^{13}C_2$, (f) 13-^{13}C, (g) 14-D, (h) 14,15-$^{13}C_2$ and (i) 14,15-$^{13}C_2$ ND derivatives.

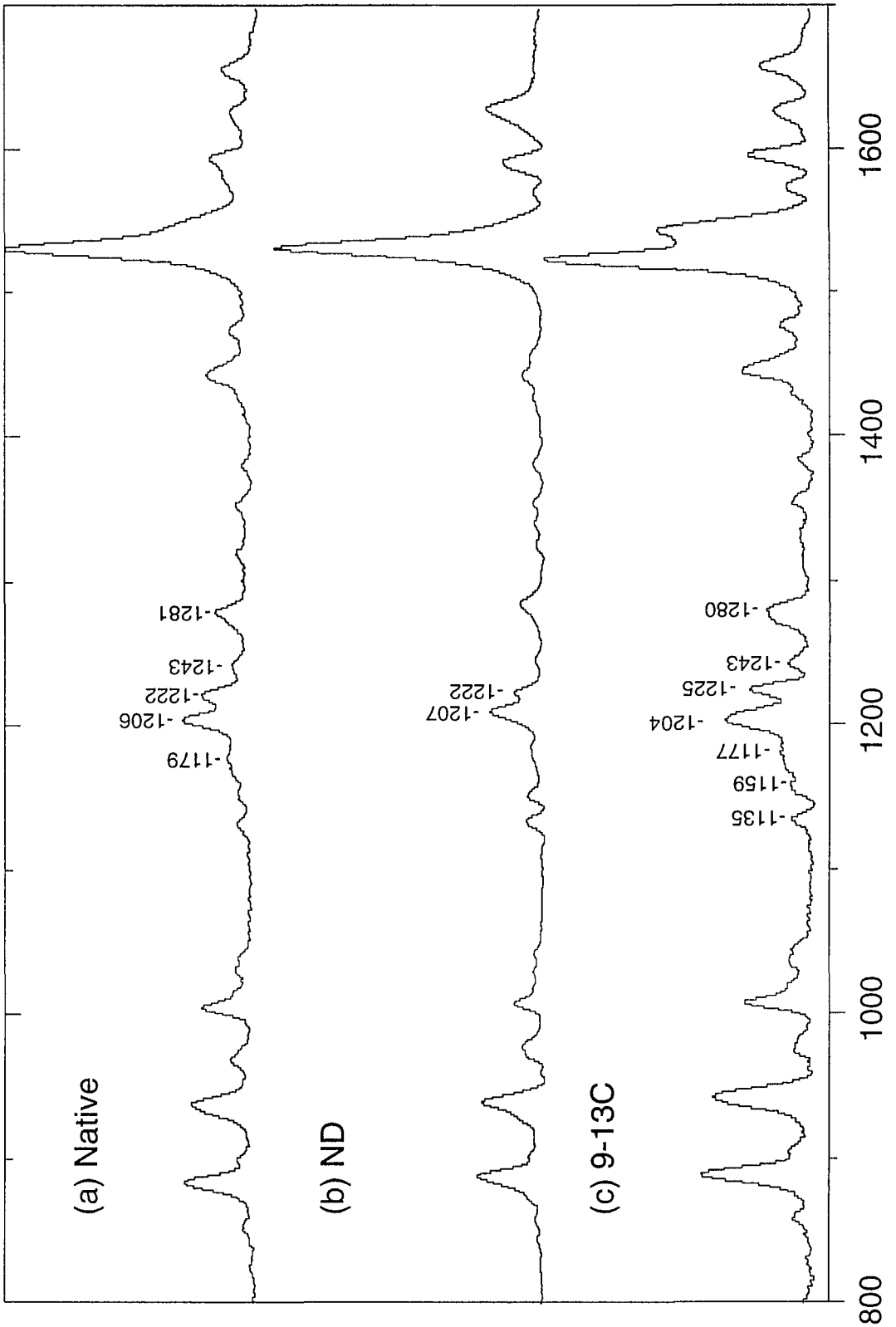
(a) Native
-1179
-1206
-1222
-1243
-1281
(b) ND
-1207
-1222
(c) 9-13C
-1135
-1159
-1177
-1204
-1225
-1243
-1280
800
1000
1200
1400
1600

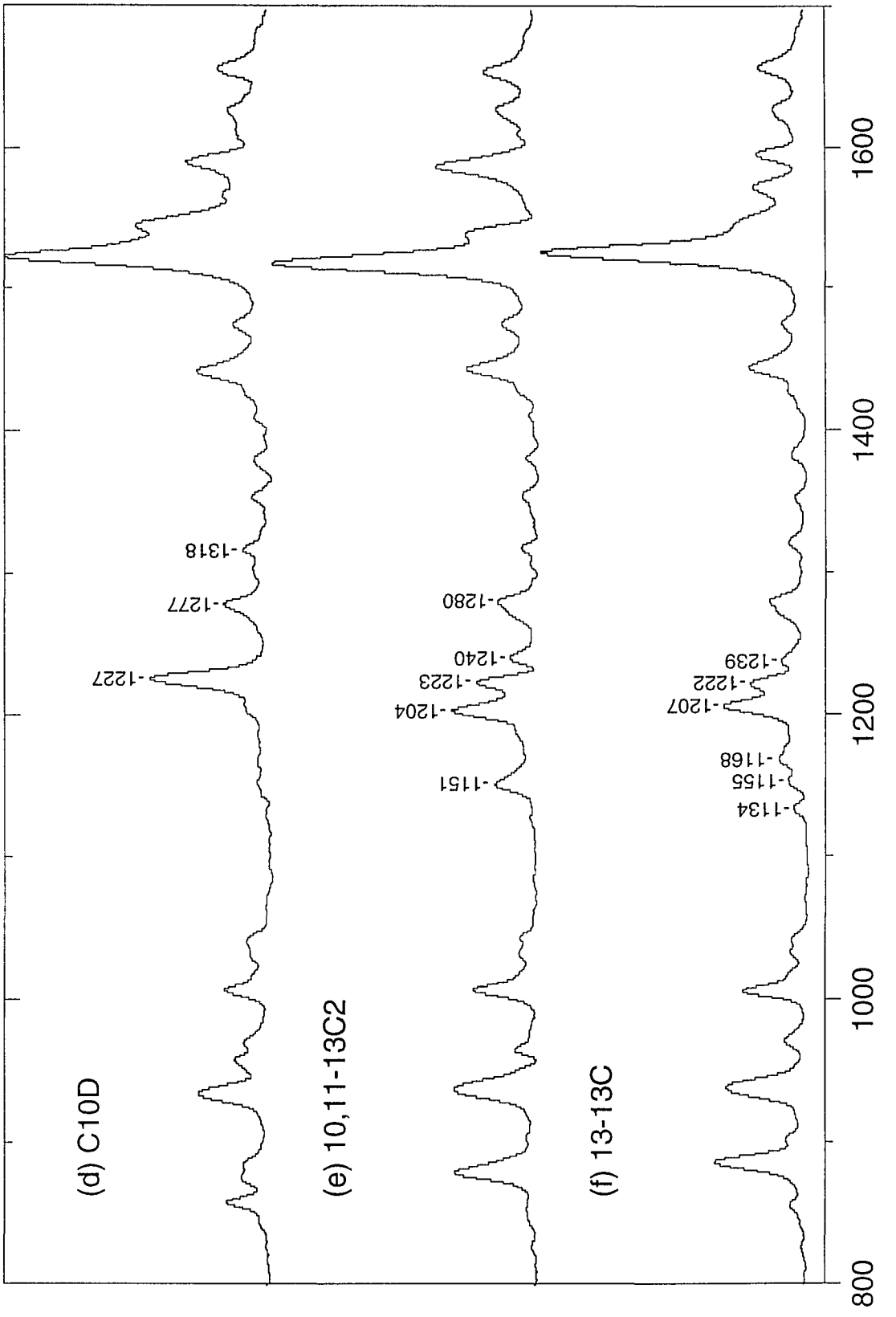
(d) C10D
-1318
-1277
-1227
(e) 10,11-13C2
-1280
-1240
-1223
-1204
-1151
(f) 13-13C
-1239
-1222
-1207
-1168
-1155
-1134
800
1000
1200
1400
1600

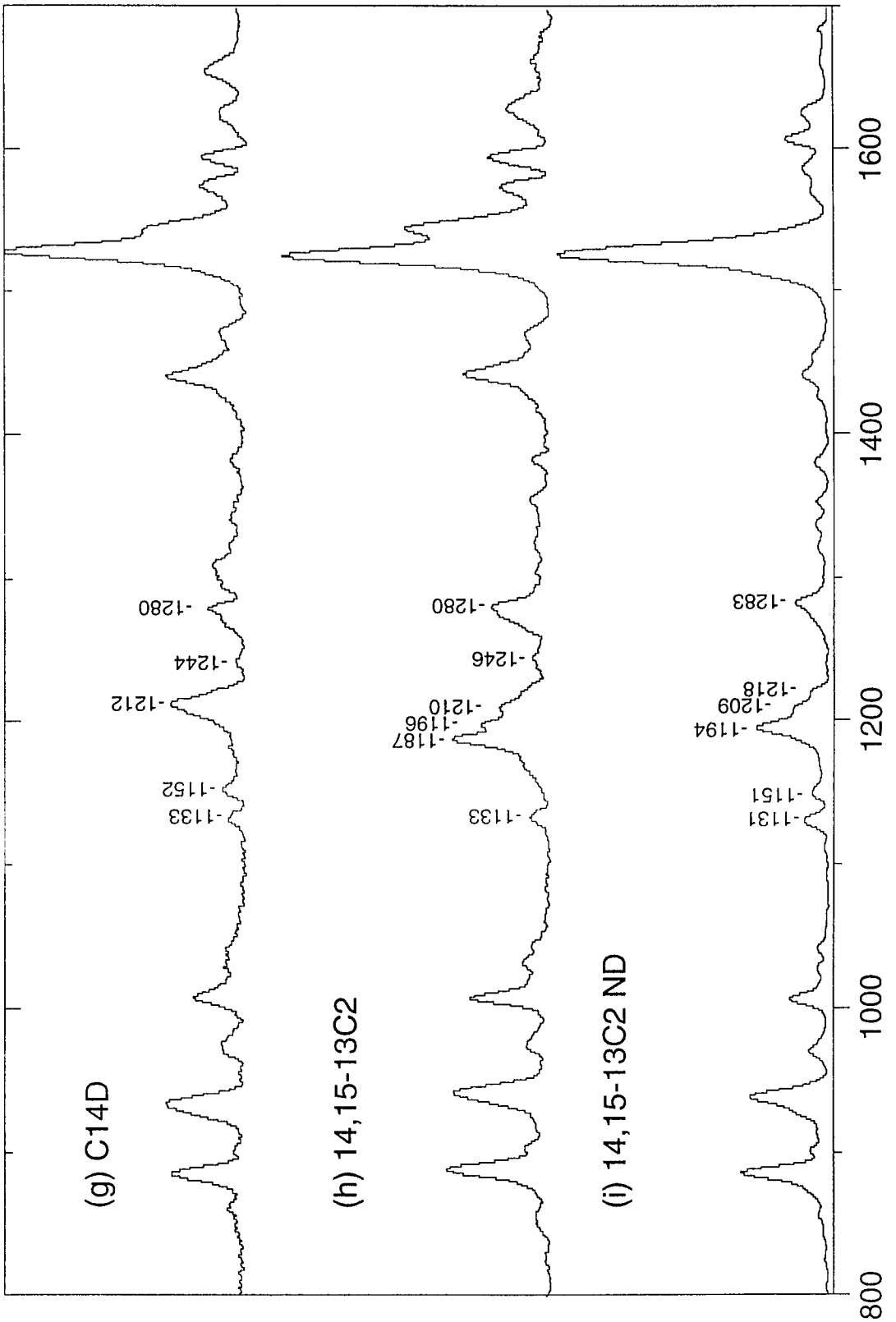
(g) C14D
(h) 14,15-13C2
(i) 14,15-13C2 ND
1133
1152
1212
1244
1280
1133
1187
1196
1210
1246
1280
1131
1151
1194
1209
1218
1283
800
1000
1200
1400
1600

Figure 5.2: The resonance Raman spectra of octopus (a) rhodopsin and its (b) ND, (c) 9-^{13}C, (d) 10-D, (e) 10,11-$^{13}C_2$, (f) 13-^{13}C, (g) 14-D, (h)14,15-$^{13}C_2$ and (i) 14,15-$^{13}C_2$ ND derivatives

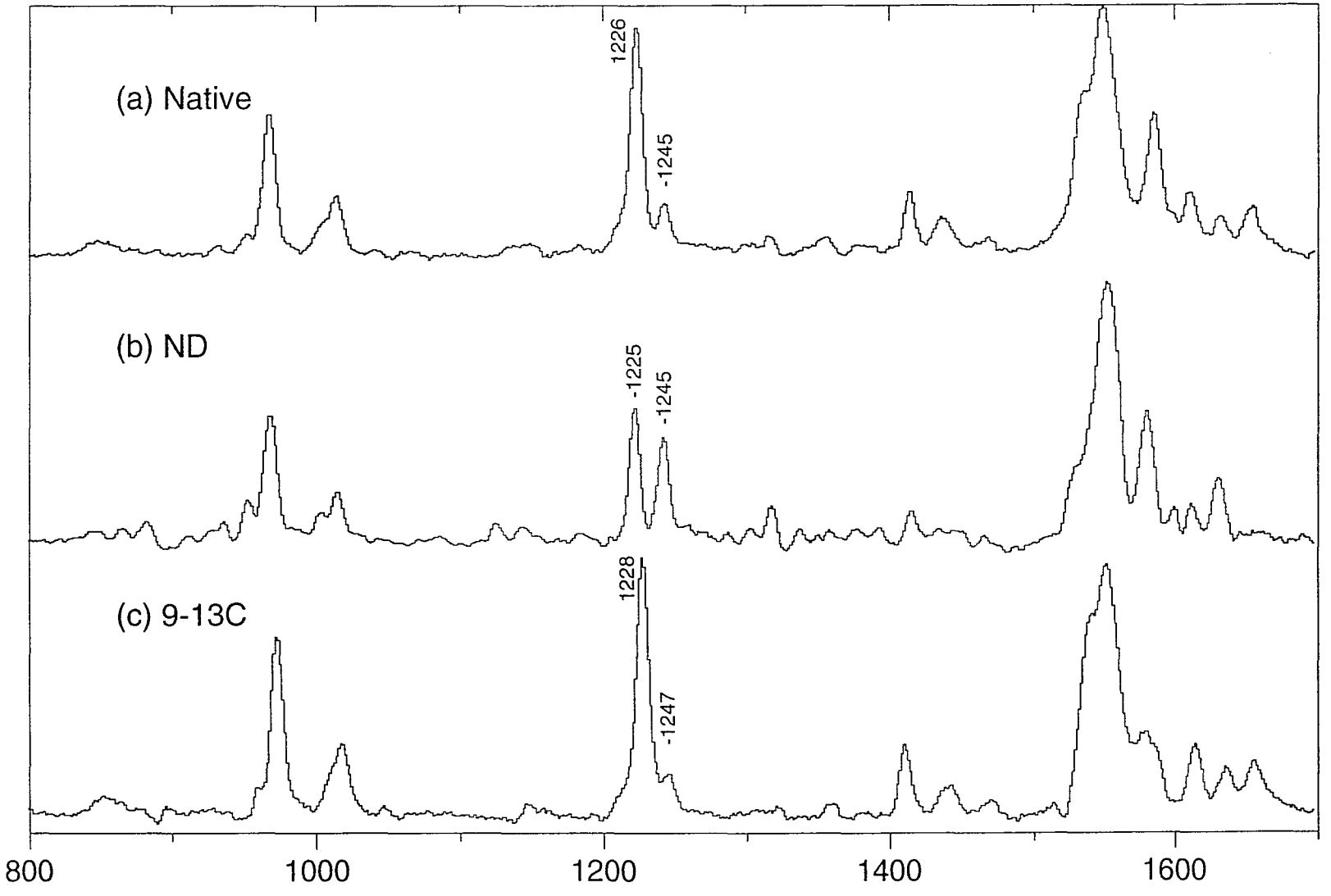
(a) Native
1226
-1245
(b) ND
-1225
-1245
(c) 9-13C
1228
-1247
800
1000
1200
1400
1600

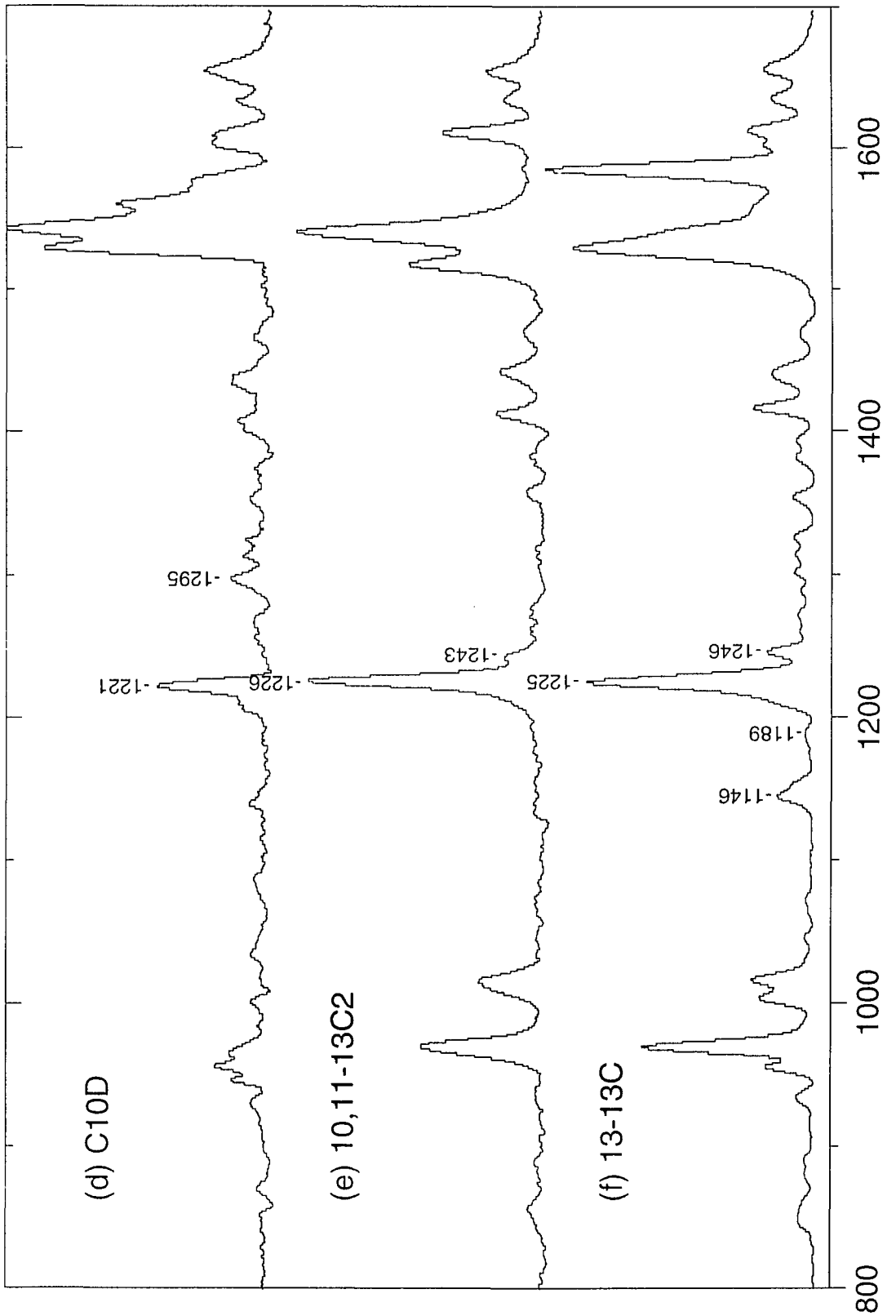
(d) C10D
(e) 10,11-13C2
(f) 13-13C
1221
1226
1295
1225
1243
1246
1146
1189
800
1000
1200
1400
1600

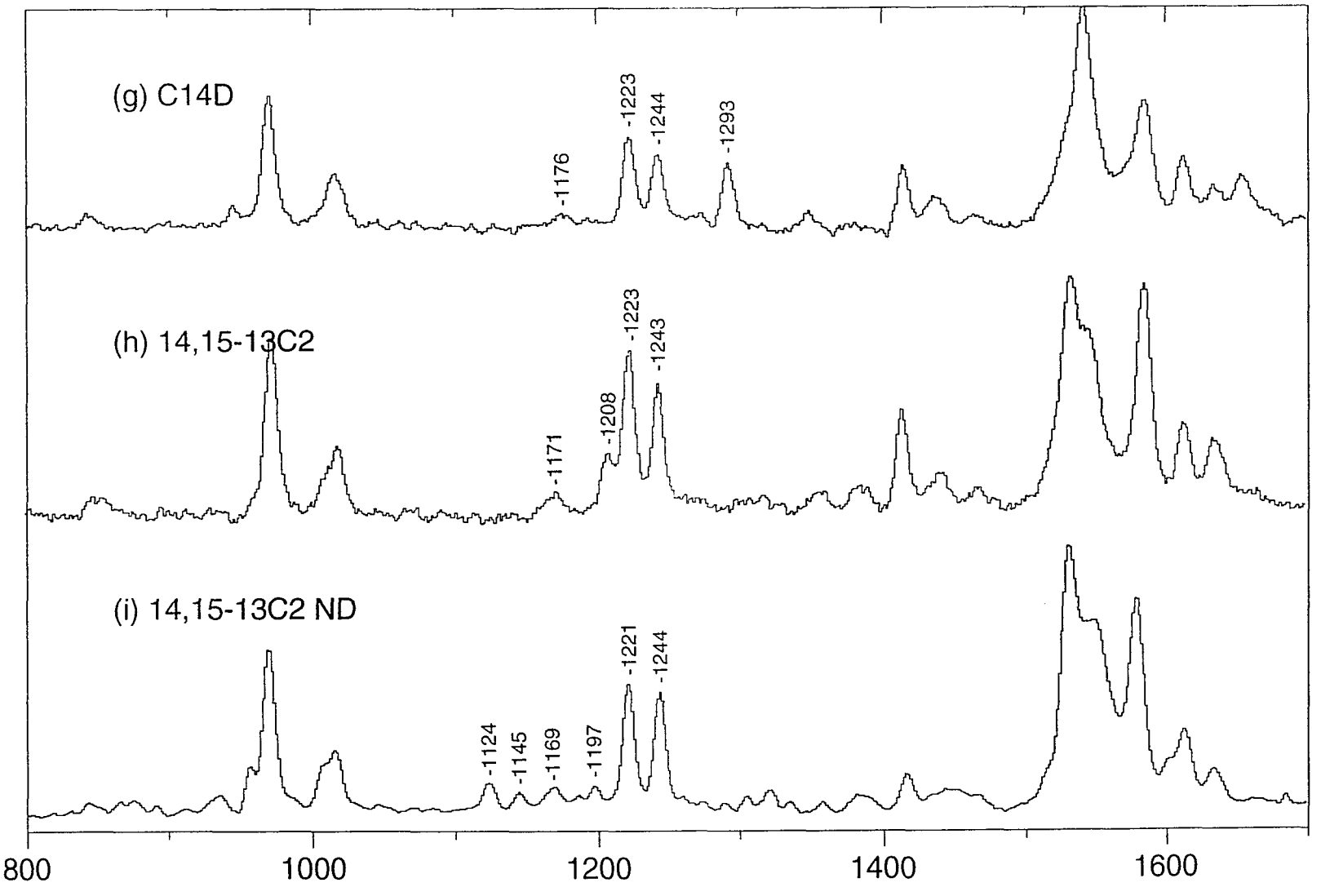
(g) C14D
-1176
-1223
-1244
-1293
(h) 14,15-13C2
-1171
-1208
-1223
-1243
(i) 14,15-13C2 ND
-1124
-1145
-1169
-1197
-1221
-1244
800
1000
1200
1400
1600

Figure 5.3: The resonance Raman spectra of octopus (a) isorhodopsin and its (b) ND, (c) 9-^{13}C, (d) 10-D, (e) 10,11-$^{13}C_2$, (f) 13-^{13}C, (g) 14-D, (h)14,15-$^{13}C_2$ and (i) 14,15-$^{13}C_2$ ND derivatives

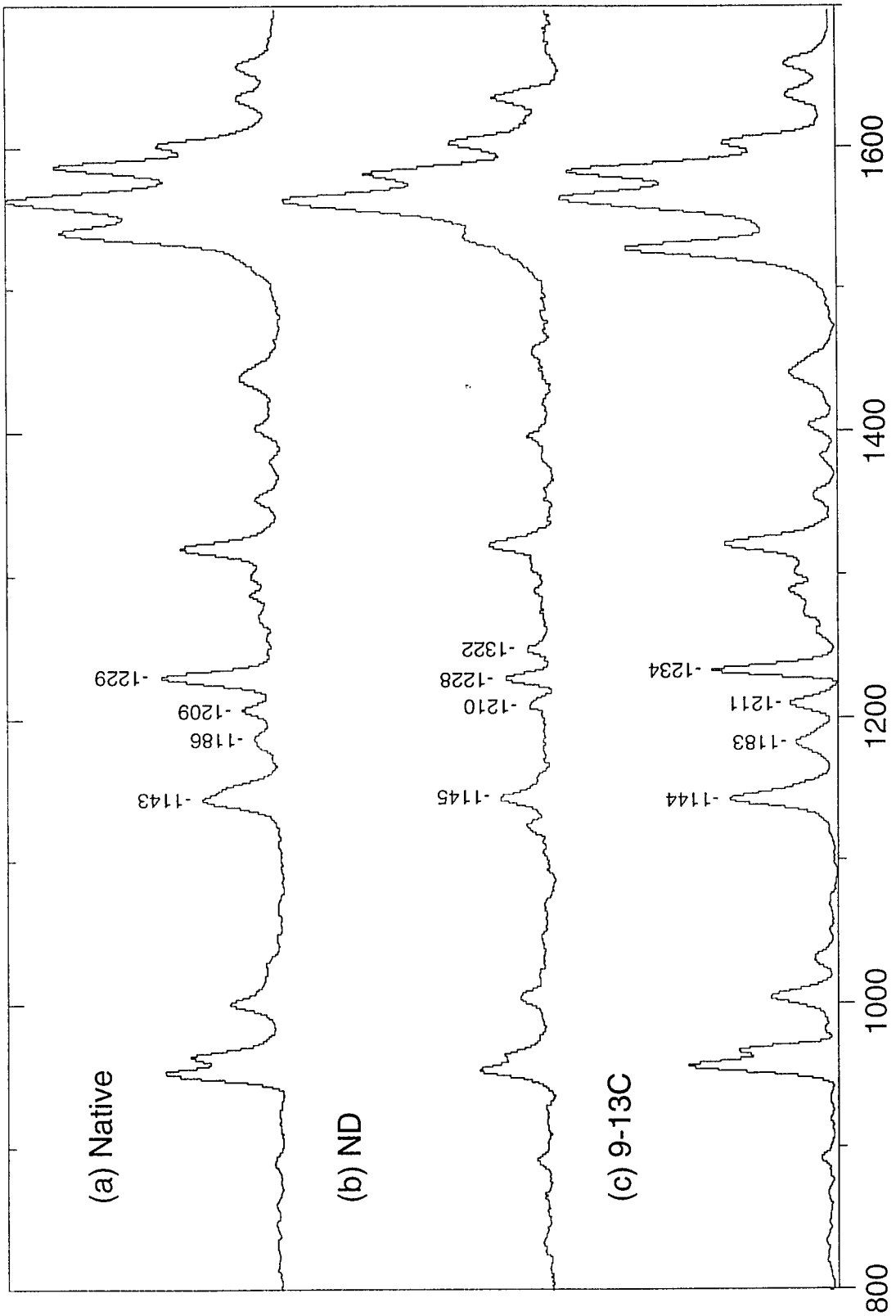
(a) Native
-1143
-1186
-1209
-1229
(b) ND
-1145
-1210
-1228
-1322
(c) 9-13C
-1144
-1183
-1211
-1234
800
1000
1200
1400
1600

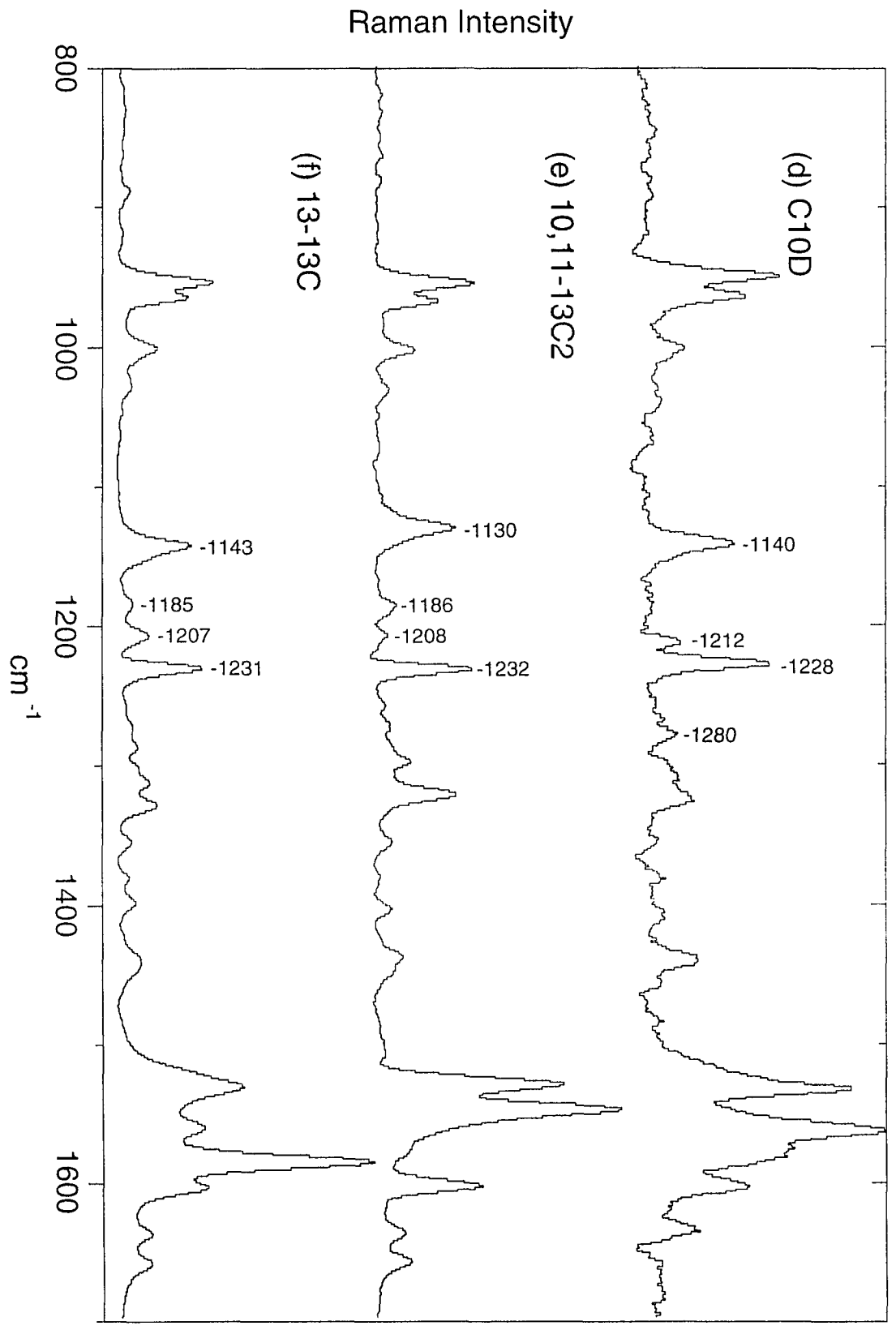
Raman Intensity
800
1000
1200
1400
1600
cm-1
(d) C10D
-1140
-1212
-1228
-1280
(e) 10,11-13C2
-1130
-1186
-1208
-1232
(f) 13-13C
-1143
-1185
-1207
-1231

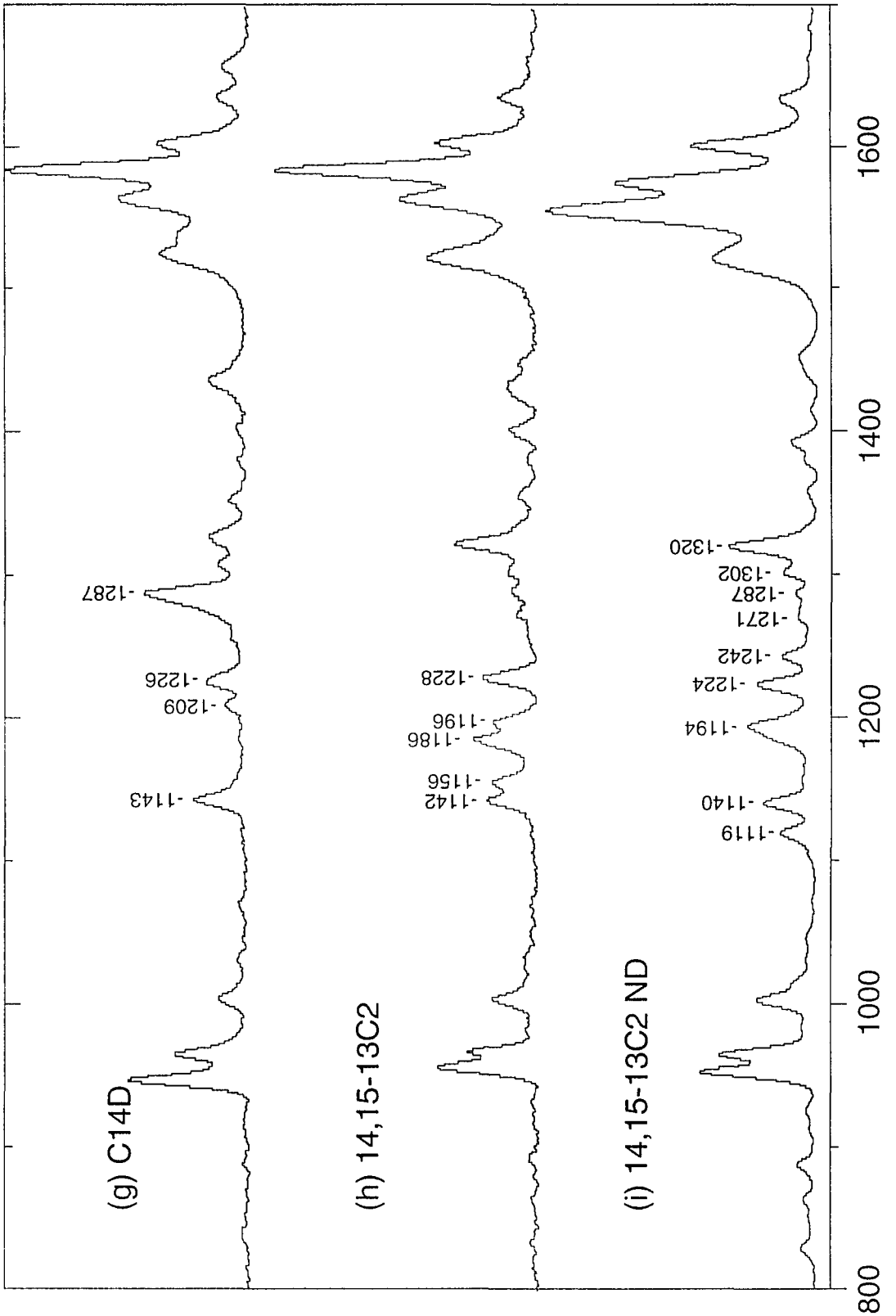
(g) C14D
-1287
-1226
-1209
-1143
(h) 14,15-13C2
-1228
-1196
-1186
-1156
-1142
(i) 14,15-13C2 ND
-1320
-1302
-1287
-1271
-1242
-1224
-1194
-1140
-1119
800
1000
1200
1400
1600

Chart 5.1: Correlation diagram in fingerprint region for all-cis-retinal with protonated Schiff base in methanol (Palings *et al.*, 1987 and octopus bathorhodopsin

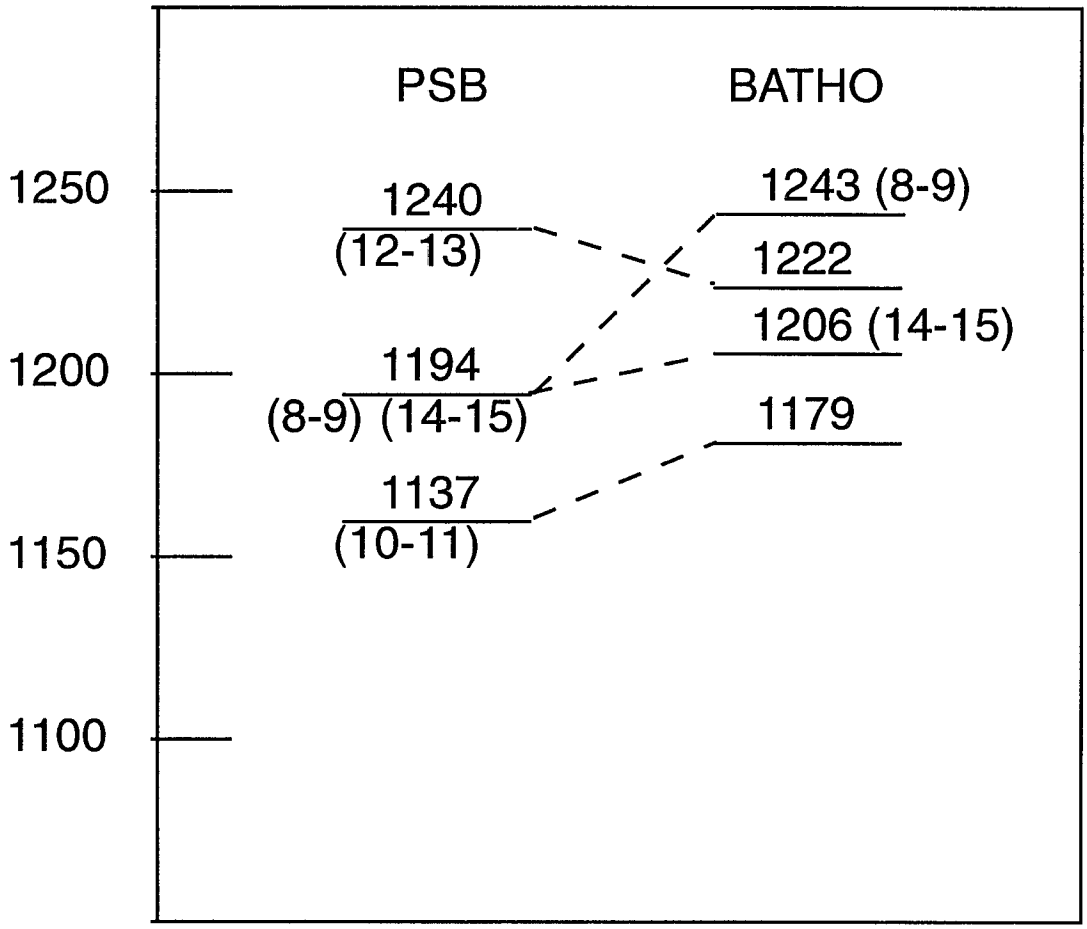

Chart 5.2: Correlation diagram in fingerprint region for 11-cis-retinal with protonated Schiff base in methanol (Palings *et al.*, 1987 and octopus rhodopsin

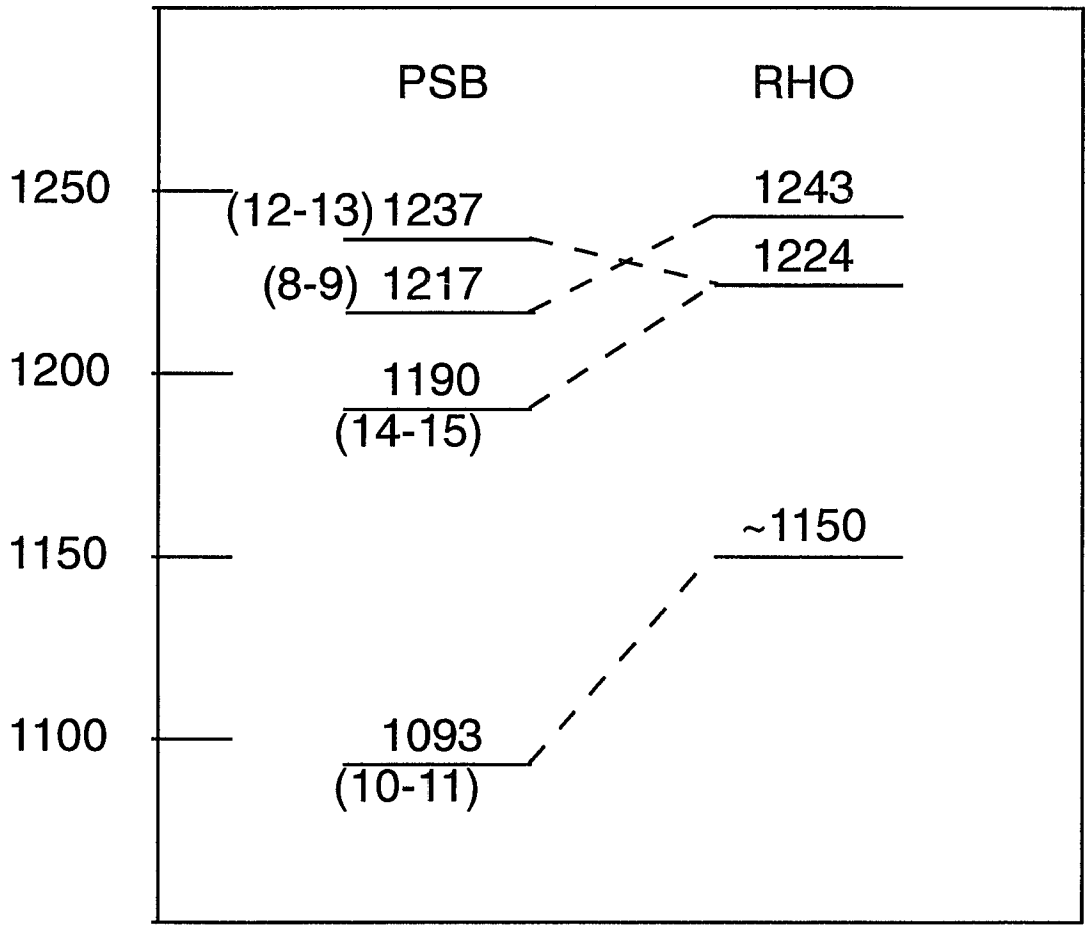

Chart 5.3: Correlation diagram in fingerprint region for 9-cis-retinal as a protonated Schiff base in methanol (Palings *et al.*, 1987) and octopus isorhodopsin

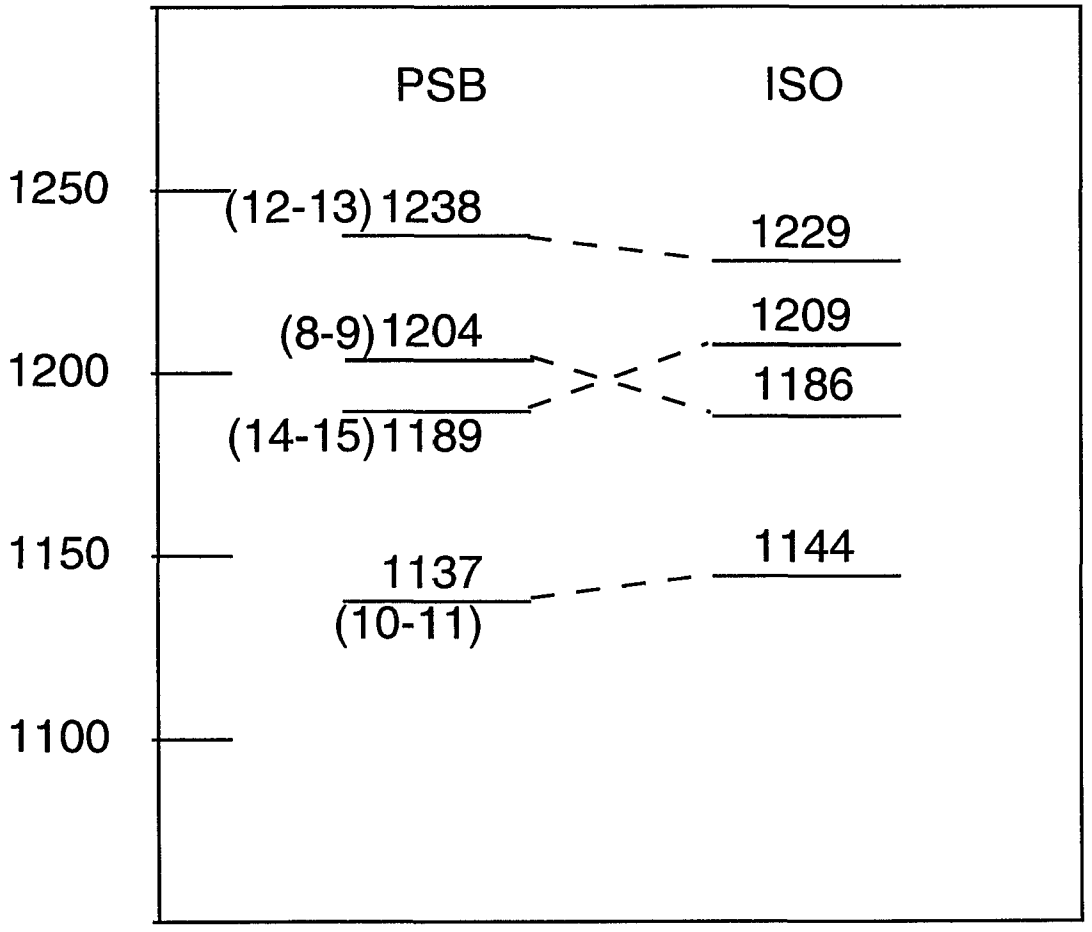

Chapter 6

RESONANCE RAMAN STUDIES OF BOVINE AND OCTOPUS VISUAL PIGMENTS WITH TRIPLET-LABELED RETINAL CHROMOPHORES

I. INTRODUCTION

In this chapter, we study the ethylenic and Schiff base modes of bovine and octopus rhodopsin, bathorhodopsin and isorhodopsin. The C=C and C=N stretching vibrations and, to a lesser extent, the CCH (or CNH) bending motions contribute to the bands in the 1500-1700 cm^{-1} region of the visual pigment Raman spectrum. For example, the C=N Schiff base stretching mode is expected to couple with NH bending and appears in the region from 1620 to 1680 cm^{-1} (Aton *et al.*, 1980). The deuterium labeling of the Schiff base nitrogen will result in a downward shift of the C=N stretching mode since this sensitivity of the coupling between this stretch and the hydrogen rocking. Normal mode analysis of retinals have shown that C=C stretching modes are also highly coupled with the corresponding CH bending modes (Curry *et al.*, 1982; Deng and Callender, 1987; Smith *et al.*, 1987). However, since the C=C stretching modes are generally tightly coupled to each other, i.e. each ethylenic band may contain contributions from several C=C stretching motions (Deng and Callender, 1987; Smith *et al.*, 1987; Smith *et al.*, 1987). Deuteration, therefore, at one double bond may affect the C=C stretching

frequency of another stretching mode. Thus, for accurate assignments one needs the data from ^{13}C-labeled chromophores (Deng *et al.*, 1991b).

Theoretical work on the Raman intensities of the conjugated polyene chain like the retinal protonated Schiff base have suggested that the $C_{12}=C_{11}$ double bond coordinate is the primary contributor to the major in-phase C=C stretching observed in Raman studies in most cases (Blazej and Peticolas, 1977; Warshel, 1977; Warshel and Dauber, 1977; Kakitani *et al.*, 1983; Deng, 1987). In the previous resonance Raman studies of octopus bathorhodopsin with deuterium labeled retinal chromophores, it was found that the major ethylenic band at 1532 cm^{-1} split into three likely uncoupled bands at 1543, 1510 and 1501 cm^{-1}, in the 11,12-D_2 doubly-labeled chromophore (Deng *et al.*, 1991b). Thus, resonance Raman data of isotopically triplet-labeled chromophores (11,12-D_2 and ^{13}C in C_8, C_{10}, C_{11}, C_{13}) may be used for the assignments of these C=C stretch bands. On the basis of these assignments and further normal mode analysis, the force constant of each C=C bond and its change in a different environment can be obtained. Such information is important in understanding the retinal chromophore-opsin-interaction in visual pigments. In this chapter, we report on the isotopic effect on ethylenic modes of rhodopsin, bathorhodopsin and isorhodopsin of both bovine and octopus as a result of selective labeling of the retinal polyene chain (11,12-D_2, 8-^{13}C-11,12-D_2, 10-^{13}C-11,12-D_2, 11-^{13}C-11,12-D_2, 13-^{13}C-11,12-D_2). This permits us to assign the Raman bands observed in the ethylenic-Schiff base region to particular internal coordinates.

II. MATERIAL AND METHODS

Octopus microvillar membranes were prepared and bleached as described in Chapter 5. The synthesis and characterization of the 11,12-D_2, 8-

^{13}C-11,12-D_2, 10-^{13}C-11,12-D_2, 11-^{13}C-11,12-D_2, and 13-^{13}C-11,12-D_2 retinals of either 11-*cis* or 9-*cis* configurations were described by Lugtenburg *et al.*, 1988.

The labeled chromophores in ethanol were added to 10 mL opsin suspension with a retinal/opsin molar ratio of 2:1. After incubation for 60 min. at room temperature, 100 μL of 2.0 *M* hydroxylamine, pH 6.5, was added. The regenerated membranes were washed once with 5 mM Tris buffer, pH 7.2, then twice with 4% bovine serum albumin (fatty acid free, Sigma Chemical Co., St. Louis, MO) in 5 m*M* Tris, pH 7.2. The membranes were stored at -60°C until further use. Approximately 50% of the opsin was regenerated using this procedure. No difference was observed in the Raman spectra of the native pigment and that regenerated with 11-*cis* or 9-*cis* unlabeled retinals. All operations were carried out in dim red light.

Bovine rhodopsin were prepared and regenerated in other papers (Wald, 1953; Shichi and Lewis, 1969; Shichi, 1970; Ebrey, 1971; Applebury *et al.*, 1974; Matsumoto *et al.*, 1978; Cusanovich, 1982; Grip, 1982; Hong *et al.*, 1982).

Resonance Raman experiments were performed at 80 K in a liquid nitrogen coldfinger as previously described (Aton *et al.*, 1980; see Chapter 4 and Chapter 5).

III. RESULTS AND DISCUSSIONS

Resonance Raman vibrational spectra of the retinal chromophore in bathorhodopsin, rhodopsin and isorhodopsin of both bovine and octopus have been obtained after regenerating visual pigments with a series of triply ^{13}C and deuterium labeled retinals, i.e., 11,12-D_2, 8-^{13}C-11,12-D_2, 10-^{13}C-11,12-D_2, 11-^{13}C-11,12-D_2, 14-^{13}C-11,12-D_2. Usually, substitution with ^{13}C in the retinal chromophore will significantly affect the frequencies of C-C and C=C stretch modes, which are normal found in the fingerprint (1100 to 1350 cm^{-1})

and the ethylenic region (1500 to 1700 cm^{-1}), respectively. They have, however, limited effect on the HOOP modes which are found in the region of 700 to 1000 cm^{-1}. Thus the analysis the resonance Raman spectra of bovine and octopus rhodopsin, bathorhodopsin and isorhodopsin with triply-labeled retinal chromophores are mainly limited to the ethylenic - Schiff base region. In this work, only the ethylenic and Schiff base mode region of the Raman data for bathorhodopsin, rhodopsin and isorhodopsin are analyzed in both the bovine and octopus pigments.

1. Bathorhodopsin

a) Bovine

Bovine bathorhodopsin has been studied, with deuterium and ^{13}C labeled chromophores, in the HOOP mode region, fingerprint region and Schiff base region (Palings *et al.*, 1987; Palings *et al.*, 1989). The Raman spectra of bovine bathorhodopsins with triply labeled chromophores are presented in Figure 6.1.

There are six bands in the ethylenic region of bovine bathorhodopsin with 11,12-D_2 labeled retinal chromophore. The isotopic shifts are summarized in Table 6.1.

In native bovine bathorhodopsin, the 1654 cm^{-1} band which is sensitive to deuteration at the ND (1626 cm^{-1}) (Palings *et al.*, 1987), has been assigned to the C=N Schiff base mode due to this well-known sensitivity (Heyde *et al.*, 1971; Aton *et al.*, 1980; Gilson *et al.*, 1988). In the $C_{11}D{=}C_{12}D$ doubly-labeled chromophore, this band lies at 1657 cm^{-1}. The $C_5{=}C_6$ stretching mode is assigned to the 1631 cm^{-1} band which is invariant upon all 8-^{13}C, 10-^{13}C, 11-^{13}C and 13-^{13}C labeling. The assignment of $C_7{=}C_8$ at 1586 cm^{-1} is supported by the spectrum of the 8-^{13}C-11,12-D_2 derivative where this

band disappears. After the down-shifting of the band, it couples with the 1538 cm^{-1} band, whose intensity is pushed down to 1513 cm^{-1}. On the basis of comparison to the 10-^{13}C-11,12-D_2 derivative, the C_9=C_{10} stretching mode can be assigned to the 1563 cm^{-1} band in the spectrum of 11,12-D_2 derivative because this mode shifts down to 1550 cm^{-1}. After the shifting, this stretching mode couples and pushes the band at 1538 cm^{-1} to about 1510 cm^{-1}. The latter becomes a shoulder of the band at 1503 cm^{-1}. The C_{11}=C_{12} stretch is assigned to the mode at 1502 cm^{-1} based upon a shift of 14 cm^{-1} in the 11-^{13}C-11,12-D_2 derivative. The intense band at 1541 cm^{-1} can be interpreted as some intensity of the band at 1563 cm^{-1} shifting down since its coupling with C_{11}=C_{12} stretch is weakened. The spectrum of the 14-^{13}C-11,12-D_2 derivative demonstrates the C_{13}=C_{14} stretching character can be assigned to the 1538 cm^{-1} band which shifts to 1525 cm^{-1} in this derivative. The decoupling of the C_{13}=C_{14} with the C_9=C_{10} stretches leads the 1563 cm^{-1} band shift to 1551 cm^{-1}.

It is surprising to note that the intensity of the C_5=C_6 stretching mode varies in the spectra of 10-^{13}C-11,12-D_2, 11-^{13}C-11,12-D_2, and 14-^{13}C-11,12-D_2 derivatives, while the frequency remains substantially the same. This implies the C_5=C_6 stretch may somehow mix with the C_9=C_{10}, C_{11}=C_{12} and C_{13}=C_{14} stretches, if the assignment of C_5=C_6 stretch is correct.

In Chart 6.1 the ethylenic-Schiff base normal modes of bovine bathorhodopsin are drawn according to the above assignments.

b) Octopus

Octopus bathorhodopsin has been studied with singly or doubly deuterium labeled chromophores in the HOOP mode region, fingerprint region and ethylenic-Schiff base region (Aton *et al.*, 1980; Pande *et al.*, 1987; Gilson *et al.*, 1988; Deng *et al.*, 1991a; Deng *et al.*, 1991b). The Raman spectra of

octopus bathorhodopsins with triply labeled chromophores are presented in Figure 6.2.

There are six bands in the ethylenic region of octopus bathorhodopsin with the 11,12-D_2 labeled retinal chromophore. The isotopic shifts of the four triply labeled chromophores are summarized in Table 6.2.

The band at 1656 cm^{-1} in native octopus bathorhodopsin has been assigned to C=N Schiff base mode due to the sensitivity to deuteration at the ND (1626 cm^{-1}) (Deng *et al.*, 1991b). This band falls at 1657 cm^{-1} in the $C_{11}D{=}C_{12}D$ doubly-labeled derivative. The $C_5{=}C_6$ stretching mode is assigned to the 1630 cm^{-1} band which is invariant upon all 8-^{13}C, 10-^{13}C, 11-^{13}C and 13-^{13}C labeling. The assignment of $C_7{=}C_8$ stretching mode to 1590 cm^{-1} is supported by the spectrum of the 8-^{13}C-11,12-D_2 derivative, where the band shifts down 19 cm^{-1}. Upon this down-shifting, the $C_7{=}C_8$ stretch couples with the band at 1543 cm^{-1} and pushed some intensity of the latter to 1516 cm^{-1}. The shifting pattern of octopus bathorhodopsin upon 8-^{13}C-11,12-D_2 substitution is similar to that of bovine bathorhodopsin. The 1543 cm^{-1} band shifting to 1535 cm^{-1} in the 10-^{13}C-11,12-D_2 derivative demonstrates that it is the $C_9{=}C_{10}$ stretching mode. The $C_{11}{=}C_{12}$ stretch is contributed to both 1500 and 1510 cm^{-1} bands based upon the intensity drop of these two modes in the 11-^{13}C-11,12-D_2 derivative. The 1500 cm^{-1} band, however, shifts more than the 1500 cm^{-1} band does (6 to 2 cm^{-1}). Thus $C_{11}{=}C_{12}$ stretch is assigned to the 1500 cm^{-1} band. The $C_{13}{=}C_{14}$ stretching character is assigned to the mode at 1543 cm^{-1}, which splits into two modes at 1532 and 1572 cm^{-1} in the 14-^{13}C-11,12-D_2 derivative spectrum.

In Chart 6.2 the ethylenic-Schiff base normal modes of octopus bathorhodopsin are shown according to the above assignments.

2. Rhodopsin

a) Bovine

Bovine rhodopsin is studied with deuterium and ^{13}C labeled chromophores in the fingerprint and Schiff base regions (Palings *et al.*, 1987). The Raman spectra of bovine rhodopsins with triply labeled chromophores are presented in Figure 6.3.

There are seven bands in the ethylenic region of bovine rhodopsin with an 11,12-D_2 labeled retinal chromophore. The isotopic shifts are summarized in Table 6.3.

The band at 1656 cm^{-1} in native bovine rhodopsin, has been assigned to the C=N Schiff base mode due to its sensitivity to deuteration at the ND (1626 cm^{-1}) (Palings *et al.*, 1987). In the $C_{11}D=C_{12}D$ doubly-labeled chromophore, this band falls at 1650 cm^{-1}. The $C_5=C_6$ stretching mode is assigned to the 1633 cm^{-1} band which is invariant upon all 8-^{13}C, 10-^{13}C, 11-^{13}C and 13-^{13}C labeling. The assignment of $C_7=C_8$ to 1610 cm^{-1} is supported by the spectrum of the 8-^{13}C-11,12-D_2 derivative where this band losses most of its intensity. The $C_9=C_{10}$ stretching character is located at 1592 cm^{-1}, shifting by 20 cm^{-1} in the 10-^{13}C-11,12-D_2 derivative. This shifting also leads to the coupling between the $C_9=C_{10}$ stretch and the 1544 cm^{-1} band. The latter is pushed down to 1528 cm^{-1}. The $C_{11}=C_{12}$ stretch is assigned to the mode at 1516 cm^{-1} based on the splitting of this band into two bands at 1499 and 1520 cm^{-1} in the 11-^{13}C-11,12-D_2 derivative. The $C_{13}=C_{14}$ stretching character is assigned to the mode at 1544 cm^{-1} on the basis of a 12 cm^{-1} shift in the 14-^{13}C-11,12-D_2 derivative.

In Chart 6.3 the ethylenic-Schiff base normal modes of bovine rhodopsin are drawn according to the above assignments.

b) Octopus

The Raman spectra of octopus rhodopsins with triply labeled chromophores are presented in Figure 6.4.

There are seven bands in the ethylenic region of octopus rhodopsin with an 11,12-D_2 labeled retinal chromophore. The isotopic shifts of the four triply labeled chromophores are summarized in Table 6.4.

In native octopus rhodopsin, the 1656 cm^{-1} band, which is sensitive to deuteration only at the ND (1632 cm^{-1}) (see Chapter 5), can be readily assigned to the C=N Schiff base mode due to this sensitivity. In the $C_{11}D=C_{12}D$ doubly-labeled chromophore, this band falls at 1657 cm^{-1}. The $C_5=C_6$ stretching mode is assigned to the 1636 cm^{-1} band which is essentially invariant upon all 8-^{13}C, 10-^{13}C, 11-^{13}C and 13-^{13}C labeling. The assignment of $C_7=C_8$ at 1612 cm^{-1} is supported by the spectrum of 8-^{13}C-11,12-D_2 derivative where this band disappears. The $C_9=C_{10}$ stretch is assigned to the mode at 1584 cm^{-1}, which shifts down by 20 to 30 cm^{-1} and couples with the band originally at 1546 cm^{-1}. This results in a strong band at 1535 cm^{-1} in the 10-^{13}C-11,12-D_2 derivative. In the 11-^{13}C-11,12-D_2 derivative, a mode shifts from 1515 cm^{-1} down to 1497 cm^{-1}, with the 1527 cm^{-1} band shifting to 1514 cm^{-1} since the coupling between this mode and $C_9=C_{10}$ stretch is weakened. These changes indicate that $C_{11}=C_{12}$ stretch is delocalized to these two modes. It is noted that the shifting pattern can also be interpreted as the 1527 cm^{-1} band shifting down 30 cm^{-1} to 1497 cm^{-1} while the 1516 cm^{-1} band remaining substantially the same position. In this case the $C_{11}=C_{12}$ stretch is assigned to the 1527 cm^{-1} band. The $C_{13}=C_{14}$ stretching character is assigned to the mode at 1546 cm^{-1}, which shifts down to 1526 cm^{-1} in the 14-^{13}C-11,12-D_2 derivative The isotopic influence of 14-^{13}C-11,12-D_2 on the $C_{13}=C_{14}$ stretch of octopus rhodopsin is similar to that of octopus bathorhodopsin.

In Chart 6.4 the ethylenic-Schiff base normal modes of octopus rhodopsin are drawn according to the above assignments.

3. Isorhodopsin

Isorhodopsin data will be reported similarly to bathorhodopsin and rhodopsin data, emphasizing the ethylenic regions.

a) Bovine

Bovine isorhodopsin was studied with deuterium and ^{13}C labeled chromophores in the fingerprint and Schiff base regions (Palings *et al.*, 1987). The Raman spectra of bovine isorhodopsins with triply labeled chromophores are presented in Figure 6.5.

There are six bands in the ethylenic region of bovine isorhodopsin with 11,12-D_2 labeled retinal chromophore. The isotopic shifts are summarized in Table 6.5.

The band at 1656 cm^{-1} in native bovine isorhodopsin has been assigned to the C=N Schiff base mode due to the sensitivity of deuteration at the ND (1637 cm^{-1}) (Palings *et al.*, 1987). In the $C_{11}D=C_{12}D$ doubly-labeled chromophore, this band is at 1659 cm^{-1}. The $C_5=C_6$ stretching mode is assigned to the 1640 cm^{-1} band which is invariant upon all 8-^{13}C, 10-^{13}C, 11-^{13}C and 13-^{13}C labeling. The assignments of $C_7=C_8$ at 1600 cm^{-1} and $C_9=C_{10}$ at 1582 are supported by the spectra of 8-^{13}C-11,12-D_2 and 10-^{13}C-11,12-D_2 derivatives, respectively, where these two bands disappear. The $C_{11}=C_{12}$ stretch is assigned to the mode at 1520 cm^{-1} based upon the splitting of this band into two bands at 1499 and 1482 cm^{-1} in the 11-^{13}C-11,12-D_2 derivative. The $C_{13}=C_{14}$ stretching character is assigned to the mode at 1549 based upon a 10 cm^{-1} shift in the 14-^{13}C-11,12-D_2 derivative.

In Chart 6.5 the ethylenic-Schiff base normal modes of bovine isorhodopsin are drawn according to the above assignments.

b) Octopus

The Raman spectra of octopus isorhodopsins with triply labeled chromophores are presented in Figure 6.6.

There are six bands in the ethylenic region of octopus isorhodopsin with 11,12-D_2 labeled retinal chromophore. The isotopic shifts of the four triply labeled chromophores are summarized in Table 6.6.

The band at 1660 cm^{-1} in native octopus isorhodopsin, which is sensitive to deuteration only at the ND (1626 cm^{-1}) (Chapter 4), can be readily assigned to the C=N Schiff base mode due to this sensitivity. In the $C_{11}D=C_{12}D$ doubly-labeled chromophore, this band remains at 1660 cm^{-1}. The $C_5=C_6$ stretching mode is assigned to the 1639 cm^{-1} band which is invariant upon all 8-^{13}C, 10-^{13}C, 11-^{13}C and 13-^{13}C labeling. The assignments of $C_7=C_8$ to 1605 cm^{-1} and $C_9=C_{10}$ to 1579 cm^{-1} are supported by the spectra of 8-^{13}C-11,12-D_2 and 10-^{13}C-11,12-D_2 derivatives, respectively, where these two bands disappear. In the 11-^{13}C-11,12-D_2 derivative, a mode shifts from 1531 cm^{-1} down to 1509 cm^{-1}, and an increase in intensity is observed at 1539 cm^{-1}. These changes allow us to assign $C_{11}=C_{12}$ stretch to one of the modes in the 1531 cm^{-1} band. The $C_{13}=C_{14}$ stretching character is assigned to the other mode of the 1531 cm^{-1} band, whose intensity shifts to 1523 cm^{-1} in the spectrum of the 14-^{13}C-11,12-D_2 derivative.

In Chart 6.6 the ethylenic-Schiff base normal modes of octopus isorhodopsin are drawn according to the above assignments.

IV. SUMMARY AND PROSPECTS

Tables 6.7-9 display the ethylenic and Schiff base modes of bathorhodopsin, rhodopsin and isorhodopsin for both bovine and octopus. It was suggested and has been tested that the ethylenic (C=C) stretching frequency of retinal-based structures is correlated with their absorption maxima (Rimai *et al.*, 1971; Aton *et al.*, 1977; Doukas *et al.*, 1978b) due to the π electron delocalization (Kakitani and Kakitani, 1975). Our data, moreover, suggests that, if the ethylenic stretching are relatively isolated, the C_{11}=C_{12} is the one that determine the absorption maxima because of the linear fitting as shown in Chart 6.7.

The above assignments shows that (1) In bovine bathorhodopsin, C_7=C_8 stretching mode is localized to 1586 cm^{-1}, while C_{11}=C_{12} and C_{13}=C_{14} stretching mode are somewhat more delocalized, and the C_9=C_{10} stretch contributes to two normal modes. It may be suggested that some disturbance is around the C_9=C_{10} bond breaks the ethylenic chain to two parts. (2) In octopus bathorhodopsin, by contrast, the C_9=C_{10} and the C_{13}=C_{14} stretching modes are localized, while the C_7=C_8 and the C_{11}=C_{12} modes are not. Thus there may be more than one disturbance affecting the chromophore chain. (3) In bovine rhodopsin, almost all bonds are delocalized, suggesting that the chromophore is pretty relaxed. This confirms the similarity of the fingerprint region of the resonance Raman spectra of bovine rhodopsin and that of the 11-cis protonated Schiff base retinal. (4) Conversely, the analysis of octopus rhodopsin clearly shows that at least the C_7=C_8, C_9=C_{10}, and C_{13}=C_{14} stretching modes are localized. This implies that there are some strong protein perturbations acting on the chromophore. This interpretation supports the proposal, which we make in Chapter 5, about the conformation of the octopus rhodopsin chromophore. (5) The ethylenic modes of both bovine and octopus isorhodopsins are delocalized. It confirms that the

spectra of bovine isorhodopsin is analogous to that of 9-cis protonated Schiff base retinal (Mathies, 1979). It also confirms the similar shifting pattern upon isotopic substitution (e.g. see Chapter 5).

As the same in Chapter 5, we wish to stress that the above assignments of the ethylenic modes of bovine and octopus pigments are quantitatively tentative because the lack of the normal mode calculation owing to limitations in calculation speed and the disk space. We propose to do the first calculation on some model compounds which do not have the β-ionyl ring. It is our hope that the specific model obtained from the normal calculation will fit the experimental data and explain the similarities and differences between bovine and octopus pigments, especially the cause of the anomalous 1226 cm^{-1} band and low λ_{max} of octopus rhodopsin in comparison to that of bovine.

Table 6.1 Bovine Bathorhodopsin Ethylenic-Schiff Base Region Vibrational Frequencies*

derivative	frequencies (cm^{-1})					
native						1654
11,12-D_2	1502	1538	1563	1586	1631	1656
8-^{13}C-11,12-D_2	-	1513(-25)	1541(-22)	1565(-21)	1627(-4)	1653(-4)
10-^{13}C-11,12-D_2	1503(+1)	1535(-3)	1550(-13)	1591(+5)	1627(-4)	1657(+3)
11-^{13}C-11,12-D_2	1504(+2)	1541(+3)	1564(+1)	1590(+4)	1631(0)	1655(-2)
14-^{13}C-11,12-D_2	1504(+2)	1525(-13)	1551(-12)	1584(-2)	1626(-5)	1656(-1)
tentative assingement	C_{11}=C_{12}	C_{13}=C_{14}	C_9=C_{10}	C_7=C_8	C_5=C_6	C=N

* a. Shifts from the 11,12-D_2 derivative are given in parentheses. b. - means not observed.

Table 6.2 Octopus Bathorhodopsin Ethylenic-Schiff Base Region Vibrational Frequencies*

derivative	frequencies (cm^{-1})					
native		1532	1545	1595	1628	1657
11,12-D_2	1500	1510	1543	1590	1630	1657
8-^{13}C-11,12-D_2	1499(-1)	-	1516(-27)	1571(-19)	1624(-6)	1657(0)
10-^{13}C-11,12-D_2	1496(-4)	1510(0)	1535(-8)	1586(-4)	1628(-2)	1657(0)
11-^{13}C-11,12-D_2	1494(-6)	1508(-2)	1542(0-1)	1587(-3)	1629(-1)	1656(-1)
14-^{13}C-11,12-D_2	1500(0)	1512(+2)	1529(-14),1572(+29)	1590(0)	1630(0)	1656(-1)
tentative assingement	C_{11}=C_{12}	C_{13}=C_{14}	C_9=C_{10}	C_7=C_8	C_5=C_6	C=N

* a. Shifts from the 11,12-D_2 derivative are given in parentheses. b. - means not observed.

Table 6.3 Bovine Rhodopsin Ethylenic-Schiff Base Region Vibrational Frequencies*

derivative	frequencies (cm^{-1})						
native							
11,12-D_2	1516	1544	1575	1592	1610	1633	1650
8-^{13}C-11,12-D_2	1519(+3)	1544(0)	-	1581(-11)	1610(0)	1635+2)	1658(+8)
10-^{13}C-11,12-D_2	1519(+3)	1528(-16)	-	-	1607(-3)	1638(+5)	1655(+5)
11-^{13}C-11,12-D_2	1499(-17)	1545(+1)	1575(0)	1592(0)	1604(-6)	1636(+3)	1654(+4)
14-^{13}C-11,12-D_2	1518(+2)	1532(-12)	1568(-7)	1596(+6)	1609(-1)	1634(+1)	1656(+6)
tentative assingement	C_{11}=C_{12}	C_{13}=C_{14}		C_9=C_{10}	C_7=C_8	C_5=C_6	C=N

* a. Shifts from the 11,12-D_2 derivative are given in parentheses. b. - means not observed.

Table 6.4 Octopus Rhodopsin Ethylenic-Schiff Base Region Vibrational Frequencies*

derivative	frequencies (cm^{-1})						
native		1536		1586	1613	1634	1657
11,12-D_2	1515	1527	1546	1584	1612	1636	1657
8-^{13}C-11,12-D_2	1514(-1)	1526(-1)	1544(-2)	1580(-4)		1634(-2)	1655(-2)
10-^{13}C-11,12-D_2	1512(-1)	-	1535(-11)	1586(+2)	1612(0)	1636(0)	1658(+1)
11-^{13}C-11,12-D_2	1514(-1)	1497(-30)	1548(+2)	1578(-6)	1613(+1)	1637(+1)	1656(-1)
14-^{13}C-11,12-D_2	1515(0)	1526(-1)		1578(-6)	1611(-1)	1637(+1)	1656(-1)
tentative assingement		C_{11}=C_{12}	C_{13}=C_{14}	C_9=C_{10}	C_7=C_8	C_5=C_6	C=N

* a. Shifts from the 11,12-D_2 derivative are given in parentheses. b. - means not observed.

Table 6.5 Bovine Isorhodopsin Ethylenic-Schiff Base Region Vibrational Frequencies*

derivative	frequencies (cm^{-1})						
native							
11,12-D_2	1520		1549	1582	1600	1640	1659
8-^{13}C-11,12-D_2	1519(-1)	1534(?)	1549(0)	-	1584(+3)	1637(-3)	1653(-6)
10-^{13}C-11,12-D_2	1519(-1)		1527(-22)	-	1601(+1)	1640(0)	1656(-3)
11-^{13}C-11,12-D_2	1499(-21)		1546(-3)	1559(-22)	1599(-1)	1637(-3)	1654(-5)
14-^{13}C-11,12-D_2	1522(+2)		1539(-10)	1578(-6)	1601(+1)	1641(+1)	1652(-7)
tentative assingement	C_{11}=C_{12}		C_{13}=C_{14}	C_9=C_{10}	C_7=C_8	C_5=C_6	C=N

* a. Shifts from the 11,12-D_2 derivative are given in parentheses. b. - means not observed.

Table 6.6 Octopus Isorhodopsin Ethylenic-Schiff Base Region Vibrational Frequencies*

derivative	frequencies (cm^{-1})					
native	1541	1564	1588	1603	1637	1660
11,12-D_2	1531	1545	1579	1605	1639	1660
8-^{13}C-11,12-D_2	1532(+1)	1538(-7)	-	1585(+6)	1639(0)	1660(0)
10-^{13}C-11,12-D_2	1525(-6)	1547(+2)		1604(-1)	1639(0)	1660(0)
11-^{13}C-11,12-D_2	1509(-12)	1539(-6)	1574(-5)	1604(-1)	1640(+1)	1659(-1)
14-^{13}C-11,12-D_2	1523(-8)	1547(+2)	1572(-7)	1604(-1)	1638(-1)	1656(-4)
tentative assingement	C_{11}=C_{12},C_{13}=C_{14}		C_9=C_{10}	C_7=C_8	C_5=C_6	C=N

* a. Shifts from the 11,12-D_2 derivative are given in parentheses. b. - means not observed.

Table 6.7: Comparison of Ethylenic Modes of Bathorhodopsin for Bovine and Octopus

bovine (cm^{-1})	stretch	octopus (cm^{-1})
1656	C=N	1657
1631	C_5=C_6	1630
1586	C_7=C_8	1590
1563	C_9=C_{10}	1543
1538	C_{13}=C_{14}	1510
1502	C_{11}=C_{12}	1500

Table 6.8: Comparison of Ethylenic Modes of Rhodopsin for Bovine and Octopus

bovine (cm^{-1})	stretch	octopus (cm^{-1})
1650	C=N	1657
1633	C_5=C_6	1636
1610	C_7=C_8	1612
1592	C_9=C_{10}	1584
1544	C_{13}=C_{14}	1546
1516	C_{11}=C_{12}	1527, 1515

Table 6.9: Comparison of Ethylenic Modes of Isorhodopsin for Bovine and Octopus

bovine (cm^{-1})	stretch	octopus (cm^{-1})
1659	C=N	1660
1640	C_5=C_6	1639
1600	C_7=C_8	1605
1582	C_9=C_{10}	1579
1549	C_{13}=C_{14}	1531
1520	C_{11}=C_{12}	1531

Figure 6.1: Resonance Raman spectra of bovine bathorhodopsin with (a) 11,12-D_2, (b) 8-^{13}C-11,12-D_2, (c) 10-^{13}C-11,12-D_2, (d) 11-^{13}C-11,12-D_2, and (e) 14-^{13}C-11,12-D_2 substituted retinal chromophores

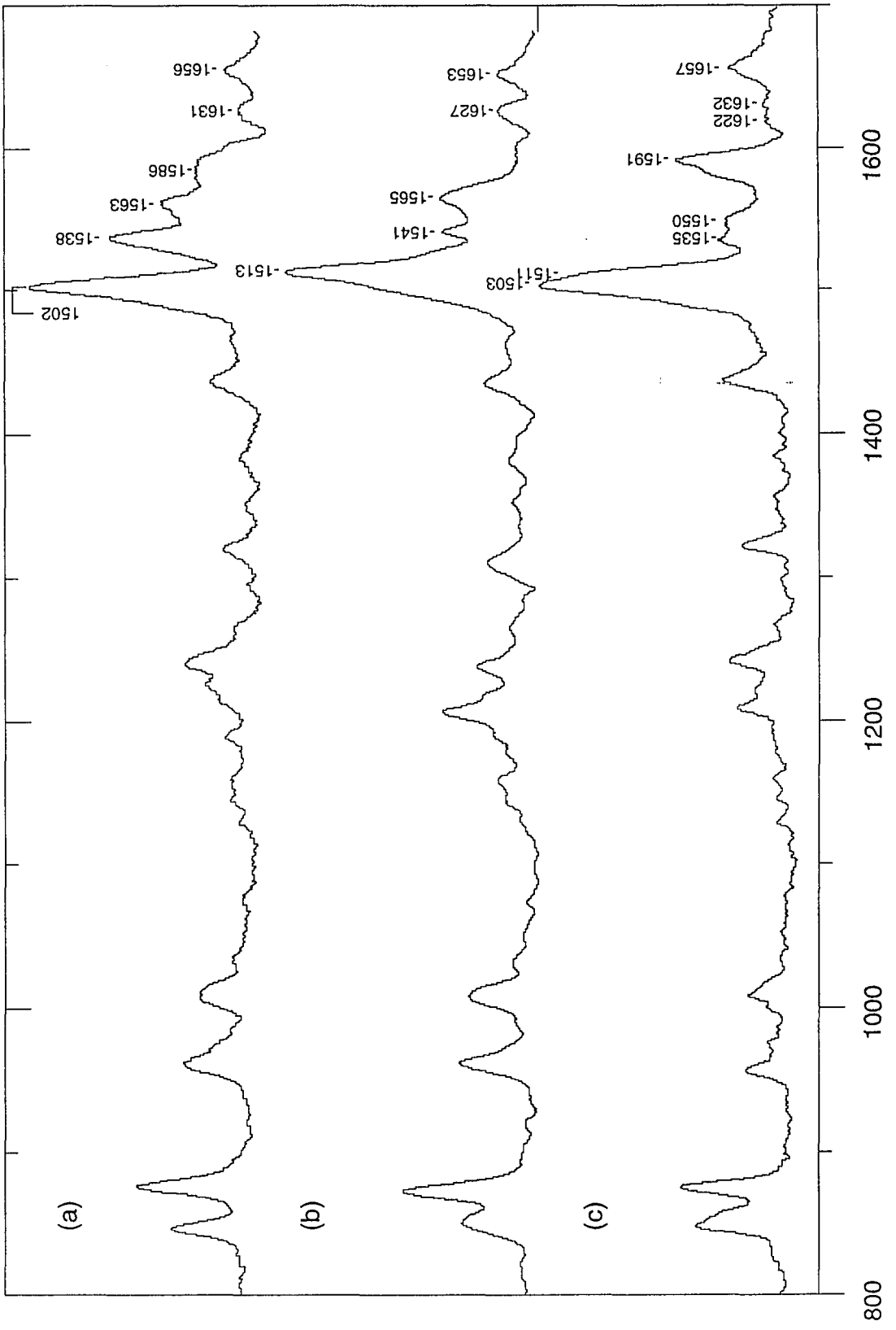
(a)
(b)
(c)
1502
1513
1538
1563
1586
1631
1656
1503
1511
1535
1550
1591
1622
1632
1657
1541
1565
1627
1653
800
1000
1200
1400
1600

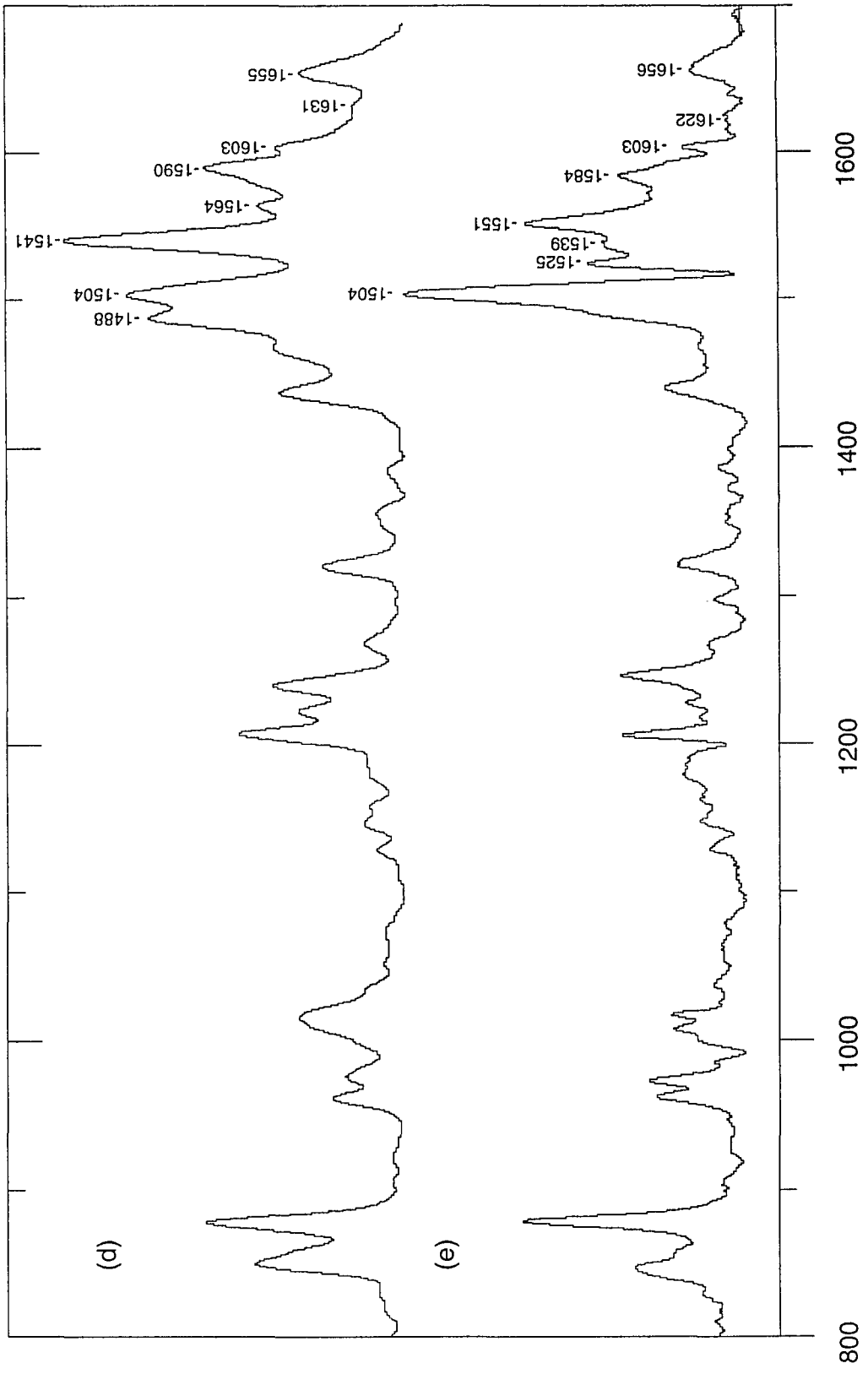
(d)
1655
1631
1603
1590
1564
1541
1504
1488
(e)
1656
1622
1603
1584
1551
1539
1525
1504
800
1000
1200
1400
1600

Figure 6.2: Resonance Raman spectra of octopus bathorhodopsin with (a) 11,12-D_2, (b) 8-^{13}C-11,12-D_2, (c) 10-^{13}C-11,12-D_2, (d) 11-^{13}C-11,12-D_2, and (e) 14-^{13}C-11,12-D_2 substituted retinal chromophores

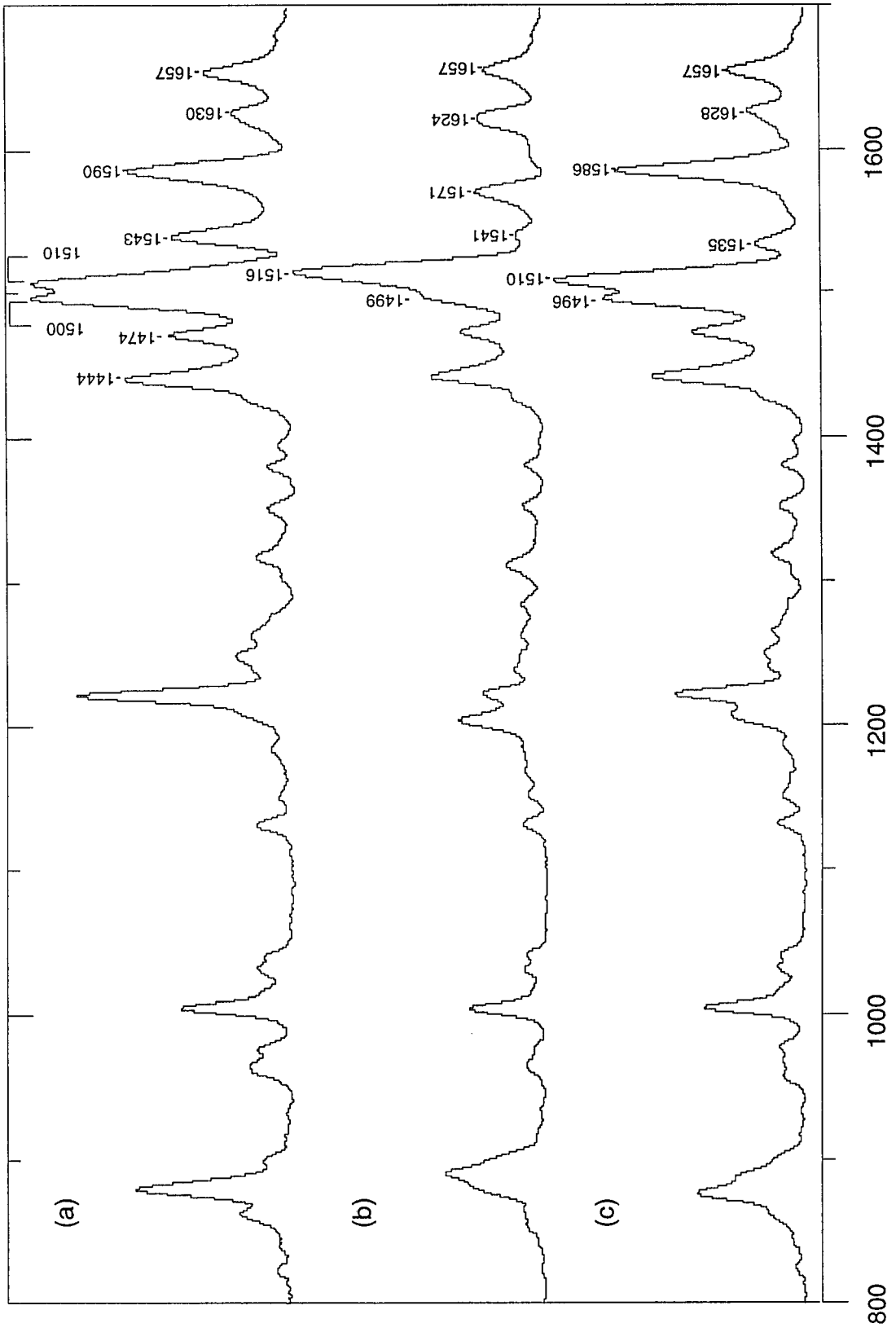
(a)
(b)
(c)
1657
1630
1590
1543
1510
1516
1499
1500
1474
1444
1657
1624
1571
1541
1657
1628
1586
1535
1510
1496
800
1000
1200
1400
1600

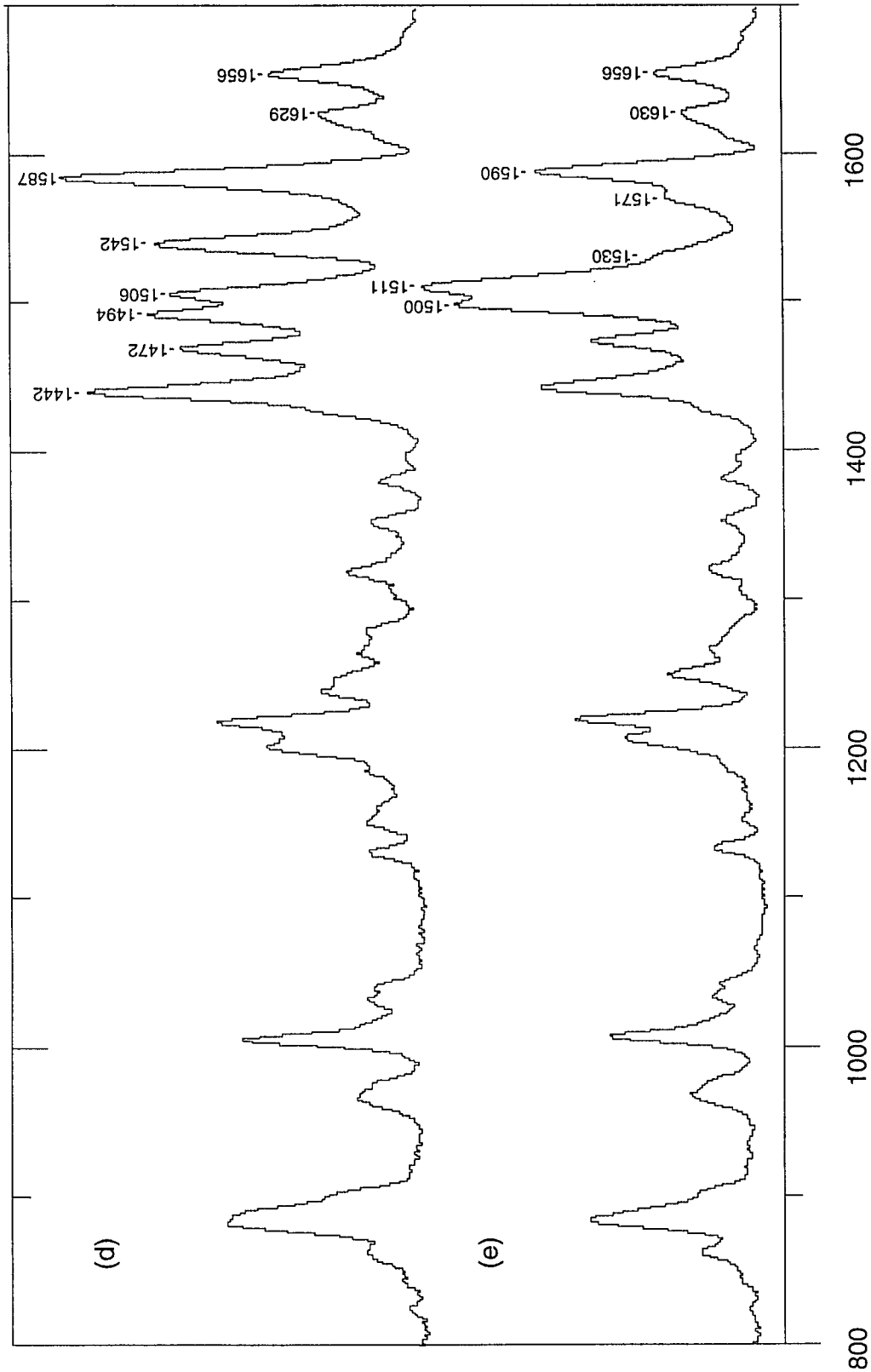
(d)
(e)
1442
1472
1494
1506
1542
1587
1629
1656
1500
1511
1530
1571
1590
1630
1656
800
1000
1200
1400
1600

Figure 6.3: Resonance Raman spectra of bovine rhodopsin with (a) 11,12-D_2, (b) 8-^{13}C-11,12-D_2, (c) 10-^{13}C-11,12-D_2, (d) 11-^{13}C-11,12-D_2, and (e) 14-^{13}C-11,12-D_2 substituted retinal chromophores

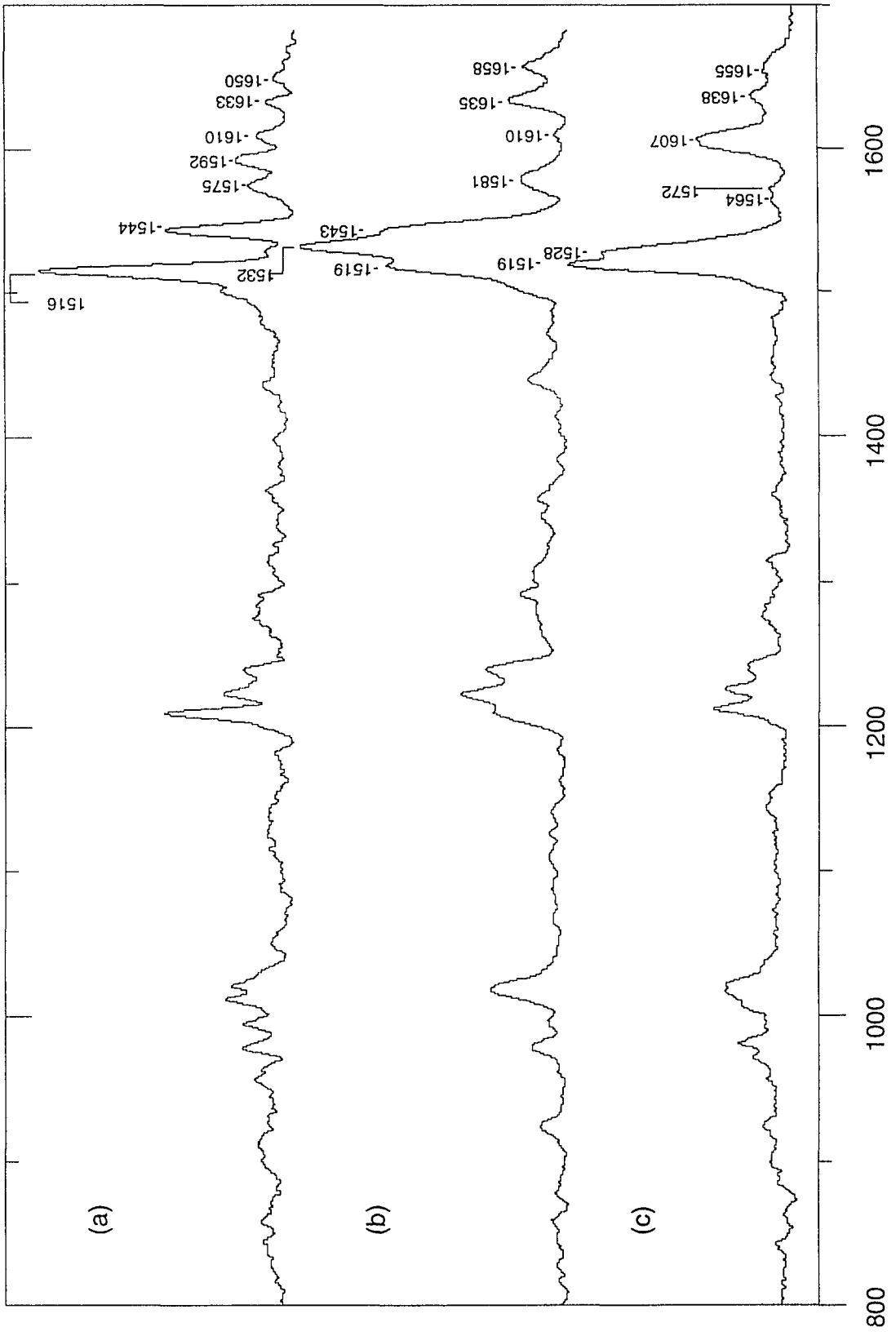
(a)
(b)
(c)
1516
1532
1544
1543
1575
1592
1610
1581
1610
1633
1635
1650
1658
1564
1572
1607
1638
1655
800
1000
1200
1400
1600

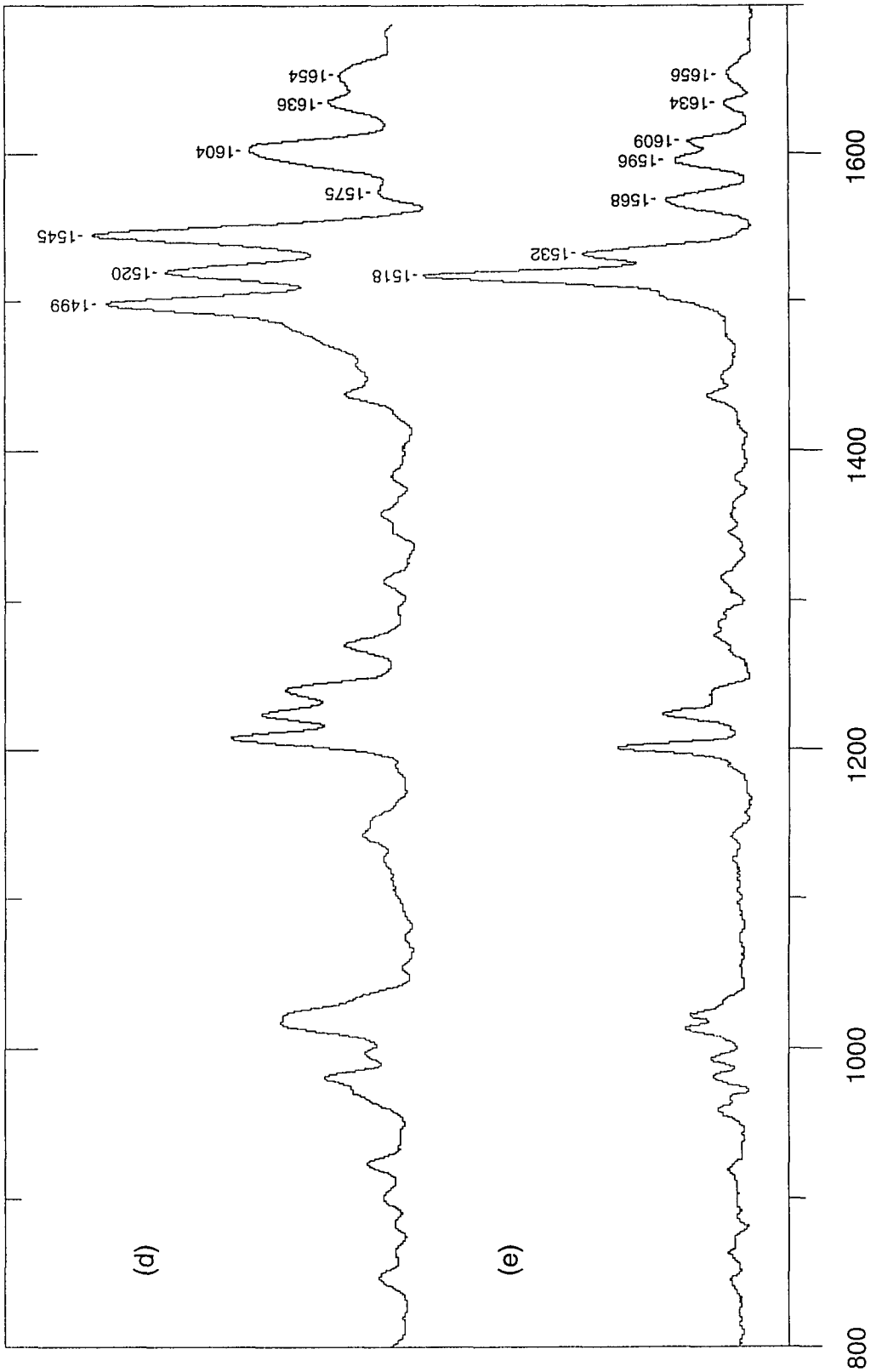
(d)
1499
1520
1545
1575
1604
1636
1654
(e)
1518
1532
1568
1596
1609
1634
1656
800
1000
1200
1400
1600

Figure 6.4: Resonance Raman spectra of octopus rhodopsin with (a) 11,12-D_2, (b) 8-^{13}C-11,12-D_2, (c) 10-^{13}C-11,12-D_2, (d) 11-^{13}C-11,12-D_2, and (e) 14-^{13}C-11,12-D_2 substituted retinal chromophores

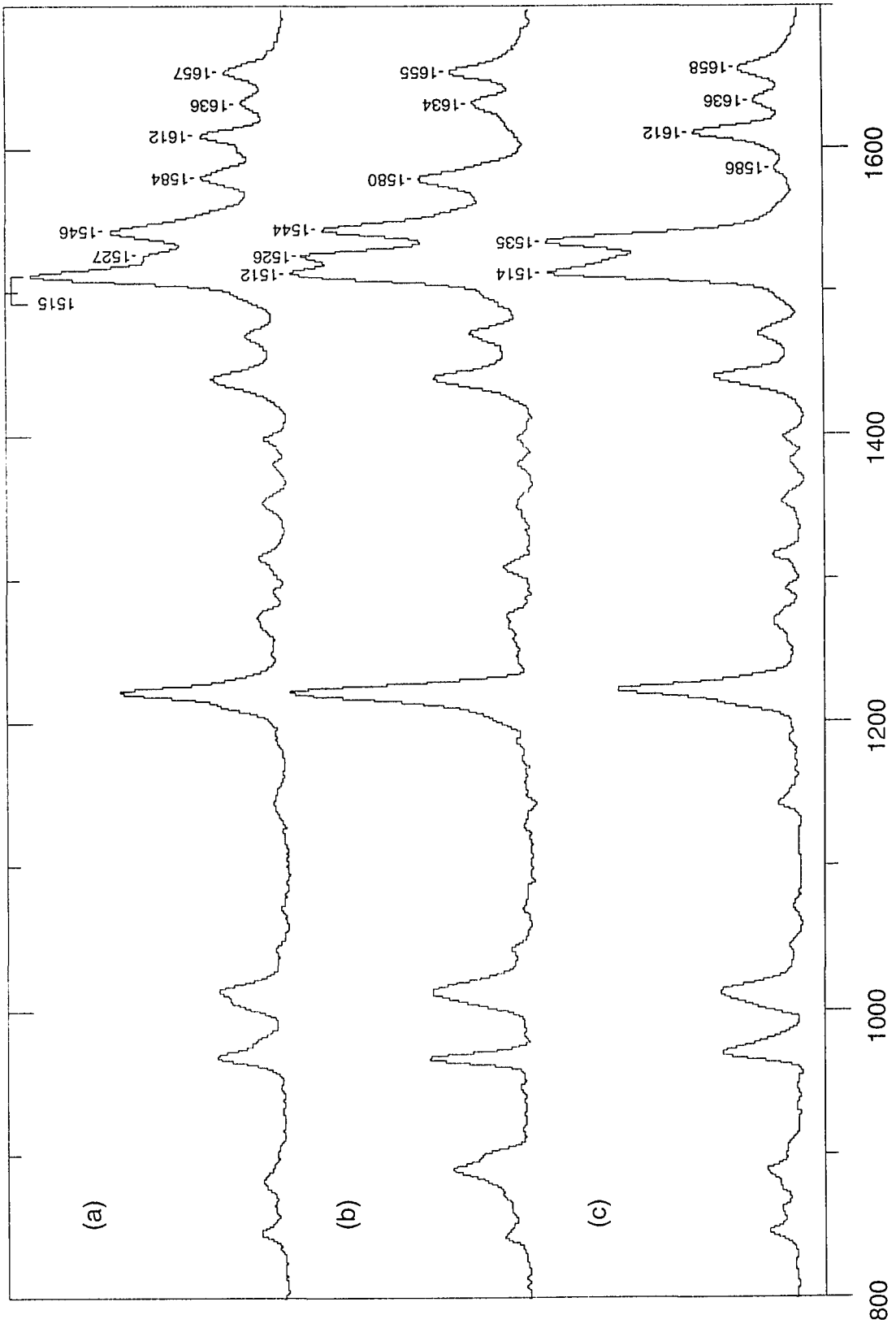
(a)
(b)
(c)
1515
1527
1546
1584
1612
1636
1657
1512
1526
1544
1580
1634
1655
1514
1535
1586
1612
1636
1658
800
1000
1200
1400
1600

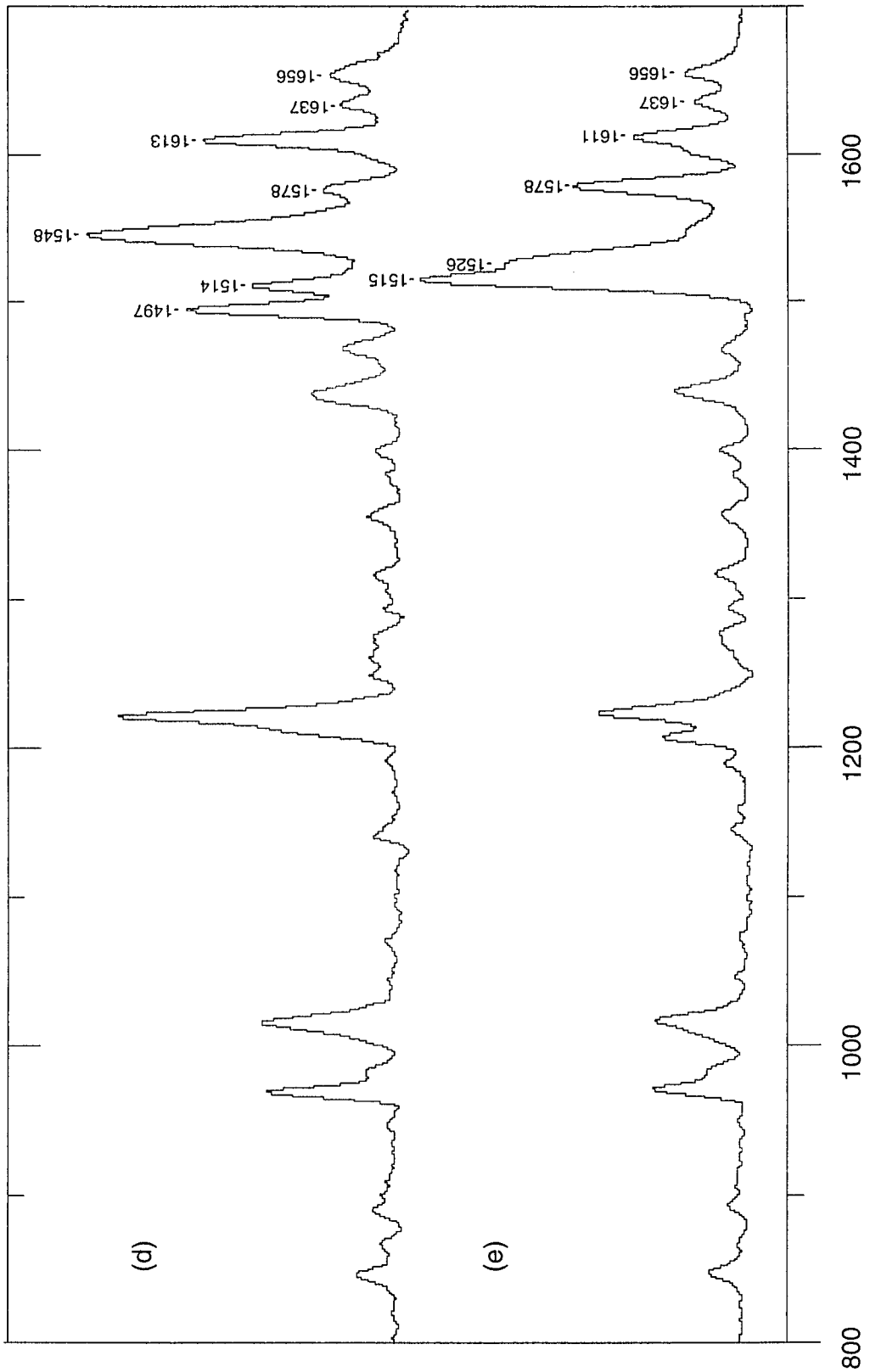
(d)
(e)
1497
1514
1515
1526
1548
1578
1578
1611
1613
1637
1637
1656
1656
800
1000
1200
1400
1600

Figure 6.5: Resonance Raman spectra of bovine isorhodopsin with (a) 11,12-D_2, (b) 8-^{13}C-11,12-D_2, (c) 10-^{13}C-11,12-D_2, (d) 11-^{13}C-11,12-D_2, and (e) 14-^{13}C-11,12-D_2 substituted retinal chromophores

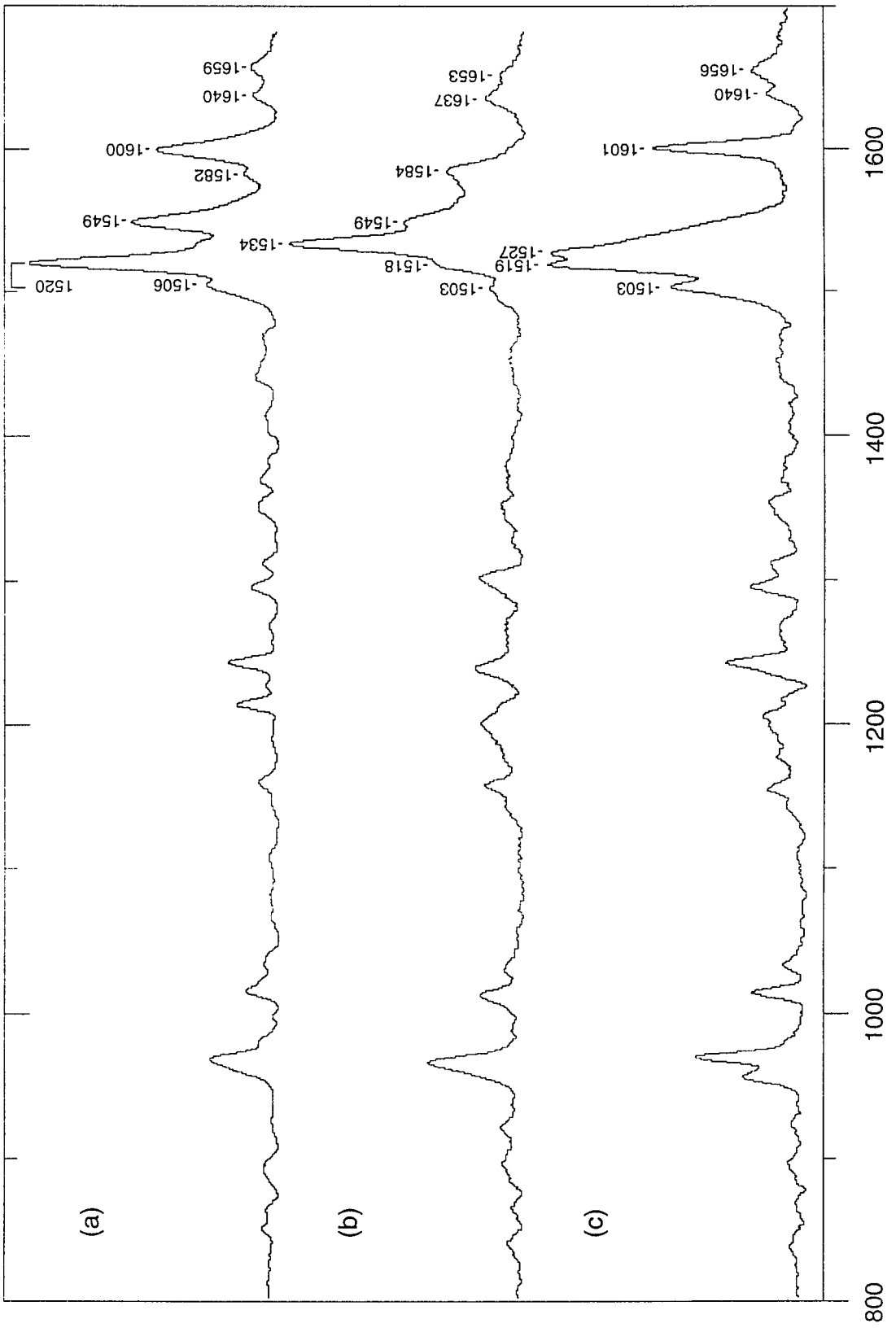
(a)
(b)
(c)
1659
1640
1600
1582
1549
1534
1520
1506
1653
1637
1584
1549
1534
1519
1518
1503
1656
1640
1601
1527
1503
800
1000
1200
1400
1600

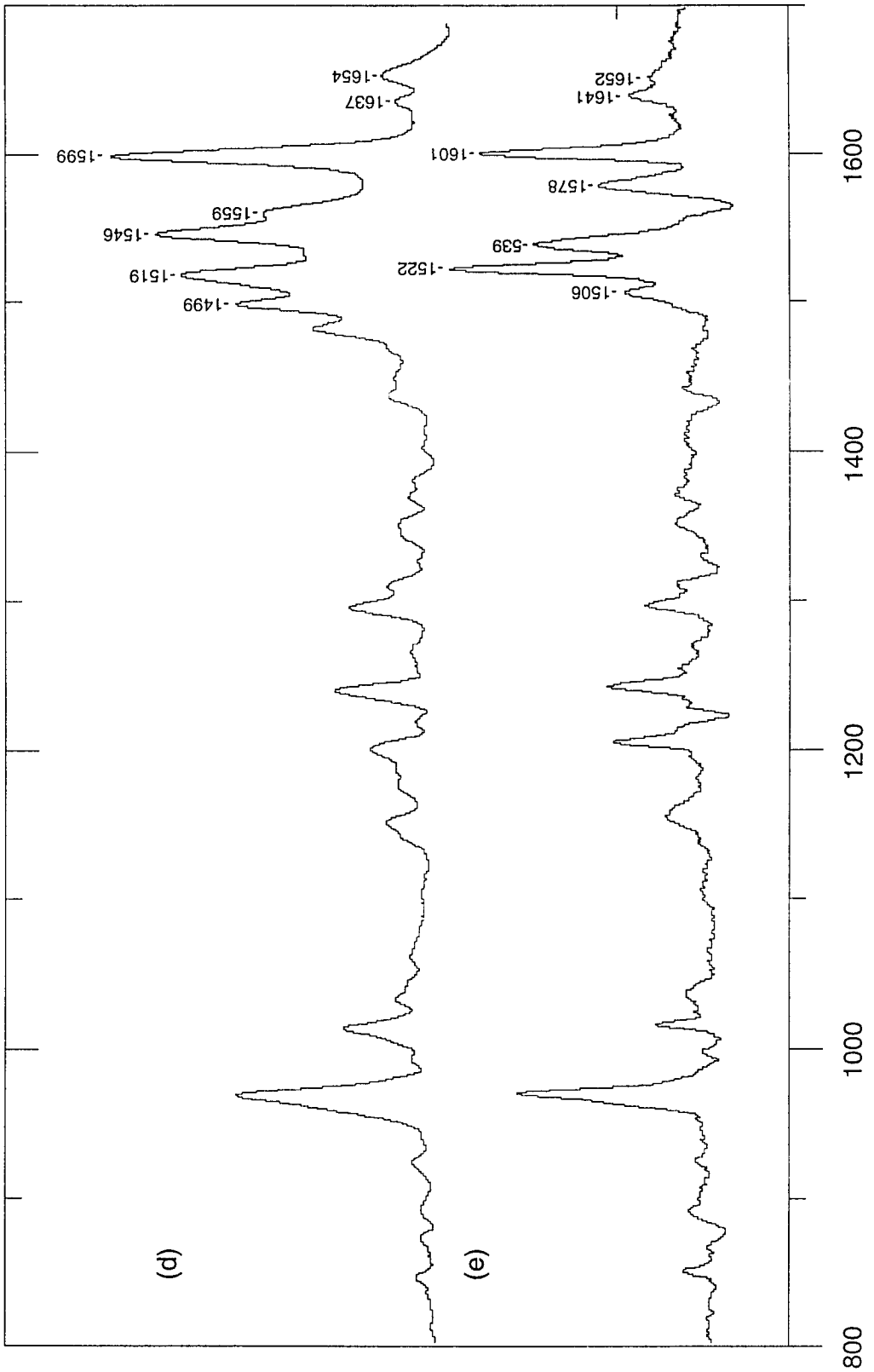
(d)
(e)
1654
1637
1599
1559
1546
1519
1499
1652
1641
1601
1578
539
1522
1506
800
1000
1200
1400
1600

Figure 6.6: Resonance Raman spectra of octopus isorhodopsin with (a) 11,12-D_2, (b) 8-^{13}C-11,12-D_2, (c) 10-^{13}C-11,12-D_2, (d) 11-^{13}C-11,12-D_2, and (e) 14-^{13}C-11,12-D_2 substituted retinal chromophores

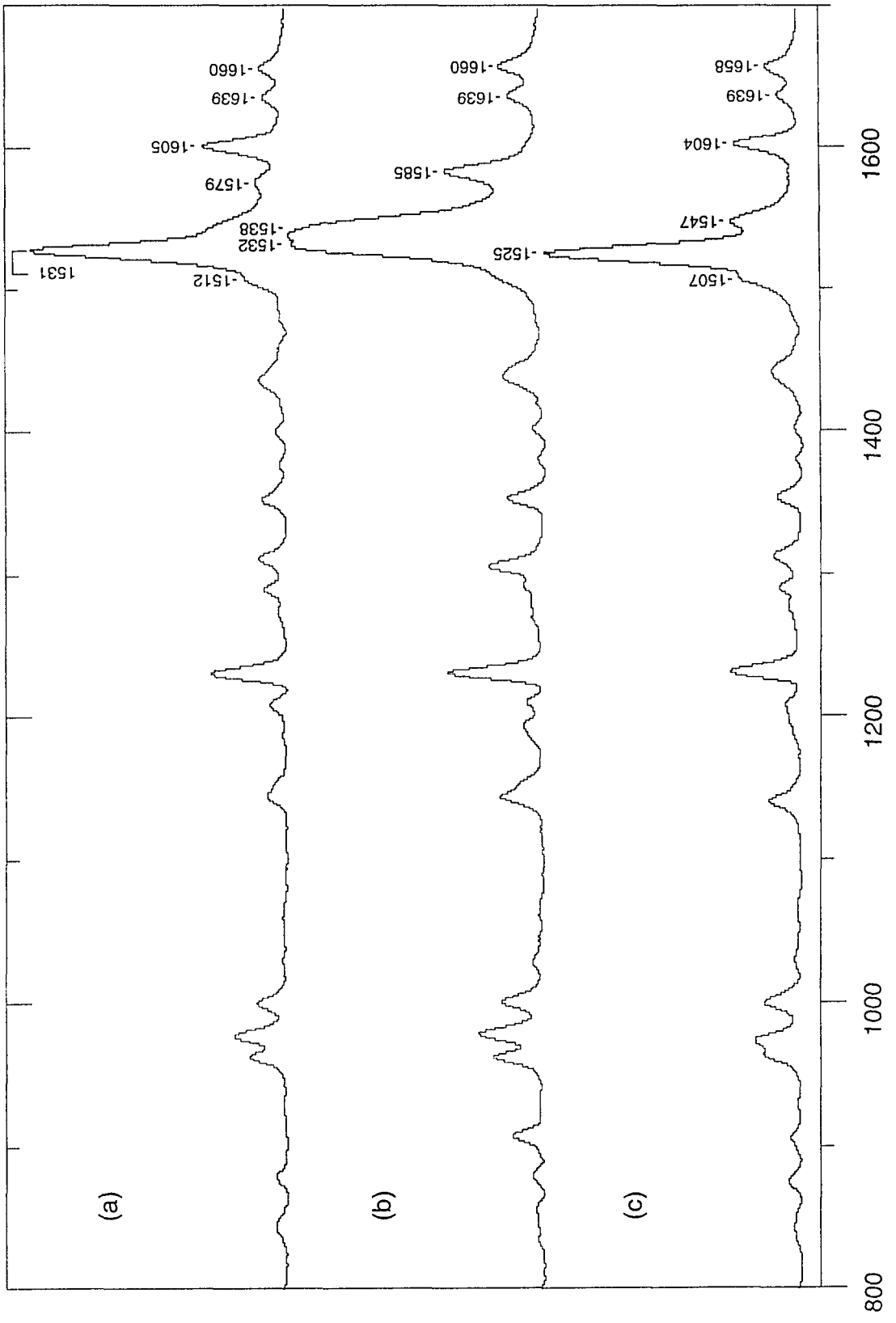
(a)
(b)
(c)
1531
1512
1532
1538
1579
1605
1639
1660
1585
1525
1547
1604
1639
1658
1507
800
1000
1200
1400
1600

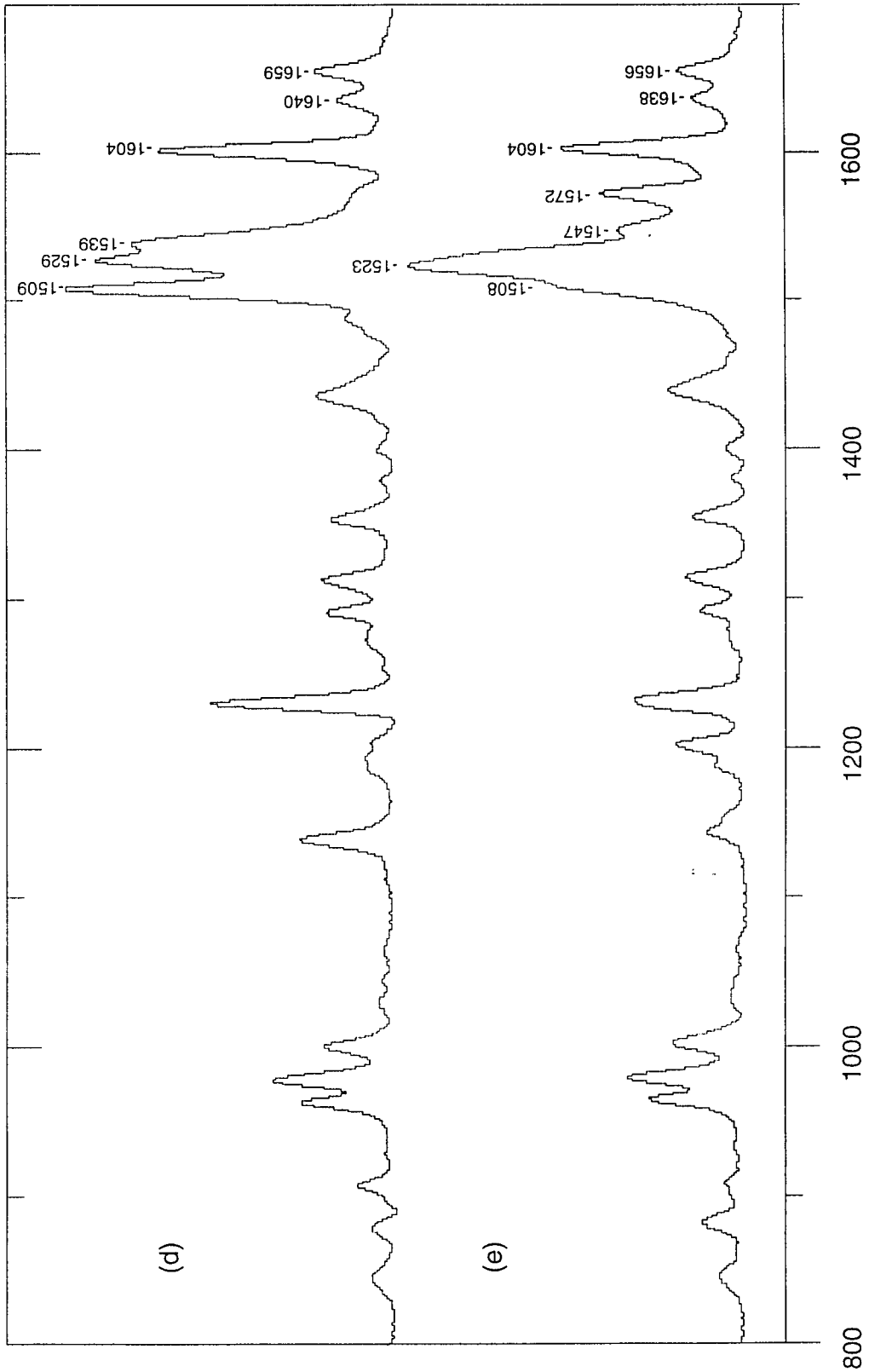
(d)
1509
1529
1539
1604
1640
1659
(e)
1508
1523
1547
1572
1604
1638
1656
800
1000
1200
1400
1600

Chart 6.1 Assignments of Ethylenic-Schiff base modes of bovine bathorhodopsin

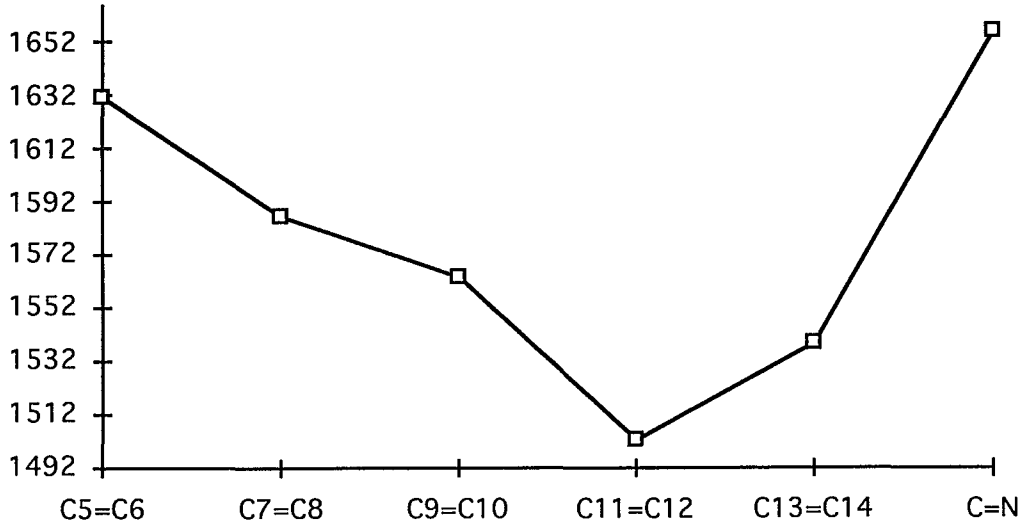

Chart 6.2 Assignments of Ethylenic-Schiff base modes of octopus bathorhodopsin

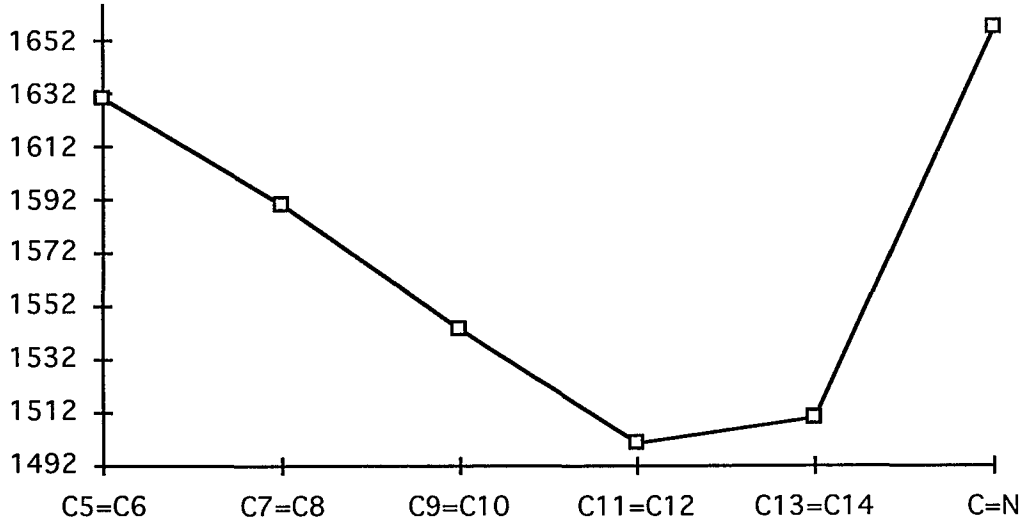

Chart 6.3 Assignments of Ethylenic-Schiff base modes of bovine rhodopsin

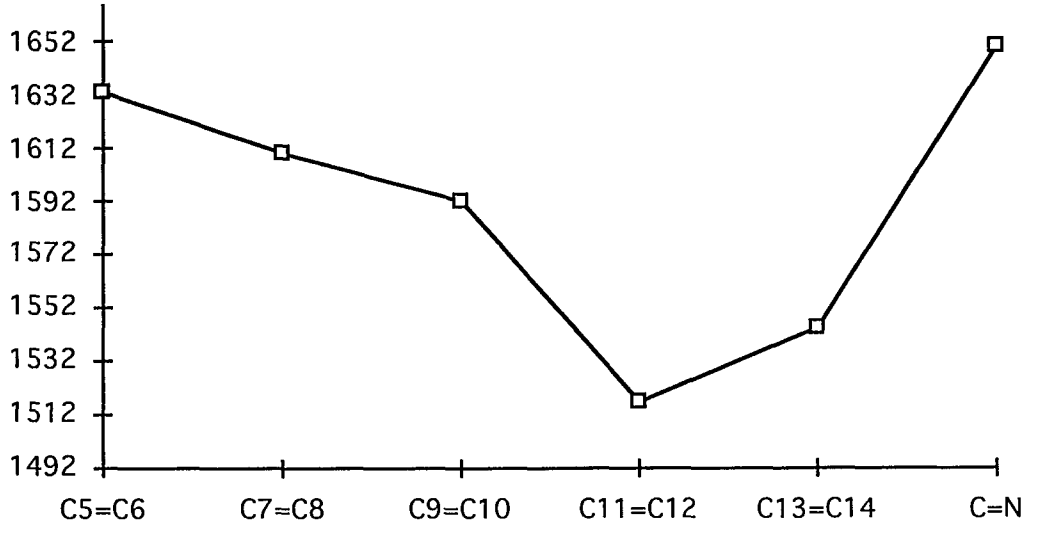

Chart 6.4 Assignments of Ethylenic-Schiff base modes of octopus rhodopsin

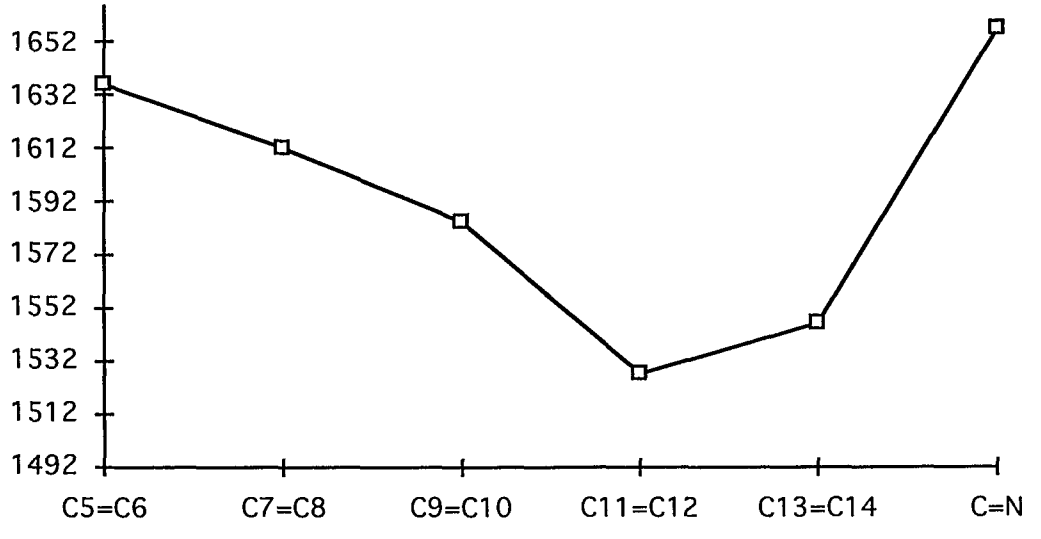

Chart 6.5 Assignments of Ethylenic-Schiff base modes of bovine isorhodopsin

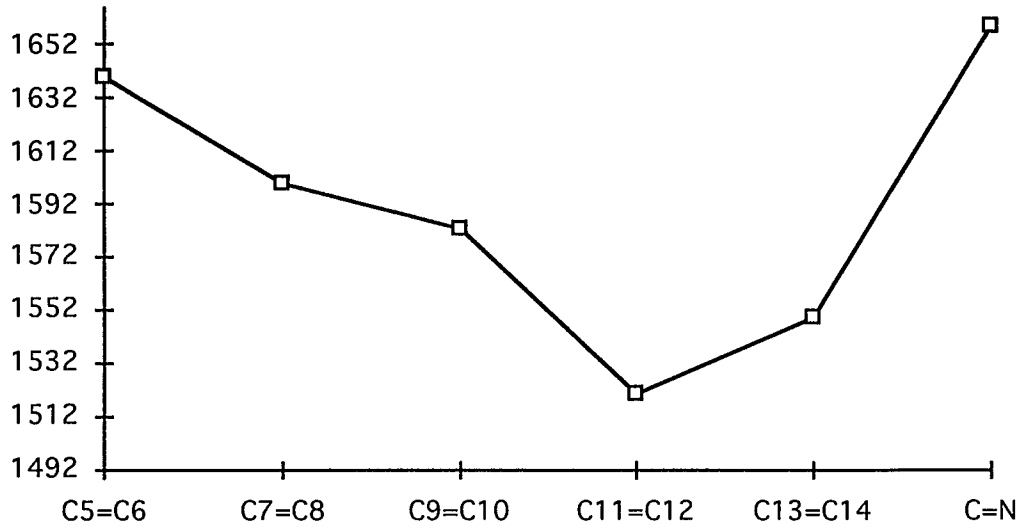

Chart 6.6 Assignments of Ethylenic-Schiff base modes of octopus isorhodopsin

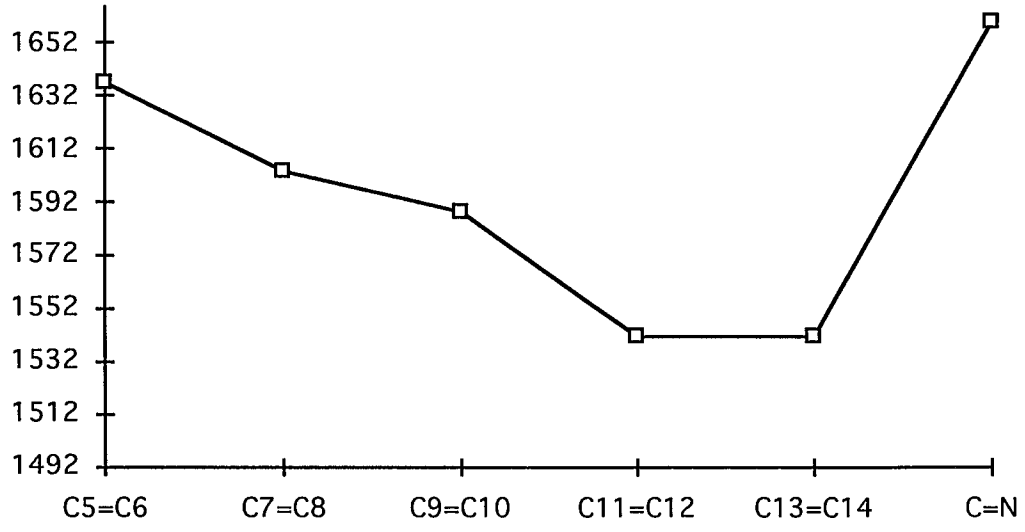

Chart 6.7: Correlation of degenerated ethylenic (C5=C6, C7=C8, C9=C10, C11=C12C, and C13=C14) stretching frequencies of bovine and octopus visual pigments with their absorption maxima. Only the C11=C12 stretch frequency has the inversely linear correlation with has been suggested for generated C=C bonds.

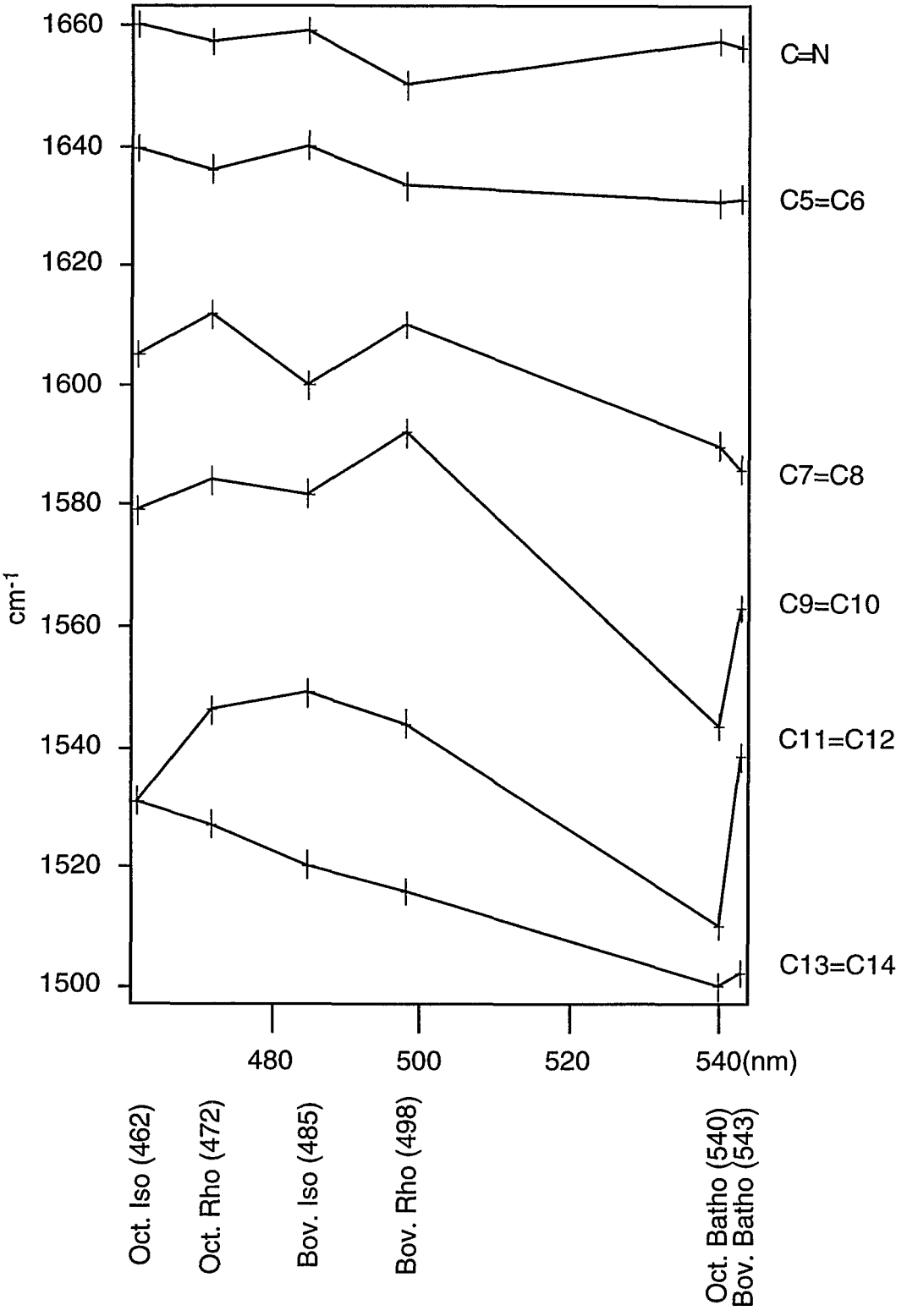
1660
1640
1620
1600
1580
1560
1540
1520
1500
cm-1
C=N
C5=C6
C7=C8
C9=C10
C11=C12
C13=C14
480
500
520
540(nm)
Oct. Iso (462)
Oct. Rho (472)
Bov. Iso (485)
Bov. Rho (498)
Oct. Batho (540)
Bov. Batho (543)

BIBLIOGRAPHY

1. Albrecht, A. C. (1961). *J. Chem. Phys.* **34**: 1476-84

2. Albrecht, A. C., and M. C. Hutley. (1971). *J. Chem. Phys.* **55**: 4438

3. Ames, J. B., S. A. Fodor, R. Gebhard, J. Raap, E. M. v. d. Berg, J. Lugtenburg, and R. A. Mathies. (1989). Bacteriorhodopsin's M412 intermediate contains a 13-cis, 14-s-trans, 15-anti-Retinal Schiff base chromophore. *Biochemistry* **28**: 3681-3687

4. Applebury, M. L., and P. A. Hargrave. (1986). Molecular Biology of the Visual Pigments. *Vision Res.* **26**: 1881-1895

5. Applebury, M. L., D. M. Zuckerman, A. A. Lamola, and T. M. Jovin. (1974). Rhodopsin. Purification and Recombination with Phospholipids Assayed by the Metarhodopsin -> Metarhodopsin II Transition. *Biochemistry* **13**: 3448-3458

6. Aton, B., R. H. Callender, and B. Honig. (1978). Photochemical cis-trans isomerisation of bovine rhodopsin at liquid helium trmperatures. *Nature* **273**: 784-786

7. Aton, B., A. Doukas, D. Narva, R. Callender, U. Dinur, and B. Honig. (1980). Resonance Raman Studies of the Primary Photochemical Event in Bovine Visual Pigment. *Biophys. J.* **29**: 79-94

8. Aton, B., A. G. Doukas, R. H. Callender, B. Becher, and T. G. Ebrey. (1977). Resonance Raman Studies of the Purple Membrane. *Biochem.* **16**: 2995-2999

9. Aton, B., A. G. Doukas, R. H. Callender, B. Becher, and T. G. Ebrey. (1979). Resonance Raman Study of the Dark-adapted Form of the Purple Membrane Protein. *Biochimica et Biophysica Acta* **576**: 424-428

10. Bagley, A. K., L. Eisenstein, G. T. Ebrey, and M. Tsuda. (1989). A Comparative Study of the Infrared Difference Spectra for Octopus and Bovine Rhodopsins and Their Bathorhodopsin Photointermediates. *Biochem.* **28**: 3366-3373

11. Bagley, K. A., V. Balogh-Nair, A. A. Croteau, G. Dollinger, T. G. Ebrey, L. Eisenstein, M. K. Hong, K. Nakanishi, and J. Vittitow. (1985). Fourier-Transform Infrared Difference Spectroscopy of Rhodopsin and Its Photoproducts at Low Temperatures. *Biochem.* **24**: 6055-6071

12. Becher, B., and J. Cassim. (1975). Improved isolation procedures for the purple membrane protein of Halobacterium Halobium. *Prep. Biochem.* **5**: 161-168

13. Bennett, N. (1978). Evidence for Differently Protonated Forms of Metarhodopsin II as Intermediates in the Decay of Membrane-bound Cattle Rhodopsin. *Biochemical and Biophysical Research Communications* **83**: 457-465

14. Birge, R. (1990). Photophysics and Molecular Electronic Applications of the Rhodopsins. *Ann. Rev. Phys. Chem.* **41**: 683-733

15. Birge, R., and R. H. Callender. (1987). Quantum Efficiencies of Primary Photochemical Processes in Vertebrate Rhodopsin. In *Biophysical Studies of Retinal Proteins*, ed. TG Ebrey, B Honig, H Fraunfelder, K Nakanishi, pp. 270-281. Urbana-Champaign: University of Illinois Press

16. Birge, R. R. (1990). Nature of the Primary Photochemical Events in Rhodopsin and Bacteriorhodopsin. *Biochim. Biophys. Acta* **1016**: 293-327

17. Birge, R. R., C. M. Einterz, H. M. Knapp, and L. P. Murray. (1988). The Nature of the Primary Photochemical Events in Rhodopsin and Isorhodopsin. *Biophys. J.* **53**: 367-385

18. Birge, R. R., and C.-F. Zhang. (1990). Two Photon Double Absorption Spectroscopy of Bacteriorhodopsin. Assignment of the Electronic and Dipolar Properties of the Low-Lying $^1A_g^{*-}$ and $^1B_u^{*+}$-like π,π^* States. *J. Chem. Physics* **92**: 7178-7195

19. Blasie, J., and C. Worthington. (1969). *J. Mol. Biol.* **39**: 417

20. Blazej, D. C., and W. L. Peticolas. (1977). Ultraviolet Resonant Raman Spectroscopy of Nucleic Acid Components. *Proc. Natl. Acad. Sci. (USA)* **1977**: 2639-2643

21. Braiman, M., and R. Mathies. (1982a). *Proc. Natl. Acad. Sci. USA* **79**: 403

22. Braiman, M., and R. Mathies. (1982b). *Meth. Enzymol* **88**: 648

23. Brown, K. G., S. C. Erfurth, E. W. Small, and W. L. Peticolas. (1972). Conformationally Dependent Low-Frequency Motions of Proteins by Laser Raman Spectroscopy. *Proc. Natl. Acad. Sci. (USA)* **69**: 1467-1469

24. Buchert, J., V. Stefancic, A. G. Doukas, R. R. Alfano, R. H. Callender, J. Pande, H. Akita, V. Balogh-Nair, and K. Nakanishi. (1983). Picosecond Kinetic Absorption and Fluorescence Studies of Bovine Rhodopsin with a Fixed 11-ene. *Biophys. J.* **43**: 279-283

25. Busch, G. E., M. L. Applebury, A. A. Lamola, and P. M. Rentzepis. (1972). Formation and Decay of Prelumirhodopsin at Room Temperature. *Proc. natl. Acad. Sci. (USA)* **69**: 2802-2806

26. Callender, R. (1979). Resonance Raman Studies of Visual Pigments. In *Light Scattering in Solids*, ed. JL Birman, HZ Cummins, pp. 391-402.

27. Callender, R. (1982a). An Introduction to Visual Pigments and Pruple Membranes and Their Primary Processes. In *Biological Events Probed By Ultrafast Laser Spectroscopy*, ed. pp. 239-258. Academic Press

28. Callender, R. (1982b). Resonance Raman Techniques for Photolabile Samples: Pump-Probe and Flow. *Methods In Enzymology* **88**: 625-633

29. Callender, R., and B. Honig. (1977). Resonance Raman Studies of Visual Pigments. *Ann. Rev. Biophys. Bioeng.* **6**: 33-35

30. Callender, R. H. (1989). The First Picosecond in Vision. In *Cell Structure and Function by Microspectrofluorometry*, ed. E Kohen, J Hirschberg, pp. 185-198. New York: Academic Press

31. Callender, R. H., A. Doukas, R. Crouch, and K. Nakanishi. (1976). Molecular Flow Resonance Raman Effect from Retinal and Rhodopsin. *Biochem.* **15**: 1621-1629

32. Carey, P. R. (1982). *Biochemical Applications of Raman and Resonance Raman Spectroscopy.* New York: Academic Press

33. Collins, F. D., and R. A. Morton. (1950). Studies in rhodopsin. 3. Rhodopsin and transient orange. *Biochem. J.* **47**: 18

34. Cone, R. (1972). *Nature* **236**: 39

35. Cooper, A. (1979). Energy Uptake in the First Step of Visual Excitation. *Nature (Lond.)* **282**: 531-533

36. Cooper, A., S. F. Dixon, and M. Tsuda. (1986). Photoenergetics of Octopus Rhodopsin: Convergent Evolution of Biological Photon Counters. *Eur. Biophys. J.* **13**: 195-201

37. Cromwell, M. M., R. Gebhard, X. Y. Li, E. S. Batenburg, J. P. Hopman, J. Lugtenberg, and R. A. Mathies. (1992). Synthesis and vibrational analysis of a locked 14-s-cis conformer of retinal. *J. Am. Chem. Soc.* **114**: 10860-10869

38. Crouch, R. K., Y. S. Or, S. Ghent, C.-H. Chang, R. Govindjee, T. G. Ebrey, R. H. Callender, and A. Pande. (1984). Neither the Retinal Ring nor the Ring Double Bond is required for Proton Pumping in Bacteriorhodopsin: Acyclic Retinal Bacterioopsin Analogues. *Journal of the American chemical Society* **106**: 8325-8327

39. Curry, B., A. Broek, J. Lugtenburg, and R. Mathies. (1982). Vibrational Analysis of All-*trans* Retinal. *J. Am. Chem. Soc.* **104**: 5274-5286

40. Curry, B., I. Palings, A. D. Breok, J. A. Pardoen, J. Lugtenburg, and R. Mathies. (1985). Vibrational Analysis of the Retinal Isomers. *Adv. Infrared and Raman Spect.* **12**: 115-178

41. Curry, B., I. Palings, A. Broek, J. A. Pardoen, P. P. J. Mulder, J. Lugtenburg, and R. Mathies. (1984). Vibrational Analysis of 13-*cis*-Retinal. *J. Phys. Chem.* **88**: 688-702

42. Cusanovich, M. A. (1982). Kinetics and Mechanism of Rhodopsin Regeneration with 11-cis-Retinal. *Methods In Enzymology* **81**: 443-447

43. Daemen, F. (1973). *Biochem. Biophys. Acta* **300**: 255

44. Deng, H. (1987). Resonance Raman Studies of Visual Pigments & Bacteriorhodopsin. *Ph. D. Thesis* :

45. Deng, H., and R. H. Callender. (1987). A Study of the Schiff Base Mode in Bovine Rhodopsin and Bathorhodopsin. *Biochem.* **26**: 7418-7426

46. Deng, H., L. Huang, R. Callender, and T. Ebrey. (1994a). Evidence For a Bound Water Molecule Next to the Retinal Schiff Base in Bacteriorhodopsin and Rhodopsin: A Resonance Raman Study of the Schiff Base Hydrogen/Deuterium Exchange. *Biophys. J.* **66**: 1129-1136

47. Deng, H., L. Huang, M. Groesbeek, J. Lugtenburg, and R. H. Callender. (1994b). Vibrational Analysis of a Retinal Protonated Schiff Base Analog. *JPC* **98**: 4776-4779

48. Deng, H., D. Manor, G. Weng, P. Rath, Y. Koutalos, T. Ebrey, R. Gebhard, J. Lugtenberg, M. Tsuda, and R. H. Callender. (1991a). Resonance Raman Studies of the HOOP Modes in Octopus Bathorhodopsin with Deuterium Labeled Retinal Chromophores. *Biochem.* **30**: 4495-4502

49. Deng, H., D. Manor, G. Weng, P. Rath, Y. Koutalos, T. Ebrey, R. Gebhard, J. Lugtenburg, M. Tsuda, and R. H. Callender. (1991b). A Resonance Raman Study of Octopus Bathorhodopsin with Deuterium Labelled Chromophores. *Photochem. Photobiol.* **54**: 1001-1007

50. Doukas, A. G., B. Aton, and R. H. Callender. (1978a). Resonance Raman Excitation profiles of All-trans Retinal: Theoretical Implications. *Chemical Physics Letters* **56**: 248-252

51. Doukas, A. G., B. Aton, and R. H. Callender. (1978b). Resonance Raman Studies of Bovine Metarhodopsin I and Metarhodopsin II. *Biochemistry* **17**: 2430-2435

52. Doukas, A. G., R. H. Callender, and R. R. Alfano. (1986). Ultrafast Photophysical Processes in Visual Pigments. In *Applications of Fluorescence in teh Biomedical Sciences*, ed. pp. 69-89. Alan R. Liss, Inc.

53. Doukas, A. G., M. R. Junnarkar, R. R. Alfano, R. H. Callender, and V. Balogh-Nair. (1985). The Primary Event in Vision Investigated by Time-Resolved Fluorescence Spectroscopy. *Biophys. J.* **47**: 795-798

54. Doukas, A. G., M. R. Junnarkar, R. R. Alfano, R. H. Callender, T. Kakitani, and B. Honig. (1984). Fluorescence Quantum Yield of Visual Pigments: Evidence for Subpicosecond Isomerization Rates. *Proc. Natl. Acad. Sci. (USA)* **81**: 4790-4794

55. Doukas, A. G., A. Pande, T. Suzuki, R. H. Callender, B. Honig, and M. Ottolenghi. (1981). On the mechanism of hydrogen-deuterium exchange in bacteriorhodopsin. *Biophys. J.* **33**: 275-280

56. Druckmann, S., M. Ottolenghi, A. Pande, J. Pande, and R. Callender. (1982). Acid-Base Equilibrium of the Schiff Base in Bacteriorhodopsin. *Biochem.* **21**: 4953-4959

57. Ebrey, T. G. (1971). The use of Ammonyx Lo in the purification of Rhodopsin and Rod Outer Segment. *Vision Res.* **11**: 1007-1009

58. Ehrenberg, B., A. Lewis, T. Porta, J. Nagle, and W. Stoeckenius. (1980). Exchange Kinetics of the Schiff base Proton in Bacteriorhodopsin. *Proc. Natl. Acad. Sci. U. S. A.* **77**: 6571-6573

59. Eigen, M. (1964). Proton Transfer, Acid-Base Catalysis, and Enzymatic Hydrolysis. *Angewandte Chemie International Edition English* **3**: 1-19

60. El-Sayed, M. A. (1982). *Methods Enzymol* **88**: 617-625

61. Englander, S. W., N. W. Downer, and H. Teitelbaum. (1972). Hydrogen exchange. *Ann. Rev. Phys. Chem.* **41**: 903-924

62. Englander, S. W., and L. Mayne. (1992). Protein folding studed using hydrogen-exchange labeling and two-dimensional NMR. *Annu. Rev. Biophys. Biomol. Struct.* **21**: 243-65

63. Eyring, G., B. Curry, A. Broek, J. Lugtenburg, and R. Mathies. (1982). Assignment and Interpretation of Hydrogen Out-of-Plane Vibrations in the Resonance Raman Spectra of Rhodopsin and Bathorhodopsin. *Biochem.* **21**: 384-393

64. Eyring, G., B. Curry, R. Mathies, A. Broek, and J. Lugtenburg. (1980a). Assignment of the Anomalous Resonance Raman Vibrations of Bathorhodopsin. *J. Am. Chem. Soc.* **102**: 5390-5392

65. Eyring, G., B. Curry, r. Mathies, R. Fransen, I. Palings, and J. Lugtenburg. (1980b). Interpretation of the Resonance Raman Spectrum of Bathorhokopsin Based on Visual Pigment Analogues. *Biochemistry* **19**: 2410-2418

66. Eyring, G., and R. Mathies. (1979). Resonance Raman Studies of Bathorhodopsin: Evidence for a Protonated Schiff Base Linkage. *Proc. Natl. Acad. Sci. U. S. A.* **76**: 33-37

67. Fahmy, K., F. Siebert, and P. Tavan. (1991). Structural investigation of bacteriorhodopsin and some of its photoproducts by polarized Fourier transform infrared spectroscopic methods-difference spectroscopy and photoselection. *Biophys. J.* **60**: 989-1001

68. Favrot, J., C. Sandorfy, and D. Vocelle. (1978). An infrared study of the basicity on non-aromatic imines: relation to visual pigments. *Photochem. Photobiol.* **28**: 271-272

69. Fodor, S. A., W. T. Pollard, R. Gebhard, E. M. v. d. Berg, J. Lugtenburg, and R. A. Mathies. (1988a). Bacteriorhodopsin's L550 intermediate contains a C14-C15-s-trans-retinal chromophore. *Proc. Natl. Acad. Sci. USA* **85**: 2156-2160

70. Fodor, S. P. A., J. B. Ames, R. Gebhard, E. M. M. v. d. Berg, W. Stoeckenius, J. Lugtenburg, and R. A. Mathies. (1988b). Chromophore Structure in Bacteriorhodopain's N Intermediate: Implications for the Proton-Pumping Mechanism. *Biochemistry* **27**: 7097-7101

71. Fransen, M. R., W. C. M. M. Luyten, J. van Thuijl, J. Lugtenburg, P. A. A. Jansen, P. J. G. M. van Greugel, and F. J. M. Daemen. (1976). *Nature (London)* **260**: 726-727

72. Friedman, J. M., and R. M. Hochstrasser. (1974). *Chem. Phys.* **6**: 155-65

73. Frisch, M. J., G. W. Trucks, M. Head-Gordon, P. M. W. Gill, M. W. Wong, J. B. Foresman, B. G. Johnson, H. B. Schlegel, M. A. Robb, E. S. Replogle, R. Gomperts, J. L. Andres, K. Raghavachari, J. S. Binkley, C. Gonzalez, R. L. Martin, D. J. Fox, D. J. Defrees, J. Baker, J. J. P. Stewart, and J. A. Pople. (1992). *Gaussian 92, Revision C.* Pittsburgh PA: Gaussian, Inc.

74. Gilson, H. S. R., B. H. Honig, A. Croteau, G. Zarrilli, and K. Nakanishi. (1988). Analysis of the Factors that Influence the C=N Stretching Frequency of Polyene Schiff Bases: Implications for Bacteriorhodopsin and Rnodopsin. *Biophys. J.* **53**: 261-269

75. Grip, W. J. D. (1982). Purification of Bovine Rhodopsin Over Concanavalin A-Sepharose. *Methods In Enzymology* **81**: 197-207

76. Grossjean, M. F., P. Tavan, and K. Schulten. (1990). Quantumchemical vibrational analysis of the chromophore of bacteriorhodopsin. *J. Phys. Chem.* **94**: 8059-8069

77. Hargrave, P. A., J. H. McDowell, D. R. Curtis, J. K. Wang, E. Juszczak, S.-L. Fong, J. K. M. Rao, and P. Argos. (1983). *Biophys. Struct. Mech.* **9**: 235-244

78. Heyde, M. E., D. Gill, R. Kilponen G., and L. Rimai. (1971). *J. Am. Chem. Soc.* **93**: 6776

79. Hildebrandt, P., and M. Stockburger. (1984). Role of Water in Bacteriorhodopsin's Chromophore: Resonance Raman Study. *Biochemistry* **23**: 5539-5548

80. Hong, K., P. J. Knudsen, and W. L. Hubbell. (1982). Purification of Rhodopsin on Hydrozyapatite Columns, Detergent Exchange, and Recombinaiton with Phospholipids. *Methods In Enzymology* **81**: 144-150

81. Honig, B., U. Dinur, K. Nakanishi, V. Balogh-Nair, M. Gawinowicz, M. Arnaboldi, and M. G. Motto. (1979a). An External Point Charge Model for Wavelength Regulation in Visual Pigments. *J. Am. Chem. Soc.* **101**: 7084-7086

82. Honig, B., T. Ebrey, R. Callender, U. Dinur, and M. Ottolenghi. (1979b). Photoisomeization, Energy Storage, and Charge Separation: A Model for Light Energy Transduction in Visual Pigments and Bacteriorhodopsin. *Proc. Natl. Acad. Sci.(USA)* **76**: 2503-2508

83. Honig, B., A. D. Greenberg, U. Dinur, and T. G. Ebrey. (1976). Visual-Pigment Spectra: Implications of the Protonation of the Retinal Schiff Base. *Biochem.* **15**: 4593-4599

84. Honig, B., B. Hudson, B. D. Sykes, and M. Karplus. (1971). *Proc. Natl. Acad. Sci. U. S. A.* **68**: 1289

85. Hubbard, R., and A. Kropf. (1958). The Action of Light on Rhodopsin. *Proc. N. A. S.* **44**: 130-139

86. Hubbard, R., and A. Kropf. (1965). *J. Gen. Physiol.* **49**: 381

87. Hubbard, R., and G. Wald. (1952). Cis-trans Isomers of Vitamin A and Retinene in teh Rhodopsin System. *J. Gen. Physiol.* : 269-315

88. Hurley, J., T. G. Ebrey, B. Honig, and M. Ottolenghi. (1977). Temperature and wavelength effects on the photochemistry of rhodopsin, isorhodopsin, bacteriorhodopsin, and their photoproducts. *Nature (Lond.)* **270**: 540-542

89. Inagaki, F., M. Tasumi, and T. Miyazawa. (1974). *J. Mol. Spectrosc.* **50**: 286-303

90. Jeng, M. F., and S. W. Englander. (1991). Stable submolecular units in a non-compact form of cytochrome c. *J. Mol. Biol.* **221**: 1045-1061

91. Johnson, B. B., and W. L. Peticolas. (1976). *Annu. Rev. Phys. Chem.* **27**: 465

92. Kakitani, H. (1979). Relative Intensity of Near Resonance Raman Lines Evaluated by the A-Term. *Chem. Phys. Lett.* **64**: 344-347

93. Kakitani, H., T. Kakatani, H. Rodman, B. Honig, and R. Callender. (1983). Correlation of Vibrational Frequencies with Absorption Maxima in Polyenes, Rhodopsin, Bacteriorhodopsin, and Retinal Analogues. *J. Phys. Chem.* **87**: 3620-3628

94. Kakitani, T., and H. Kakitani. (1975). Molecular Mechamism for the Initial Process of Visual Excitation. I. Model of Photoisomerization in Rhodopsin and its Theoretical Basis by a Quantum Mechanical Calculation of the Adiabatic Potential. *J. Phys. Soc. Jpn.* **38**: 1455-1463

95. Kim, P. S. (1986). Amide proton exchange as a probe of protein folding pathways. *Methods in Enzymology* **131**: 136-156

96. Kitagawa, T., and M. Tsuda. (1980). Resonance Raman Spectra of Octopus Acid and Alkaline Metarhodopsins. *Biochem. Biophys. Acta* **624**: 211-217

97. Kosower, E. M. (1988). *Proc. Natl. Acad. Sci. U.S.A.* **85**:

98. Koutalos, Y., T. G. Ebrey, H. R. Gilson, and B. Honig. (1990). Octopus photoreceptor membranes Surface charge density and pK of the Schiff base of the pigments. *Biophy. J.* **58**: 493-501

99. Koutalos, Y., T. G. Ebrey, M. Tsuda, K. Odashima, T. Lien, M. H. Park, N. Shimizu, F. Derguini, K. Nakanishi, H. R. Gilson, and B. Honig. (1989). Regeneration of Bovine and octupus opsins in situ with natural and artificial retinals. *Biochem.* **28**: 2732-2739

100. Lam, E., A. Pande, R. Callender, E. F. Hilinski, P. M. Rentzepis, and L. Packer. (1984). Spectroscopic Characterization of Nitrated Purple membranes. *Biochemistry International* **8**: 217-224

101. Lewis, A. (1982). Resonance Raman Spectroscopy of Rhodopsin and Bacteriorhodopsin; An Overview. *Methods In Enzymology* **88**: 561-585

102. Lews, A., J. Spoonhower, R. Bogomolni, R. Lozier, and W. Stoeckenius. (1974). *PNAS USA* **71**: 4462

103. Lin, S. W., Y. Imamoto, Y. Fukada, Y. Shichida, T. Yoshizawa, and R. A. Mathies. (1994). What Makes Red Visual Pigments Red? A Resonance Raman Microprobe Study of Retinal Chromophore Structure in Iodopsin. *Biochemistry* **33**: 2151-2160

104. Lin, S. W., T. P. Sakmar, R. R. Frank, H. G. Khorana, and R. A. Mathies. (1992). Resonance Raman Microprobe Spectroscopy of Rhodopsin Mutants: Effect of Substitutions in the Third Transmembrane Helix. *Biochemistry* **31**: 5105-5111

105. Liu, R. S. H., and A. E. Asato. (1985). The primary process of vision and the structure of bathorhodopsin: A mechanism for photoisomerization of polyenes. *Proc. Natl. Acad. Sci. USA* **82**: 259-263

106. Livnah, N., and M. Sheves. (1993). The Schiff base bond configuration in bacteriorhodopsin and in model compounds. *Biochemistry* **32**: 7223-7228

107. Loppnow, G. R., B. A. Barry, and R. A. Mathies. (1989). *Proc. Natl. Acad. Sci. U.S.A.* **86**: 1515-1518

108. Loppnow, G. R., M. E. Miley, R. A. Mathies, R. S. H. Liu, H. Kandori, Y. Shichida, Y. Fukada, and T. Yoshizawa. (1990). Structure of the retinal Chromophore in 7,9-dicis-Rhodopsin. *Biochemistry* **29**: 8985-8991

109. Lugtenburg, J., R. A. Mathies, R. G. Griffin, and J. Herzfield. (1988). Structure and Function of Rhodopsins from Solid State NMR and Resonance Raman Spectroscopy of Isotopic Retinal Derivatives. *Trends Biochem. Sci.* **13**: 388-393

110. Maeda, A., J. Sasaki, Y. J. Ohkita, M. Simpson, and J. Herzfeld. (1992). Tryptophan Perturbation in the L Intermediate of Bacteriorhodopsin: Fourier Transform Infrared Analysis with Indole -^{15}N Shift. *Biochemistry* **31**: 12543-12545

111. Mathies, R. (1979). . In *Chemical and Biochemical Applications of Lasers*, ed. CB Moore, pp. 55. New York: Academic Press

112. Mathies, R., A. R. Oseroff, and L. Stryer. (1976). Rapid-flow Resonance Raman Spectroscopy of Photolabile Molecules: Rhodopsin and Isorhodopsin. *Proc. Natl. Acad. Sci. (USA)* **73**: 1-5

113. Mathies, R. A., S. W. Lin, J. B. Ames, and W. T. Pollard. (1991). From Femtoseconds to Biology: Mechanism of Bacteriorhodopsin's Light-Driven Proton Pump. *Ann. Rev. Biophys. Biophys. Chem.* **20**: 491-518

114. Mathies, R. A., S. O. Smith, and I. Palings. (1987). Determination of Retinal Chromophore Structrue in Rhodopsins. *Biological Applications of Raman spectroscopy* **2**: 59-108

115. Matsumoto, H., K. Horiuchi, and T. Yoshizawa. (1978). Effect of Digitonin Concentration on Regeneration of Cattle Rhodopsin. *Biochimica et Biophysica Acta* **501**: 257-268

116. Monger, T. G., R. R. Alfano, and R. H. Callender. (1979). Photochemistry of Rhodopsin and Isorhodopsin Investigated on a Picosecond Time Scale. *Biophys. J.* **27**: 105-116

117. Morrison, D. F., P. J. O'Brien, and D. R. Pepperberg. (1991). Depalmitylation with Hydroxylamine Alters the Functional Properties of Rhodopsin. *The Journal of Biological Chemistry* **266**: 20118-20123

118. Narva, D., and R. Callender. (1980). On the State of Chromophore Protonation in Rhodopsin: Implication for Primary Photochemistry in Visual Pigments. *Photochem. Photobiol.* **32**: 273-276

119. Narva, D. L., R. H. Callender, and T. G. Ebrey. (1981). Low temperature Resonance Raman Study of the L Intermediate of Bacteriorhodopsin. *Photochemistry and Photobiology* **33**: 567-571

120. Nathans, J., D. Thomas, and D. S. Hogness. (1986). *Science* **232**: 193-202

121. Ohtani, H., T. Kobayashi, M. Tsuda, and T. Ebrey. (1988). Primary Processes in Photolysis of Octopus Rhodopsin. *Biophys. J.* **53**: 17-24

122. Oseroff, A. R., and R. Callender. (1974). Resonance Raman Spectroscopy of Rhodopsin in Retinal Disk Membranes. *Biochem.* **13**: 4243-4248

123. Ottolenghi, M. (1980). The Photochemistry of Rhodopsins. In *Adv. Photochem.*, ed. pp. 97-200.

124. Ovchinnikov, Y. (1982). *FEBS Lett.* **148**: 179

125. Ovchinnikov, Y. A., N. G. Abdulaev, A. S. Zolotarev, I. D. Artamonov, I. A. Bespalov, A. E. Dergachev, and M. Tsuda. (1988). Octopus rhodopsin
Amino acid sequence deduced from cDNA. *FEBS LETTERS* **232**: 69-72

126. Page, M. I., and W. P. Jencks. (1971). Entropic Contributions to Rate Acceleration in Enzymic and Intramolecular Reactions and the Chelate Effect. *Proc. Nat. Acad. Sci. USA* **68**: 1678-1683

127. Pajares, M. A., and R. R. Rando. (1989). The Active-site Environment of Rhodopsin. *The Journal of Biological Chemistry* **264**: 6804-6809

128. Palings, I., J. A. Pardoen, E. van der Berg, C. Winkle, J. Lugtenburg, and R. Mathies. (1987). Assignment of Fingerprint Vibrations in the Resonance Raman Spectra of Rhodopsin, Isorhodopsin, and

Bathorhodopsin: Implications for Chromophore Structure and Environment. *Biochem.* **26**: 2544-2556

129. Palings, I., E. M. M. van den Berg, J. Lugtenburg, and R. A. Mathies. (1989). Complete Assignment of the Hydrogen Out-of-Plane Wagging Vibrations of Bathorhodopsin: Chromophore Structure and Energy Storage in the Prinary Photoproduct of Vision. *Biochem.* **28**: 1498-1507

130. Pande, A., R. Callender, T. Ebrey, and M. Tsuda. (1984). Resonance Raman Study of the Primary Photochemistry of Visual Pigments Hypsorhodopsin. *Biophys. J.* **45**: 573-576

131. Pande, C., R. H. Callender, J. Baribean, F. Boucher, and A. Pande. (1989). Effect of Lipid Protein Interaction on the Color of Bacteriorhodopsin. *Biochim. Biophys. Acta* **973**: 257-262

132. Pande, C., R. H. Callender, C.-H. Chang, and T. G. Ebrey. (1986). Pesonance Raman Study of the Pink Membrane Photochemically Prepared From the Deionized Blue Membrane of H. Halobium. *Biophys. J.* **50**: 545-549

133. Pande, C., R. H. Callender, R. Henderson, and A. Pande. (1989). Purple Membrane: Color, Crystallinity, and the Effect of DMSO. *Biochem.* **28**: 5971-5977

134. Pande, C., A. Pande, K. T. Yue, R. Callender, T. Ebrey, and M. Tsuda. (1987). Resonance Raman Spectroscopy of Octopus Rhodopsin and its Photoproducts. *Biochem.* **26**: 4941-4947

135. Pande, J., R. H. Callender, and T. G. Ebrey. (1981). Resonance Raman Study of the Primary Photochemistry of Bacteriorhodopsin. *Proc. Natl. Acad. Sci. (USA)* **78**: 7379-7382

136. Pande, J., M. McDermott, R. H. Callender, and A. Spector. (1991). The Calf Gamma Crystallins - A Raman Spectroscopic Study. *Exp. Eye Res.* **52**: 193-197

137. Pande, J., A. Pande, and R. H. Callender. (1982). On the Chromophore Configuration of Metarhodopsin II. *Photochem. Photobiol.* **36**: 107-109

138. Papermaster, D. S., and W. J. Dryer. (1973). Rhodopsin content in the Outer Segment Membranes of Bovine and frog Retinal rods. *Biochem.* **13**: 2438-2444

139. Peters, K., M. L. Applebury, and P. M. Rentzepis. (1977). Primary Photochemical Event in Vision: Proton Translocation. *Proc. Natl. Acad. Sci. (USA)* **74**: 3119-3123

140. Placzek, G. (1934). UCRL Translation no. 526L Leipzig:Akademische Verlagsgesellschaft VI. In *Handbach der Radiologie*, ed. E Marx, pp. 209-374.

141. Poo, M., and R. Cone. (1974). *Nature (London)* **274**:

142. Pugh, E. N. J., and T. D. Lamb. (1993). Amplification and kinetics of the activation steps in phototransduction. *Biochimica et Biophysica Acta* **1141**: 111-149

143. Rafferty, C. N., and H. Schchi. (1981). The involvement of water at the retinal binding site in rhodopsin and early light-induced intramolecular proton transfer. *Photochem. Phoptobiol.* **33**: 229-234

144. Raman, C. V., and K. S. Krishnan. (1928). *Nature (London)* **121**: 501

145. Rao, V. J., F. Derguini, and K. Nakanishi. (1986). 5-(Trifluoromethyl)bacteriorhodopsin Does Not Translocate Protons. *J. Am. Chem. Soc.* **108**: 6077-6078

146. Rimai, L., D. Gill, and J. L. Parsons. (1971). Raman Spectra of Dilute Solutions of Some Stereoisomers of Vitamin A Type Molecules. *J. Am. Chem. Soc.* **93**: 1353-1357

147. Rimai, L., R. G. Kilponen, and D. Gill. (1970). *Biochem. Biophys. Res. Commun.* **41**: 492

148. Roothaan, C. C. J. (1951). A Study of Two-Center Integrals Useful in Calculations on Molecular Structure. I. *TThe Journal of Chemical Physics* **19**: 1445-1457

149. Rosenfeld, T., B. Honig, and M. Ottolenghi. (1977). *Cis-Trans* Isomerization in the Photochemistry of Vision. *Pure and Appl. Chem.* **49**: 341-351

150. Sakmar, T. P., R. R. Franke, and G. Khorana. (1989). Glutamic Acid-113 Serves as the Retinylidene Schiff Base Counterion in Bovine Rhodopsin. *Proc. Natl. Acad. Sci. (USA)* **86**: 8309-8313

151. Schoenlein, R. W., L. A. Peteanu, R. A. Mathies, and C. V. Shank. (1991). The First Step in Vision: Femtosecond Isomerization of Rhodopsin. *Sci.* **254**: 412-414

152. Sheves, M., A. Albeck, N. Friedman, and M. Ottobenghi. (1986). Controlling the pKa of the bacteriorhodopsin Schiff base by use of atificial retinal analogues. *Proc. Natl. Acad. Sci. USA* **83**: 3262-3266

153. Shichi, H. (1970). Spectrum and Purity of Bovine Rhodopsin. *Biochemistry* **9**: 1973-1977

154. Shichi, H., and M. S. Lewis. (1969). Biochemistry of Visual Pigments Purification and Properties of Bovine Rhodopsin. *The Journal of Biological Chemistry* **244**: 529-536

155. Smith, S. O., M. S. Braiman, A. B. Myers, J. A. Pardoen, J. M. L. Courtin, C. Winkel, J. Lugtenburg, and R. A. Mathies. (1987). Vibrational Analysis of the all-*trans* Retinal Chromophore in Light Adapted Bacteriorhodopsin. *J. Am. Chem. Soc.* **109**: 3108-3125

156. Smith, S. O., I. Hornung, R. V. D. Steen, J. A. Pardoen, M. S. Braiman, J. Lugtenburg, and R. A. Mathies. (1986). Are C_{14}-C_{15} single bond isomerizations of the retinal chromophore involved in the proton-pumping mechainism of bacteriorhodopsin? *Proc. Natl. Acad. Sci. USA* **83**: 967-971

157. Smith, S. O., J. Lugtenburg, and R. A. Mathies. (1985a). Determination of Retinal Chromophore Structure in Bacteriorhodopsin with Resonance Raman Spectroscopy. *J. Membrane Biol.* **85**: 95-109

158. Smith, S. O., A. B. Myers, R. A. Mathies, J. A. Pardoen, C. Winkel, M. M. van der Berg, and J. Lugtenburg. (1985b). Vibrational Analysis of the All-*Trans* Retinal Protonated Schiff Base. *Biophys. J.* **47**: 653-664

159. Smith, S. O., A. B. Myers, J. A. Pardoen, C. Winkel, P. P. J. Mulder, J. Lugtenburg, and R. Mathies. (1984). Determination of Retinal Schiff Base Configuration in Bacteriorhodopsin. *PNAS* **81**: 2055-2059

160. Smith, S. O., J. A. Pardoen, J. Lugtenburg, and R. A. Mathies. (1987). Vibrational analysis of the 13-*cis*-retinal chromophore in dark-adapted bacteriorhodopsin. *J. Phys. Chem.* **91**: 804-819

161. Solomons, T. W. G. (1988). *Organic Chemistry.* New York: John Wiley & Sons

162. Spiro, T. G., ed. (1987), Resonance Raman Spectra of Polyenes and Aromatics. In *Biological Applications of Raman Spectroscopy*, Vol. 2. New York: Wiley & Sons

163. Steinberg, G., M. Ottolenghi, and M. Sheves. (1993). pK_a of the Protonated Schiff Base of Bovine Rhodopsin. A Study with Artificial Pigments. *Biophysical J.* **64**: 1499-1502

164. Stockburger, M., W. Klusman, H. Gattermann, G. Massig, and R. Peters. (1979). *Biochem.* **18**: 4886

165. Strackee, L. (1972). Photodichroism of rhodopsin solutions at -196C. *Photochem. Photobiol.* **15**:

166. Suzuki, T., and R. H. Callender. (1981). Primary Photochemistry and Photoisomerization of Retinal at 77K in Cattle and Squid Rhodopsins. *Biophys. J.* **34**: 261-265

167. Tang, J., and A. C. Albrecht. (1970). . In *Raman Spectroscopy, 2*, ed. HA Szymanski, pp. 33-68. New York: Plenum

168. Tavan, P., and K. Schulten. (1986). Evidence for a 13,14-cis Cycle in Bacteriorhodopsin. *Biophys. J.* **50**: 81-89

169. Tavan, P., K. Schulten, and D. Oesterhelt. (1985). *Biophys. J.* **47**: 415-430

170. Terner, J., C. Hsieh, A. Burns, and M. El-Sayed. (1979). *PNAS* **76**: 3046

171. Tonomura, B., H. Nakatani, M. Ohnishi, J. Yamaguchi-Ito, and K. Hiromi. (1987). Test Reactions for a Stopped Flow Apparatus. *Anal. Biochem.* **84**: 370-383

172. Tsuda, M. (1979a). *Methods Enzymol.* **88**: 552-561

173. Tsuda, M. (1979b). Optical Activity of the Metarhodopsins. *Biochim. Biophys. Acta* **578**: 372-380

174. Tsuda, M. (1979c). Transient Spectra of the Intermediates in the Photolytic Sequence of Octopus Rhodopsin. *Biochim. Biophys. Acta* **545**: 537-546

175. Tsuda, M. (1982). *Methods Enzymol.* **81**: 392-399

176. Tsuda, M., Y. Terayama, and M. Takahashi. (1982). Absorption Spectra and Molar Extinction Coefficients of Octopus Rhodopsin and its Photoproducts. *J. Lib. Arts & Sci. Sapporo Med. College* : 37-41

177. Tsuda, M., F. Tokunaga, T. E. Ebrey, K. T. Yue, J. Marque, and L. Eisenstein. (1980). Behaviour of Octopus Rhodopsin and its Photoproducts at Very Low Temperatures. *Nature* **287**: 461-462

178. Tsuda, M., T. Tsuda, Y. Terayama, Y. Fukada, T. Akino, G. Yamanaka, L. Stryer, T. Katada, M. Ui, and T. Ebrey. (1986). Kinship of cephalopod photoreceptor G-protein with vertebrate transducin. *FEBS LETTERS* **198**: 5-10

179. van der Meer, K., J. J. C. Mulder, and J. Lugtenburg. (1976). *Photochem. Photobiol.* **24**: 363-367

180. Van Vleck, J. H. (1929). *Proc. Natl. Acad. Sci. USA* **15**: 754-64

181. Wald, G. (1953). *Ann. Rev. Biochem.* **22**: 497

182. Wald, G. (1968). *Science* **162**: 230-239

183. Wald, G., J. Durell, and R. C. C. S. George. (1950). The Light Reaction in the Bleaching of Rhodopsin. *Science* **111**: 179-181

184. Warshel, A. (1977). Interpretation of Resonance Raman Spectra of Biological Molecules. *Ann. Rev. Biophys. Bioeng.* **6**: 273-300

185. Warshel, A., and N. Barboy. (1982). Energy Storage and Reaction Pathways in the First Step of the Vision Process. *J. Am. Chem. Soc.* **104**: 1469-1476

186. Warshel, A., and P. Dauber. (1977). Calculations of Resonance Raman Spectra of Congugated Molecules. *J. Chem. Phys.* **66**: 5477-5488

187. Warshel, A., and M. Karplus. (1974). Calculation of π–π^* Excited State Conformations and Vibronic Structure of Retinal and Related Molecules. *J. Am. Chem. Soc.* **96**: 5677-5689

188. Wilson, E. B. J., J. C. Decius, and P. C. Cross. (1955). *Molecular Vibrations.* New York: Mcgraw-Hill

189. Yan, M., D. Manor, G. Weng, H. Chao, L. Rothberg, T. M. Jedju, R. R. Alfano, R. H. Callender, L. Rothberg, and T. Jedju. (1991). Ultra-Fast Spectroscopy of the Visual Pigment Rhodopsin. *Proc. Natl. Acad. Sci. (USA)* **88**: 9809-9812

190. Yoshizawa, T. (1972). *Handbook of Sensory Physiology-Photochemistry of Vision.*

191. Yoshizawa, T., and Y. Shichida. (1982). Low-Temperature Spectrophotometry of Intermediates of Rhodopsin. *Methods In Enzymology* **81**: 333-354

192. Yoshizawa, T., and G. Wald. (1963). Pre-Lumirhodopsin and the Bleaching of Visual Pigments. *Natr.* **197**: 1279-1285

193. Yue, K. T., H. Deng, and R. Callender. (1989). Raman Difference Spectroscopy in Measurements of Molecules and Molecular Groups Inside Proteins. *J. Raman Spec.* **20**: 541-546

194. Zhou, F., A. Windemuth, and K. Schulten. (1993). Molecule Dynamics Study of the Proton Pump Cycle of Bacteriorhodopsin. *Biochemistry* **32**: 2291-2306

195. Zhukovsky, E. A., and D. D. Oprian. (1989). Effect of Carboxylic Acid Side Chains on the Absorption Maximum of Visual Pigments. *Sci.* **246**: 928-930

INDEX